Universitetet i Stavanger

FACULTY OF SCIENCE AND TECHNOLOGY

MASTER'S THESIS

Study programme/specialisation: Petroleum Engineering/ Reservoir Engineering	Spring Semester, 2019 Confidential - Two years (2021)
Author: Cathrine Bergo	Cathrine Bergo ..... (signature of author)

Faculty Supervisor:
Pål Østebø Andersen (Department of Energy Resources, University of Stavanger)

Company Supervisor:
Joseph Dowley (Wintershall Norge AS)

Title of master's thesis:

Reservoir Simulation of Chemical Inflow Tracers in Horizontal Wells

Credits: 30 ECTS

Keywords: Maria Field RESMAN Inflow Tracer Technology Horizontal Wells Reservoir Simulation History Matching Multisegment Well Model Local Grid Refinement	Number of pages: 100 + supplemental material/other: 6 Stavanger, 14.06.2019 date/year

Abstract

Conventional production logging tools can be challenging to deploy and interpret in long horizontal wells. Inflow tracer technology can address these challenges, by allowing continuous monitoring of the horizontal section. These oil and water activated tracers are permanently embedded into the sandscreen completion of the Maria field producer H-4. The quantitative inflow contribution, obtained from the unique tracers, is interpreted at two well events; Initial clean-up and after six months of production. All zones were contributing to inflow during clean-up, while samples after restart showed no/minor heel contribution, which is not fully understood. This study aims to demonstrate how inflow profiles from tracer data can be used in a simulation model and how the inflow behavior of H-4 can be explained.

To improve the prediction of the existing Maria reservoir model, it is history matched against interpreted tracer inflow profile, in addition to the traditionally used matching parameters; Pressure and oil production rate. By tuning the horizontal permeability and porosity, within acceptable margins, good matches to the clean-up profile were achieved. Less satisfactory matches were achieved to the restart profile, giving no clear explanation of the mechanism causing such behavior. No major reduction in the well productivity could indicate that the heel zones are really flowing during restart, but the tracer signals are lost somehow.

To increase the understanding of the complex reservoir model, a simplified model was constructed, based on assumptions of single-phase oil and Darcy's law with radial geometry at steady state conditions. Interpretation using both models imply a higher permeability trend in zones with higher inflow. The simplifying assumptions of constant reservoir pressure and depth of the horizontal section are considered to have greatest impact on the oil rate results. Thus, by taking these into account, higher accuracy of drawdown and hence, permeability distribution, is expected. The reservoir model, on the other hand, takes more parameters, mechanisms and equations into account. Hence, it is more representative of real systems.

Considering the multisegment well option in the Maria reservoir model, it was concluded that the pressure losses of producer H-4 have a minor impact on the reservoir model results. Moreover, from a sensitivity study of Local Grid Refinement around the H-4 wellbore, it was concluded that the current grid blocks are appropriate to capture the dynamic trends of the reservoir.

Table of Contents

List of Figures

List of Tables

List of Abbreviations

BHP	Bottom Hole Pressure
BS&W	Basic Sediments and Water
CPU	Computer Processing Unit
EOR	Enhanced Oil Recovery
GOR	Gas Oil Ratio
GS	Gas-soluble System
ICD	Inflow Control Device
IPR	Inflow Performance Relationship
LSOBM	Low Solid Oil-Based Mud
MD	Measured Depth
MICP	Mercury Injection Capillary Pressure
OBM	Oil Based Mud
OOIP	Original Oil In Place
OS	Oil-soluble System
OWC	Oil Water Contact
PBU	Pressure Build Up
PDO	Plan for Development and Operation
PLT	Production Logging Tool
PPT	Parts Per Trillion
STOOIP	Stock Tank Oil Originally In Place
THP	Tubing Head Pressure
TPR	Tubing Performance Relationship
TVDSS	True Vertical Depth from Mean Sea Level
VFP	Vertical Flow Performance
WINO	Wintershall Norge
WS	Water-soluble System

Nomenclature

B_o	Oil Formation Volume Factor
c_f	Unit conversion factor
C_i	Total tracer concentration for tracer *i*
$C_{s,i}$	Concentration of tracer *i* at steady state
$C_{0,i}$	Initial concentration built up in the annular area during shut-in for tracer *i*
D	Well diameter
f	Friction factor
g	Gravity acceleration
Δh_i	Horizontal length of zone *i*
k	Permeability of formation
kh	Flow capacity
k_h	Horizontal permeability
k_i	Concentration decline coefficient for tracer *i*
k_i	Permeability for zone *i*
k_s	Permeability of skin zone
k_v	Vertical permeability
l	Running position along the horizonal section calculated from well toe
N_{Re}	Reynolds number
P_b	Bubble point pressure
P_{gauge}	Pressure at gauge depth
P_{res}	Reservoir pressure
P_{ref}	Reference pressure
P_w	Well pressure
P_{wh}	Wellhead pressure
Q	Cumulative volumetric flow rate along the well
Q_i	Volumetric flow rate for zone *i*
r_e	Drainage radius
r_s	Radius of skin zone
r_w	Well radius
S	Skin factor
T_{ref}	Reference temperature
U	Flow velocity
v	Fluid velocity
V	Cumulative production volume
ε	Tubing roughness
μ_i	Viscosity for fluid phase *i*
ρ_i	Density for fluid phase *i*

Acknowledgments

The MSc thesis “Reservoir Simulation of Chemical Inflow Tracers in Horizontal Wells” has been carried out during the Spring of 2019 at the University of Stavanger, Department of Energy Resources, in collaboration with Wintershall Norge AS, on the occasion of terminating MSc degree in Reservoir Engineering.

First and foremost, I would like to express my sincere gratitude towards my supervisors Pål Østebø Andersen, Associate Professor at the Department of Energy Resources at University of Stavanger, and Joseph Dowley, Subsurface Team Leader of the Maria field in Wintershall Norge, for their professional, continuous guidance and valuable insights throughout the completion of this thesis.

Moreover, I would also like to express my special thanks to Gyunay Namazova and Leidulf Mæland, Reservoir Engineers in Wintershall Norge, for their great patience and support during the training of the software Petrel and ECLIPSE. A great thanks goes to Wintershall Norge for giving me the opportunity and experience to collaborate.

I would also like to thank RESMAN for taking their time to show me around at their laboratory in Trondheim – a really interesting visit. Eventually, a great thanks go to the University of Stavanger for these interesting five years of education.

Cathrine Bergo

Stavanger, June 2019

1 Introduction

1.1 Background

The Maria Oil Field is located in the Haltenbanken area of the Norwegian Sea, operated by Wintershall Norge AS. The field was discovered in 2010 and started producing December 2017, from the upper part of the Garn sandstone formation. Maria is developed as a subsea multi-host tieback, tied to already existing infrastructure in the area; Well stream is transported to Kristin, water supply from Åsgard B and gas supply from Heidrun. As per today, Maria has five producers, all characterized by long horizontal sections, with reservoir section lengths between 1600 and 2800 m, and two slanted water injectors. The producer wellbores are equipped with permanently installed inflow oil and water activated tracers in the inflow control device sandscreen completion, to monitor the zonal inflow contribution along the reservoir (Wintershall, 2015a). This inflow tracer technology is particularly created for long horizontal wells, invented to counter the challenges of conventional production logging in horizontal wells, related to risk and cost (Anopov et al., 2018).

The inflow profile along the horizontal section of the field producers was sampled and the tracer concentrations interpreted, to quantify how much each reservoir zone is producing, at two occasions; During initial clean-up and after approximately six months of production (Mehdiyev, 2018). Clean-up of the well is performed to remove drilling mud, completion fluids and debris that could interfere with the production (Fleming & Appleby, 2006). The inflow profile obtained during clean-up for producer H-4 showed good results, in which all zones were contributing to inflow. The profile obtained after six months of production indicated that something had happened in the reservoir; The heel zones, initially expected to give the highest zonal inflow, were not flowing (Mehdiyev, 2018).

During the development of the Maria field, a reservoir model was created to predict the reservoir performance, to optimize the production and assess economics, in addition to guiding development decisions. With the historical data available, following production start at the end of 2017, the observed oil production rates are entered in the model and further matched against the well bottom hole pressure, for each producer. To date, the simulated inflow contribution of the model has not been matched against the interpreted inflow from tracer response, for any of the Maria producers. Therefore, in this thesis, the simulation inflow

rate of the reservoir model will be history matched against the interpreted inflow profile for Maria producer H-4, for the two occasions, to look into if the tracer results add value to open-hole log information to characterize the simulation model properties.

To begin with, an introduction to the Maria field will be given, followed by fundamental theory related to chemical inflow tracers, well performance and reservoir simulation. Moreover, the Maria inflow tracers are presented, along with the interpreted tracer inflow contribution from producer H-4. Then, a description of the Maria model is given; Base Case assumptions, uncertainties and mechanisms built into the model. In the next chapter, Method, the approach of the simulation cases to be performed will be explained. The simulated results will be presented and eventually discussed and concluded.

1.2 Objectives

The main goal in this thesis is to understand how the interpreted tracer inflow results from Maria can be implemented in a simulation model and how the inflow behavior can be explained. To meet the set goal, a full field simulation model and analytical, simplified model are used. The following objectives are to be investigated for Maria producer H-4;

- How does the interpreted inflow results of producer H-4 match the expected inflow contribution from simulated horizontal production wells?
- Which parameters must be tuned to obtain a better match of the inflow results?
- What causes the deviations between interpreted tracer inflow and simulated inflow contribution?
- What causes the deviations between the Simplified Model results and the reservoir model?
- How will the simulation results change when the grid is locally refined around the wellbore and the producer redefined as a multisegment well, i.e. when frictional well effects are modeled?
- What are the limitations and advantages of production logging tools to measure horizontal well inflow compared to inflow tracers?

2 Maria Field Introduction

The producing Maria field is located 230 km from the Norwegian coastline, in blocks 6406/3, 6407/1 and 6507/10 in the Haltenbanken area of the Norwegian Sea (**Figure 2.1**). The oil field is operated by Wintershall Norge AS. Maria is surrounded by a number of producing fields and discoveries and is contributing to lifetime extension of the nearby infrastructure in Haltenbanken (Wintershall, 2017b). To the supplier market, the field has been a significant contributor over the last year (Wintershall, 2018).

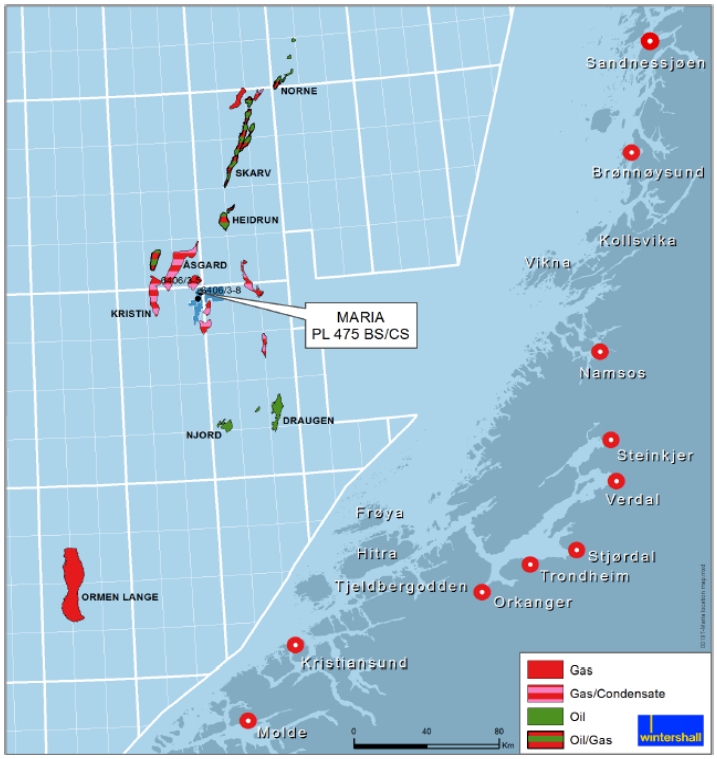

Figure 2.1: Location of the Maria Field (Wintershall, 2017b).

2.1 Project History

The field was discovered in August 2010. For Wintershall Norge (WINO), Maria was the first operated discovery developed all the way to production, in cooperation with the license partners, Petoro AS (30%) and Spirit Energy Norway AS (20%). The Plan for Development and Operation (PDO) was submitted in May 2015 and the approval by the authorities was received in September 2015. Only two years after the approval of PDO, 16th December 2017, the production started (Wintershall, 2017b).

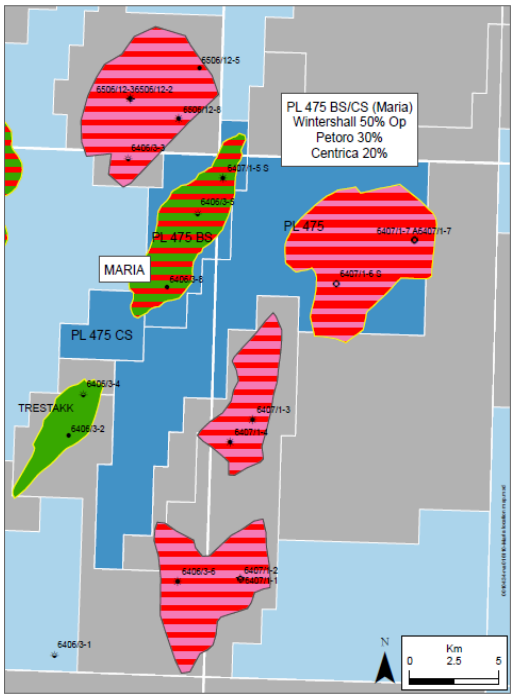

Figure 2.2: Regional license map (Wintershall, 2015a).

In 1988, former Statoil drilled the first exploration well, 6406/3-5, found dry with oil shows, in the area

where the Maria field is located today. In January 2009, Wintershall was awarded the operatorship (30%) of the PL 475 BS license, resulting in the discovery of the Maria field by the exploration well, 6406/3-8 T2, in August 2010. The PL 475 CS license was awarded in February 2011, which in 2012 gave rise to the appraisal well, 6407/1-5 S, to determine the lateral size of the reservoir in the northern part. Maria lies fully within the PL 475 BS and PL 475 CS licenses (Wintershall, 2015a). A map of the regional licenses can be seen in **Figure 2.2**.

2.2 Development Solution

The Maria subsea field, located at approximately 300 m water depth, has two 4-slot subsea templates installed. The installations are located three km apart and are called Maria H and G. Maria is developed as a subsea multi-host tieback, where each template is involving one water injector. The semisubmersible rig, Deepsea Stavanger, drilled the seven wells at Maria; Five producers and two injectors (Wintershall, 2017b).

97 km of pipeline are linking the Maria reservoir to the nearby Equinor-operated installations; Kristin, Heidrun and Åsgard B **(Figure 2.3)**. The Maria field is located 20 km east of Kristin platform and the entire well stream is transported here for processing. Furthermore, the processed oil is shipped to Åsgard C for storage and offloading to tanker ships, while the gas is exported through the Åsgard transportation pipeline system to Kårstø. 15 km northwest of Maria is the Åsgard B located and it is providing the lift gas to Maria via the existing Tyrihans D subsea template. Moreover, the supply of water for water

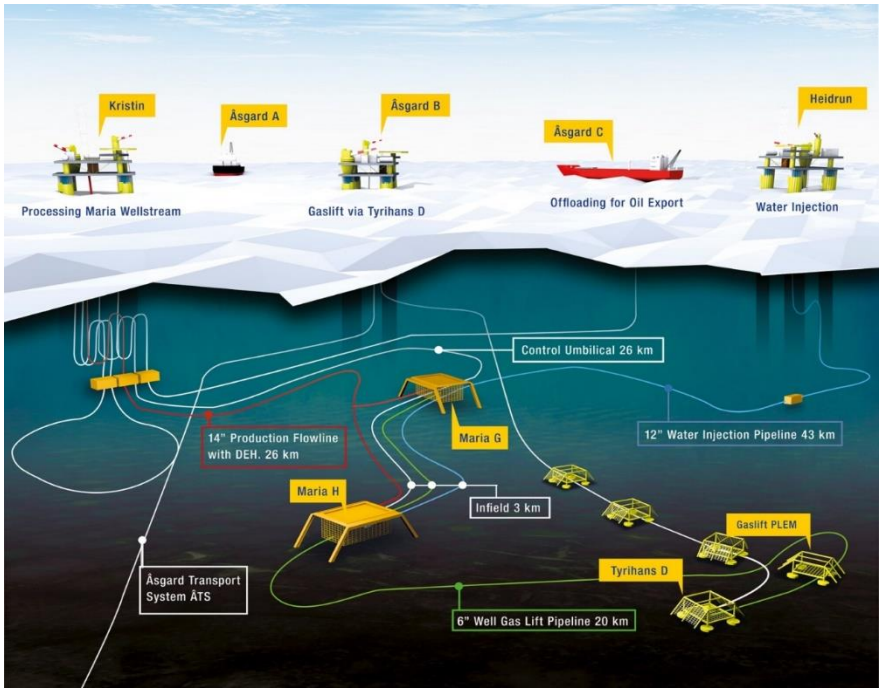

Figure 2.3: Maria development concept (Wintershall, n.d.).

injection to the Maria reservoir is provided by the Heidrun platform, located 45 km north of Maria (Wintershall, 2017b, 2018).

Kristin is the key host for Maria and is responsible for the daily operations at Maria, along with cooperation with Åsgard and Heidrun, and reporting. For WINO, Kristin is the only contact point. The responsibility for operating and maintaining all equipment on the host facilities is assigned Equinor, while WINO is responsible for the reservoir management (Dowley, 2016).

2.3 Reservoir

Maria consists of a sandstone reservoir with a mean top depth of 3770 m True Vertical Depth, measured from Mean Sea Level (TVDSS), in the Garn Formation of the Middle Jurassic age. The formation has a thickness of 90 to 100 m with silt layers within between the massive sand.

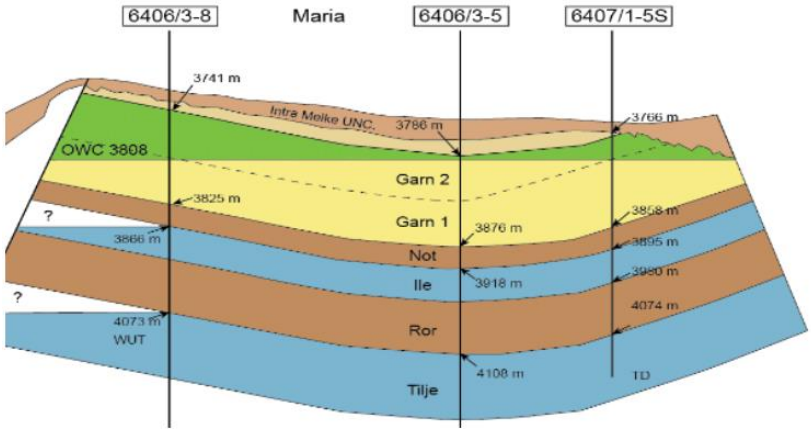

Figure 2.4: The Maria reservoir structure (Dowley, 2016).

The structure is defined as a distinct horst, trending northeast-southwest, with erosional components in the northern part. The quality of the reservoir, in general, is moderate, but better in the southern part, i.e. better for the H-wells than for the G-wells. Despite this, the Maria reservoir is considered to be relatively homogeneous related to porosity and permeability (Wintershall, 2015b).

The Garn Formation of the Fangst Group is a shallow marine deposit, that can be subdivided into two units; Lower Garn, Garn 1, and Upper Garn, Garn 2. Garn 1 can further be subdivided into A and B, and are most likely generated by currents. Garn 2 can be divided into A, B, C and D and deposited in a wave-influenced environment with some current influence. The subunits are mainly implemented due to silt barriers of lower permeability separating the layers (Wintershall, 2015a).

In the reservoir formation, there is zonal prevalence of calcite, either as calcite nodules or cement. The latter can be explained by cementation of the reservoir rock, which is a chemical process where minerals precipitate into the pore space between the sediment grains. Thus, the cementation is contributing to reduced porosity and permeability, i.e. resulting in poorer reservoir quality (Fossen, 2008). Calcite is prevalent in a greater amount in the southern part of the Maria field. Garn 1 has better reservoir quality than Garn 2, as calcite is present to a lesser extent. As it can be observed in **Figure 2.4**, the Oil Water Contact (OWC) is located at a depth of 3808 mTVDSS, resulting in Garn 1 being primarily filled with water. Hence, the underlying sandstone formations, Ile and Tilje, are in this field water bearing (Wintershall, 2015b).

The reservoir has normal pressures and temperatures, with a maximum temperature of 137˚C. Consequently, there are no major risks identified such that conventional drilling methods can be used and within sufficient margins (Wintershall, 2015a).

2.4 Wells and Drainage Strategy

The five Maria production wells have open-hole completions and are drilled vertically into the overburden, deviated horizontally prior to the drilling of the reservoir sections. All the producers are characterized by long horizontal sections, with a length between 1600 to 2800 m into Garn 2D formation. They have an average total well length of 6400 m (Wintershall, 2015a). The two water injectors, on the other hand, are slanted, deviating with an inclination between 45˚ and 60˚ in the reservoir section, with an approximate length of 300 m. The injectors have an average total well length of 4500 m (Wintershall, 2015a). The well

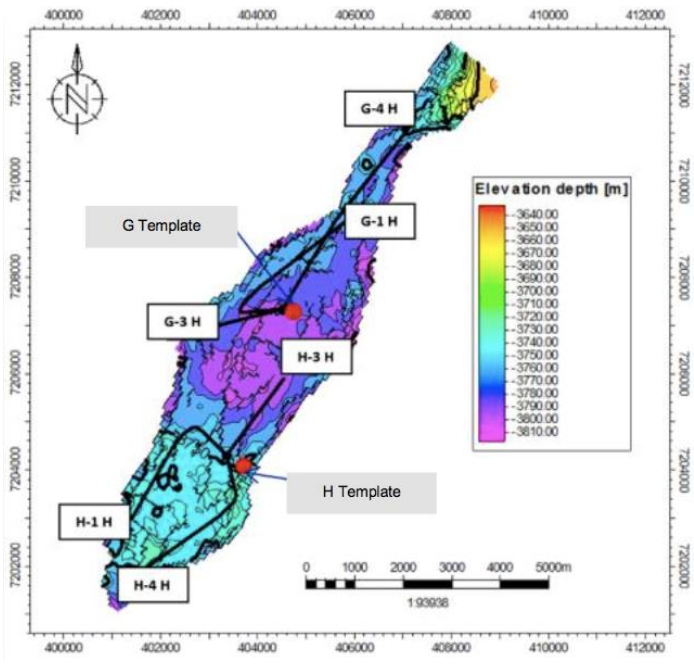

Figure 2.5: Location of the well trajectories in the Maria field (Dowley, 2016).

trajectories in the Maria field can be seen in **Figure 2.5** below.

The drainage strategy for Maria is production supported by injection of water, used to pressure-support the field. Water injection is performed to maximize the recovery of the reserves by sweeping the remaining oil through the reservoir towards the production wells. The main strategy was to inject water mostly in the high permeable water zone, to maintain a reservoir pressure above the bubble point pressure. Hence, the water was initially injected into the Garn 1 Formation, below the producing interval in Garn 2, such that the water could migrate upwards through barriers and faults. The injection started one month after start-up of the production (Wintershall, 2017b).

The injected water is Sulphate-reduced seawater, as there is a potential risk of scale formation in the production wells with increased seawater cut, due to the Maria formation water containing a high amount of Barium. Consequently, chemical injection valves are equipped at each production well for injection of scale inhibitor when required (Wintershall, 2017b). To optimize the production, two gas lift mandrels are installed at each production well, where gas can be injected into the production tubing for artificial lift (Wintershall, 2017b).

2.5 Completion Design

A service company provided Wintershall with a simulation study to evaluate which completion design that would give the most efficient flow solution for the Maria producers. The most efficient design, and thus, the chosen concept, turned out to be sandscreens installed with a multiport Inflow Control Device (ICD) at every reservoir-facing joint. The screen-only completion was ranked to be less efficient for the given reservoir (LR Senergy, 2016).

The ICD systems are choking devices used to manage the distribution of flow along the horizontal well section and hence, deliver an even profile regardless of location and variation in permeability (Bybee, 2010; Kumar et al., 2015). Zones containing high permeability, has a high pressure drop across the ICDs, reflecting a higher annular pressure. Consequently, the drawdown and flow rates in the corresponding zones are reduced. In other words, the fastest flowing zones are retarded by the ICDs, as the pressure drop increases with the fluid flow rate. This reduces the risk of sanding and coning. For low-permeability zones, the opposite is

applicable (Youngs et al., 2010).

The ICD nozzles regulate the flow from the reservoir into the main flow stream. For conventional sandscreens, the fluid flows directly from the reservoir into the tubing through the mesh grid in the sandscreen, while for ICDs two types of inflows are defined; First, the inflowing fluid flows from the reservoir to the annulus, then from the annulus to the tubing via the sandscreens and ICD nozzles. In **Figure 2.6** and **Figure 2.7**, the difference in the fluid flow path of conventional sandscreens and ICD sandscreens and definitions of the fluid inflow can be observed, respectively. The ICDs at the Maria producers are placed every 30 m. They have four ICDs per joint of screen, where each nozzle has a diameter of four mm (LR Senergy, 2016).

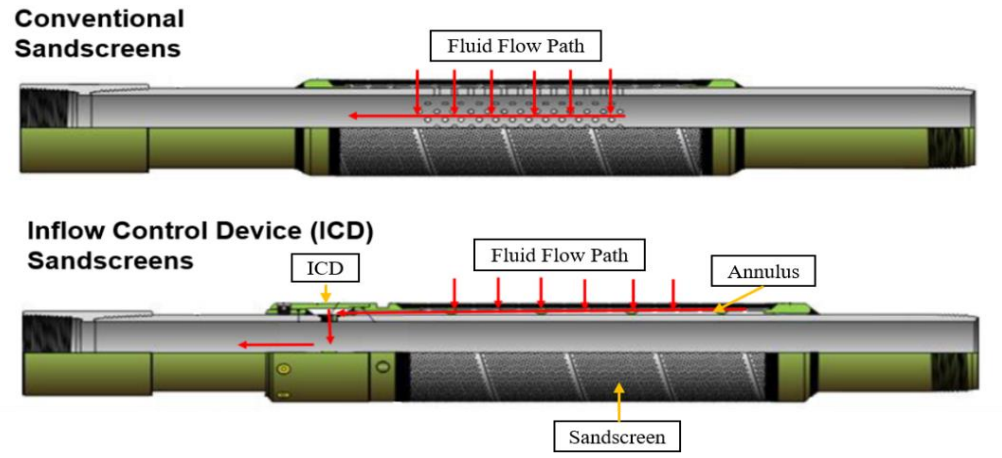

Figure 2.6: Illustrating the difference in the fluid flow path of conventional sandscreens and ICD sandscreens (LR Senergy, 2016).

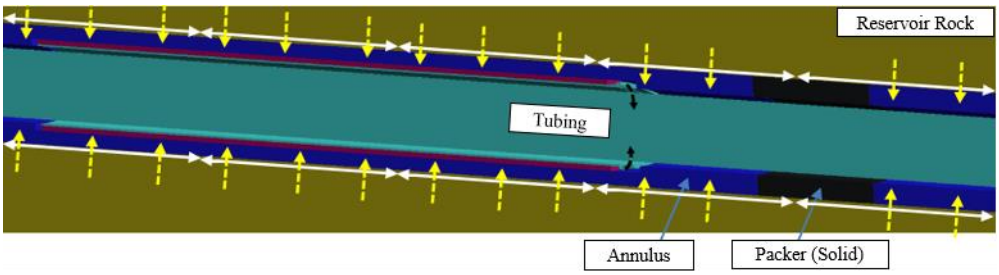

Figure 2.7: Fluid inflow definitions (LR Senergy, 2016).

As observed in **Figure 2.7** above, packers installed in an ICD completion can reduce the

inflow. In screen-only completions, strong annular flow can be observed, where fluids rush towards the first screen to flow into the tubing. Consequently, the inflow efficiency is reduced. In this case, packers can contribute positively by reducing the annular flow. Annular flow is eliminated in the ICD completions, as the fluid is forced to flow through the nozzles of the ICD into the tubing (LR Senergy, 2016). Hence, the inflow is representative for the given zone and only a small number of packers are included in the Maria producer's completion.

3 Fundamental Theory

The intention of this chapter is to present the fundamental aspects of tracers in general, challenges with conventional production logging in horizontal wells and the RESMAN Inflow Tracer Technology. The interpretation method, Flush Out model, used to quantify the inflow contribution along the horizontal reservoir section from tracer response will be presented, followed by theory related to the well performance and pressure drop in horizontal wells. Moreover, the reservoir simulation concepts of multisegment wells and Local Grid Refinement will be explained. Eventually, the simulation programs used throughout this thesis are presented.

3.1 Tracers

A tracer, also called a marker, can be chemical or radioactive compounds with at least one characteristic distinguishing it from the reservoir fluid (Dyrli & Leung, 2017). All tracers have their unique chemical signature to ensure that the detected signal correlates to the correct well location, for the intention of later producing it (Carpenter, 2018). The tracer must be stable, non-degradable and inert under reservoir conditions and must not adsorb onto the reservoir rock. Thus, not interact chemically with the porous media. In addition, the tracer detection limit must be very low and have minimal impact on the environment. Tracer compounds which are soluble in the water, oil or gas phase are called chemical tracers (Salman et al., 2014).

Reservoir tracers are used for various purposes and are accordingly typically classified as inter-well or single-well tracers. Their purposes will be shortly explained below. In the Maria field, a new tracer technology has been used to quantify the wellbore inflow and this RESMAN technology will be described in **Section 3.3**. It is used for different purposes than the inter-well and single-well tracers.

3.1.1 Inter-Well Tracer Testing

In inter-well tracer testing, tracers are added to the water in an injection well to provide information on the well-to-well communication, for instance, to characterize reservoir properties, volumetric sweep efficiency and flow pattern of the reservoir. The tracer results

are primarily qualitatively analyzed, where the arrival and non-arrival of the tracers are documented (Guan et al., 2005). The time is recorded for the injected tracer to arrive in the production well and then it will be back-produced to surface (Bjørlykke & Avseth, 2010, p. 457). Furthermore, fluid samples will be collected and analyzed at the laboratory using advanced chromatography, together with spectroscopy. From this, it is feasible to predict how the fluids are flowing in the reservoir (Dyrli & Leung, 2017).

3.1.2 Single-Well Tracer Testing

Single-well tracer testing is an in-situ method to provide information on the reservoir fluid saturation. It is used for testing Enhanced Oil Recovery (EOR) processes to determine the residual oil saturation and hence, measuring the displacement of oil by an EOR slug to give a direct indication of the process effectiveness to mobilize the residual oil (Tomich et al., 1973). Tracers are added to the water injected into the well, before the well is shut-in for the tracers to interact. After this, the water is back-produced to surface and the tracer concentration profiles are analyzed. The residual oil saturation is indicated by the separation between the tracer's arrival times (Sheely, 1978).

3.2 Challenges with Conventional Production Logging in Horizontal Wells

Horizontal wells have increased reservoir contact compared to vertical wells, which allows it to achieve greater production efficiency. Nevertheless, one of the main challenges for the industry is to comprehend the inflow profile from a horizontal well (Andresen et al., 2012). Initially, the conventional Production Logging Tools (PLTs) were developed for vertical wells. Thus, by using these tools in horizontal wells, optimal results will not be obtained (Ovchinnikov et al., 2017). Accordingly, production logging in horizontal wells is way more challenging than in vertical wells (Chandran et al., 2005).

Even though conventional PLTs can provide measurements of high resolution in long horizontal wells, they can be challenging to run and the data acquisition is highly expensive (Anopov et al., 2018). Moreover, the PLTs are non-efficient related to the operation, production optimization, time and well intervention at a low cost. Hence, a coiled tubing, often combined with a tractor, is needed for intervention to deploy the PLTs into long horizontal wells, as the gravity cannot assist, like in vertical wells. These can be challenging

to deploy in complex, offshore environments. There is a risk that the coiled tubing will go into helical buckling before the toe of the well is reached. The latter will result in an incomplete well log (Siddiqui et al., 2017). An additional risk related to running the coiled tubing with a tractor is that it can affect the pressure in the wellbore, which further influences the flow distribution (Semikin et al., 2015). Hence, the original flow condition is disturbed, resulting in inaccurate measurements (Ozkan et al., 2002).

One type of PLT technique, spinner components, can be used to identify the fluid phases and the corresponding phase's velocities in the wellbore. One of the main limitations of the spinners for use in horizontal wells is presence of multi-phase fluid flows, due to gravitational fluid segregation in the borehole. The restricted size of the spinners will primarily enable us to measure the middle phase, oil. Consequently, the oil rate is overestimated. Hence, when single-phase flow is present, the spinners are expected to provide accurate data (Al-Ali et al., 2000). On the other hand, additional logging problems can be encountered in horizontal wells due to the stratified layers traveling at different speeds (Ovchinnikov et al., 2017). The flow patterns can change laterally due to an uneven increase or decrease in the fluid rates (Chandran et al., 2005).

To counter the challenges of production logging in horizontal wells, permanently installed, inflow tracer technology was invented as an alternative (Anopov et al., 2018). The RESMAN Intelligent Tracer Technology will be considered in this study. This innovative and wireless technology is a cost-efficient way to continuously monitor the inflow contribution along the wellbore. It is specifically created for long horizontal wells and wells with complex completions, where the conventional techniques imply risks and are expensive (Siddiqui et al., 2017). In addition, it does not require any downhole well intervention or expensive completion tools. Thereby, causing no extra operational risk. Another advantage is that it is robust for the downhole conditions and health, safety and environmentally friendly, as extremely low amounts of chemicals are used (Williams & Carvalho, 2013). It provides a chemical tracer production log, which can be obtained periodically, whenever needed; Up to 10 years for zonal inflow quantification and potentially throughout the well lifetime for water breakthrough detection. Thus, the inflow tracer technology is not limited to a one-time report, which is the case for the PLTs (Bennetzen & Hviding, 2019; RESMAN, n.d.). An advantage with the PLTs is that it provides measurements of higher resolution than the inflow tracer

technology. Except this, tracer technology is an economical and productive alternative to conventional PLTs. In the following section, the technology will be explained into closer details.

3.3 RESMAN Inflow Tracer Technology

The Intelligent Inflow Tracer Technology allows continuous surveillance of the reservoir section (Bennetzen & Hviding, 2019). Unique tracers are installed at strategic locations in the completion of the horizontal section of the production well, for the inflowing fluids to contact the tracers (Carvalho et al., 2015). The tracer systems can easily be integrated on any completion device, e.g. conventional sandscreens, ICD sandscreens, multi-stage fracking equipment and pup joints (Williams & Carvalho, 2013). The resolution of the digital oilfield model is improved by installing these chemical tracers. By understanding the reservoir performance, the uncertainty of the subsurface is reduced, thereby allowing improved and proactive reservoir management strategies. In the long-term, this might imply an improved performance of the well (Bennetzen & Hviding, 2019). The main objectives of inflow tracers in horizontal wells are to determine the zonal inflow distribution across the reservoir, either qualitatively or quantitatively, in addition to identifying the water breakthrough locations (Carpenter, 2018).

The chemical tracers are incorporated in porous polymer material (**Figure 3.1**) and have an affinity to either oil, gas or water, i.e. they can be Oil-soluble Systems (OS), Gas-soluble Systems (GS) or Water-soluble Systems (WS) (Carvalho et al., 2015). The tracer marking periods, i.e. lifetime, are limited. The polymer strips, containing unique tracers, are incorporated into joints, referred to as tracer joints. They are installed onshore and an example of how the strips are installed can be observed in **Figure 3.2** (Anopov et al., 2018). The amount of tracer joints is dependent on the horizontal well section length. **Figure 3.3** illustrates a horizontal well, stretching from a Measured Depth (MD) of 4500 to 7000 m, with eight tracer joints installed.

Figure 3.1: Polymers with chemical tracers incorporated (Mehdiyev, 2018).

Each unique tracer is represented by a unique color. Over 80 unique chemical tracer signatures have been developed for oil and another 80 for water. As they are unique in nature, the signatures will not be mistaken for being other chemicals under production (Carpenter, 2018).

Figure 3.2: Polymer strips installed along the completion of the well pipe (Gashimov et al., 2017).

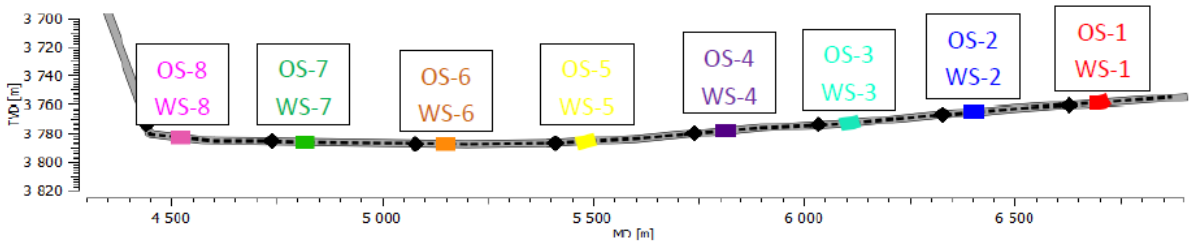

Figure 3.3: Distribution of tracers along the completion (Mehdiyev & Rivero, 2018).

The chemical tracers are designed to remain dormant until wetted by the target fluid. Thus, OS tracers will remain dormant when in contact with water and active when in contact with oil. For WS tracers, the opposite is applicable. In air, both tracer types will remain dormant. When the polymer material is in contact by the target fluid, low concentrations of the respective tracer molecules are gradually released, through diffusion, into the well flow and hence, their chemical signature is released (Carvalho et al., 2015). The tracer release is not dependent on the flow velocity of the surrounding fluids. Tracer molecules are instead released at a constant rate when in contact with the target fluid. Thus, this implies that tracer molecules will be released no

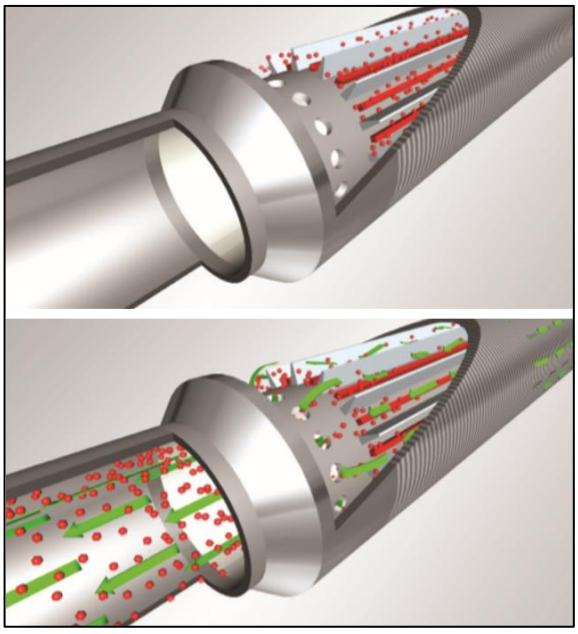

Figure 3.4: Tracer molecules (red dots) are flushed to surface with the well stream when contacted by the inflowing target fluid (Carvalho et al., 2015).

matter if the well is producing or shut-in (Siddiqui et al., 2017). The molecules are carried to the surface, carrying information about their specific zones and are produced together with the main flow stream (**Figure 3.4**).

Production fluid samples are taken at the surface and provide qualitative information of the inflow contribution; Which zones are flowing/not flowing. No tracer detection from one zone indicates that there is no inflow through that zone and hence, there is a restriction in the annular to flow. Moreover, no tracer detection from any of the zones indicates that an obstruction inside the wellbore has developed and a clean-out may be needed (Williams, 2017). The samples can further be sent to the laboratory for a quantitative analysis for the determination of the tracer molecule concentrations to quantify the inflow distribution. The concentrations can be detected in ultra-low concentrations, down to parts per trillion (PPT) (Carpenter, 2018).

3.4 Interpretation Events

After the production fluid samples are analyzed, the results are interpreted, addressing all phases in a well's lifetime; Transient and steady state. The program and objectives vary depending on the well operation phase (Carpenter, 2018).

3.4.1 Transient Analysis

In the first flowing phase of the well it is said to be in a transient state, where the tracer concentration is varying with time. In transient mode, tracer shots are registered as peaks of high tracer concentration. They can be explained by the step change of pressure drop at start-up of the well (Morozov et al., 2017). A transient analysis is used to estimate the relative flow contributions in each reservoir section and to monitor the well clean-up, which is information used for the qualitative evaluation (Mehdiyev, 2018). Samples taken during well clean-up and shut-in/restart are analyzed during transient state.

3.4.1.1 Well Clean-up

To encounter the problems of reduced permeability in critical areas of the formation, several solutions have been developed (Rollins & Taylor, 1959). The wellbore must be cleaned up by

well intervention to remove solids that interfere the production, down to acceptable limits. Another objective is to facilitate the completion operations and minimize the formation damage. Moreover, to clean up the mud residue (Fleming & Appleby, 2006).

Several requirements have to be met for a clean-up to be terminated. As some fields/operator have different criteria, some generalized criteria are; A pre-specified wellbore volume back-produced to surface, fluid rates and wellhead/Bottom Hole Pressure (BHP) stable for a given time period, in addition to stable trends for the last measurements of pH, Basic Sediments and Water (BS&W) and Chloride of water content from choke manifold (Wintershall, 2017a). Moreover, a "clean well" must have tracer sample response from 70 to 75 % of the reservoir section (Wintershall, 2017b). During the clean-up process, a back-production of the following fluids is expected; Wellbore fluids, reservoir fluids and drilling fluids that have leaked into the formation while drilling (Wintershall, 2017a).

The objective of samples taken after a well clean-up is to qualify the clean-up efficiency of each section, i.e. to estimate the well productivity. Clean-up samples are collected at intervals of minimum 30 minutes, increasing gradually to 6 to 12 hours, with a total duration of 2 to 3 days (Morozov et al., 2017). The samples are collected at the end of the clean-up, to avoid contamination if injected chemicals and Oil Based Mud (OBM) are used (Wintershall, 2017a). Already from the start-up of the well, the Intelligent Tracer Technology allows monitoring of the horizontal section to determine the lowest productive interval, which is an advantage for the planning of well interventions in an early phase (Morozov et al., 2017).

3.4.1.2 Well Shut-in/Restart

The objective of samples taken after restart of a well is to quantify the inflow profile. The well must be shut-in for a short period, 6 to 24 hours (Morozov et al., 2017). During shut-in periods, tracers of high concentration, so-called tracer shots, can form in the annular area of the reservoir compartment at each traced location, by continuous diffusion in contact with the target fluid. Along with the main well stream, the tracer shots are flushed out with the initial production, when production is restarted (Williams & Carvalho, 2013). By determining the volume or time interval required for flush out of the tracers from each reservoir section and by history-matching the reservoir simulation parameters with the measured production data, a quantitative evaluation of the inflow profile can be obtained (Carpenter, 2018). Fluid samples

at the wellhead are collected in intervals, varying from 5 to 60 minutes, with a total duration of 1 to 2 days (Morozov et al., 2017).

3.4.2 Steady State Analysis

When the tracer shots are flushed out of the well, the concentration of the flow is usually stabilized (Morozov et al., 2017). When the well is flowing at a steady rate, a steady state analysis is used to identify the breakthrough locations of water, in addition to determining the production performance of oil and water (Mehdiyev, 2018). The reservoir fluid is routinely sampled during the well operation, typically once a week. Hence, it is continuously monitored. The fluid samples are sent to the lab for a proper analysis when a water breakthrough is suspected. The interpreted results will include critical information on the dynamics of the increasing water cut for each section, throughout the period of sampling. These tracer systems are important to recover reserves by quickly detecting the flooded sections and thereby isolating them. In addition, they can be used for decisions of successive well intervention, without any use of downhole logging (Morozov et al., 2017; Siddiqui et al., 2017).

In **Figure 3.5** below, it can be observed that samples are collected more frequently in the beginning, during the transient regime, and less frequently when the steady state is reached. The water samples taken at the beginning of the transient regime are from the back-production of fluids during the clean-up process.

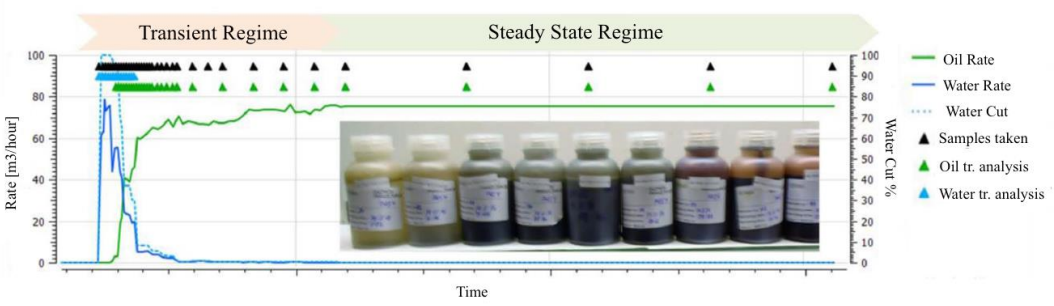

Figure 3.5: Illustrating the transient and steady state regimes.

3.5 Tracer Interpretation Models

A powerful analytical and visual technique is to plot and correlate data. Trends in patterns can be recognized, involving changes in slopes and data anomalies, by human and artificial cognition and algorithms. The changes in production data can be correlated with tracer signal and hence, well behavior in specific zones can be interpreted (Bennetzen & Hviding, 2019). Two tracer transport model techniques have been developed by RESMAN for interpretation, to determine the zonal inflow distribution of the reservoir section after restart:

1) Flush Out Model
2) Arrival Time Model

The Arrival Time model is not suitable in wells with long tie-backs, as the sampling should be performed at the wellhead to avoid time separations (Carpenter, 2018). Moreover, it is not well-suited for wells completed with ICDs, as the tracers will more or less arrive at the same time. Both the exceptions are present in the Maria producers. Hence, it is not used. Therefore, the Arrival Time model will not be presented.

3.5.1 Flush Out Model

The physical and mathematical Flush Out model technique is used to model the response of tracer concentrations developed during restart of a well after it has been shut-in, by interpreting the decline rate of the tracer concentrations from each zone. In the model, the tracer concentration is a function of the volume produced, i.e. the cumulative production (Carvalho et al., 2015). The model is mainly used for quantitative evaluation; A representative percentage of total inflow from each monitored zone is obtained by history matching the measured production sample concentrations to the simulated data (Morozov et al., 2017).

The back-production of tracer shots is rate dependent and the performance of the reservoir zones is proportional to the flush out productivity (Morozov et al., 2017). From the shape of the tracer shots captured at surface, quantitative estimates of the inflow contribution can be derived. A quick flush out of the annulus is indicated by a steep concentration decline rate

profile towards the steady state level and hence, correspond to high inflow rates and more productive zones. Thus, the resulting response can be seen by tracer zone 1 in **Figure 3.6** and OS-2 in **Figure 3.7**. On the contrary, a less effective flush out indicates zones with lower inflow rates and hence, less productive zones (Williams & Carvalho, 2013). As the tracer concentration that is flushed out from a less productive zone becomes more diluted when released to the well stream, it will get a less steep decline rate profile, seen by tracer zone 2 in **Figure 3.6** and tracer OS-1 in **Figure 3.7** (Carvalho et al., 2015).

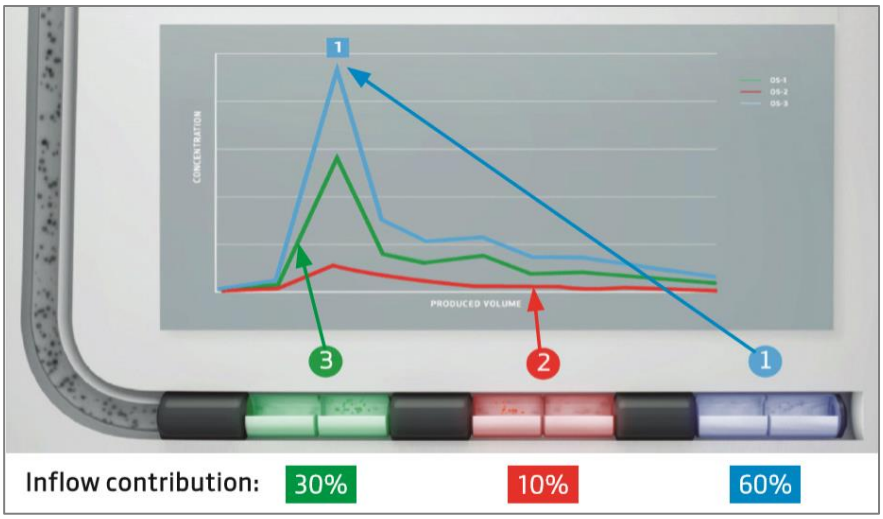

Figure 3.6: Quantitative inflow evaluation, based on the shape of the tracer shots captured at surface (Carvalho et al., 2015).

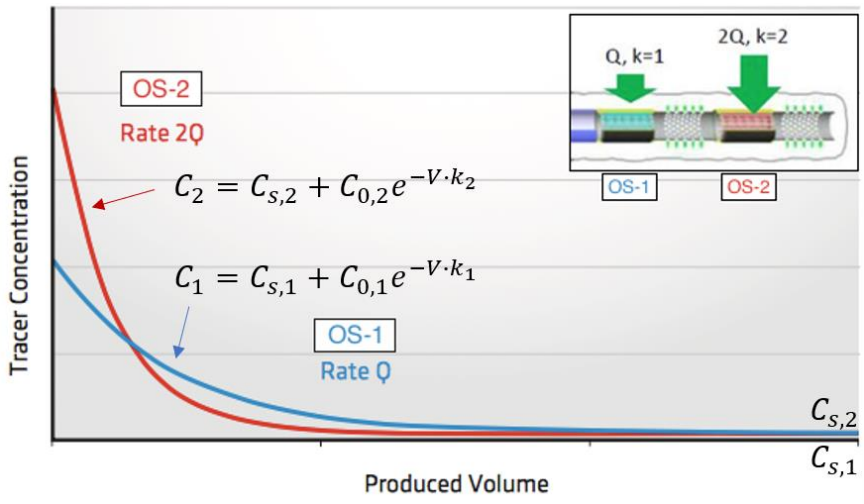

Figure 3.7: Illustration of the Flush Out model with mathematical equations (Carvalho et al., 2015; Mehdiyev, 2018).

Under ideal conditions, the total concentration of tracer molecules for tracer *i*, as a function of time, can be expressed mathematically by (Langaas et al., 2017):

$$C_i(t) = C_{s,i} + C_{0,i}e^{-V \cdot k_i} \quad (3.1)$$

Where,

C_i Total tracer concentration for tracer *i* as a function of time,

$C_{s,i}$ Concentration of tracer *i* at steady state

$C_{0,i}$ Initial concentration build-up in the annular area during shut-in for tracer *i*, corresponding to the height of the tracer peak

V Cumulative production volume

k_i Concentration decline coefficient for tracer *i*

The tracer concentration decline coefficient, k, can be determined for each reservoir section by usage of the well model, nodal analysis and mathematical tools (Morozov et al., 2017). The coefficient expresses how fast the tracer shot is flushed out and it is directly proportional to the fluid inflow at the tracer location. It can therefore, describe the local flow rate and hence, be used to quantify the performance of each section (Williams, 2017). From **Figure 3.7**, OS-2 is flushed out at twice the rate of OS-1, which implies that the oil with a high concentration of OS-2 will be recovered nearly twice as fast, resulting in a doubled k-factor (Morozov et al., 2017).

3.6 Well Performance

The production driving force is the differential pressure driving the reservoir fluid into the wellbore, referred to as pressure drawdown (Skaugen, 2010). The term reservoir deliverability is defined as the achievable fluid production rate from reservoir at a specified BHP, which significantly affects the well deliverability. The well delivery capacity is determined by a combination between inflowing rates from reservoir to well, given by Inflow Performance Relationship (IPR), and flow conditions

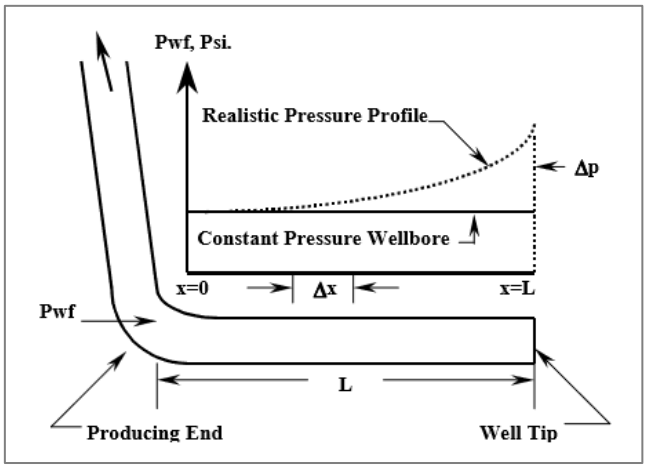

Figure 3.8: Pressure profile along a horizontal wellbore (Saavedra & Reyes, 2001).

through the tubing, described by Vertical Flow Performance (VFP) and Tubing Performance Relationship (TPR) (Guo et al., 2007, p. 30,70). The IPR is a function of the pressure difference between the reservoir and well, while VFP is given by the pressure difference between the well and well head. Adjustments of the well head pressure will influence the well pressure and hence, the IPR and VFP. The pressure drop in the production tubing is given by two main components; Hydrostatic and frictional loss. The frictional loss accounts for pressure drop due to the roughness of tubing and is increasing with flow rate (Skaugen, 2010).

One of the main factors determining the delivery factor of the well is the drawdown needed to lift the fluid through the production tubing, while still maintaining a sufficient flow rate (Skaugen, 2010). Therefore, it is required to have some pressure drop from toe to heel, resulting in the pressure of the toe having a higher well pressure than of the heel. (Joshi, 1991, p. 379). This implies that the fluid inflow will drop as it approaches the toe (Archer & Agbongiator, 2005). To maintain stable flow conditions, the inflow rates must balance the outflow rates (Skaugen, 2010). The pressure profile in a horizontal well is illustrated in **Figure 3.8**.

3.6.1 Formation Damage

"Formation damage is an undesirable operational and economic problem that can occur during the various phases of oil and gas recovery from subsurface reservoirs" (Civan, 2016, p. 1). Formation damage can be caused by several processes, e.g. related to chemical, hydrodynamic, thermal, mechanical and biological processes (Civan, 2016, p. 3). For instance, foreign materials, such as mud filtrate, cement slurry and clay particles, can invade the formation during drilling operations and hence, cause impairment of the near-well permeability. This flow-restricting effect is commonly referred to as "wellbore damage" and the altered permeability region as "skin zone". Skin is a dimensionless quantity, which might limit the drawdown (Lu et al., 2013). Mechanical skin can be calculated using Hawkins' equation, **Equation (3.2)** (Morales et al., 1996). The pressure drop due to skin is defined as the difference between the reservoir's actual and ideal pressure drop (Joshi, 1991, p. 193).

$$S = \left(\frac{k}{k_s} - 1\right) \cdot ln\frac{r_s}{r_w} \qquad (3.2)$$

Where,

S	Skin factor
k	Permeability of the formation
k_s	Permeability of the skin zone
r_w	Wellbore radius
r_s	Radius of skin zone

According to Civan (2016), the drilling fluid loss is greatest at the heel of horizontal wells and reducing towards the toe. Hence, the skin of the heel is typically greater than of the toe. Skin damage removal in horizontal wellbores may be quite complicated. Stimulation treatments, such as acidizing and fracture treatments, are very costly and problematic in long horizontal wells. Additionally, the treatment volumes required are large. For horizontal well productivity, skin can be very destructive (Cho & Shah, 2001). Moreover, the effect of formation damage is much higher in a horizontal well compared to a vertical well, drilled in the same formation (Yan et al., 1998).

The effective wellbore radius is an alternative concept to the skin effect. A stimulated well, i.e. a well with improvement, defined by negative skin values, will have an effective wellbore radius greater than drilled well radius and a reduced pressure drop in the near-well area. On the other hand, a well with damage will have a smaller effective wellbore radius and an increased pressure drop in the near-well area, defined by positive skin values (Joshi, 1991, p. 43).

3.6.2 Effect of Wellbore Pressure Drop on Horizontal Well Performance

According to Ohaegbulam et al. (2017), a common complication for several petroleum researchers concerns the effect of the wellbore pressure drop along the well, on the performance of the horizontal well. The pressure loss increases the tendency of water and gas coning at the well heel. Furthermore, the oil production in some parts of the horizontal wellbore can be choked due to the pressure loss, leaving that wellbore part unproductive. This is especially significant for long horizontal wellbores. Accordingly, there exists a limitation where the advantage of increasing the length of the horizontal wellbore restricts the well deliverability due to the wellbore pressure losses. They concluded that beyond a certain length of the horizontal section, the well productivity will no longer be proportional to the well

length (Ohaegbulam et al., 2017).

In a homogeneous reservoir, the flow contribution of the heel is expected to be greater than of the toe. This can be explained by long horizontal producers resulting in significant pressure drop over its length. Inflow at the toe must overcome this pressure drop, while oil produced at the heel is not affected. This is defined as the heel-to-toe effect (Denney, 2010).

Several studies have investigated the performance of the wellbore pressure drop in horizontal wells on the well deliverability. The first author to analytically describe the link between turbulent flow in the horizontal wellbore to the reservoir flow was Dikken (1990), using material balance equations. His analytical model assumed single-phase pressure drop in the well under steady state conditions. In the analytical approach, he considered the horizontal well to have an infinite length, while in the numerical approach, a finite well length was considered. From his work, he drew the conclusion that beyond a certain well length, the frictional pressure losses will give rise to a constant oil production when increasing the well length.

A generalization of Dikken's work is completed by Novy (1995). He developed both single-phase oil and single-phase gas flow equations, using boundary value formulations and finite difference schemes for solving. Novy concluded that the frictional pressure loss is negligible in wells with short horizontal well lengths since the well then acts as a uniform pressure sink. On the other hand, friction often becomes important in long horizontal wells, as the drawdown is depleted by the frictional pressure loss.

When the flow turbulence in the wellbore is increased, the pressure loss due to friction increases. This is most likely caused by the inflow of fluids along the horizontal section (Brice & Miranda, 1992). Cho & Shah (2001) recommenced the work on Dikken's model and concluded that by neglecting frictional pressure losses in long horizontal wells, the oil production rate will be significantly overestimated. They further concluded that the frictional pressure losses were of less importance when considering low flow rates in horizontal wellbores, up to a critical well length.

When the near-wellbore area is damaged, an increased drawdown is required for a well to

produce a given rate. Despite that a positive skin value is not preferable, Dikken (1990) demonstrated that it reduces the frictional pressure loss when present in horizontal wells.

3.7 Reservoir Simulation

For a reservoir engineer, a reservoir simulator is one of the most powerful tools. The computer program is designed to model the flow of fluids through a reservoir (Fanchi, 2006, p. 1).

3.7.1 Multisegment wells with Inflow Control Devices

For solving complex simulation cases, robust reservoir models must be made. Thus, an extra option is to construct a multisegment well to account for the frictional pressure effects in horizontal wells. This can be done by dividing the reservoir section of the well into multiple contiguous segments (Youngs et al., 2010). The lateral part of the reservoir can exhibit heterogeneities and permeability contrasts, and thus, segmentation becomes essential (Abbasy et al., 2010).

Each segment consists of a node and a flow path (**Figure 3.9**); At the segment node, the variables are calculated and by the flow paths, the connectivity between the segments are indicated (Youngs et al., 2010). Hence, a multisegment well provides a comprehensive description of the wellbore fluid flow (Schlumberger, 2014). In a Black Oil model with three phases, there are four equations per segment; Three material balance equations and one pressure drop equation. Hydrostatic, acceleration and friction effects are defined by the pressure drop equation (Youngs et al., 2010). Combined, the equations can solve for four variables per segment; Fluid pressure, total flow rate and the flowing fractions of water and gas (Schlumberger, 2014).

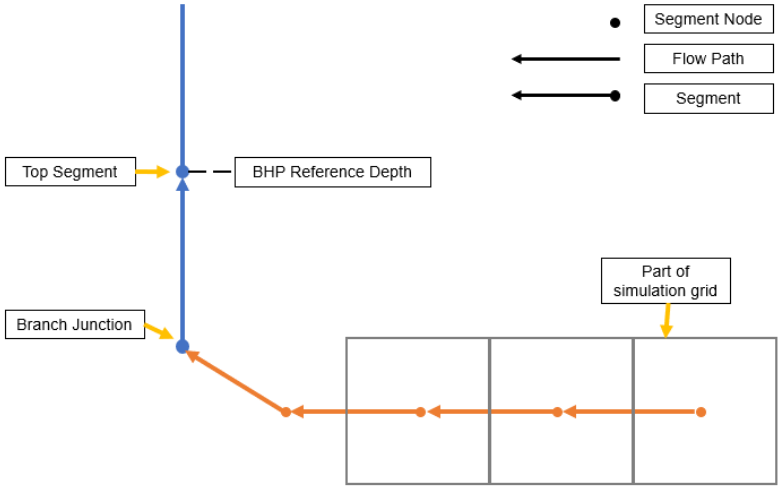

Figure 3.9: Illustration of the concept of a multisegment well (Figure made with inspiration from (Bao, 2016)).

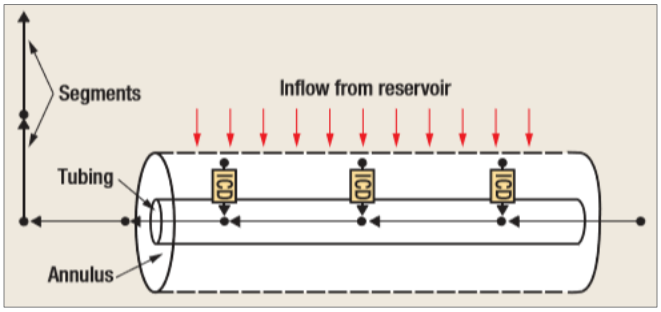

Figure 3.10: Multisegment model, equipped with ICDs.

Some of the many advantages with multisegment well models over the simple reservoir models are that multilateral branches can be evaluated and that changes in fluid phases can be accounted for, in addition to crossflow between segments. This makes it possible to model the downhole devices, within a high level of detail (Youngs et al., 2010).

When the completion is equipped with ICDs, they can be represented by discrete segments, such that it is possible to model their effect on flow. The ICDs are modeled perpendicular to the tubing segments and designed as short segments (**Figure 3.10**). When each ICD is isolated by a packer, it can be defined as individual segments. On the other hand, when there are multiple ICDs between packers, as in the Maria producers, they cannot be modeled individually. This can be explained by potential interaction between the ICDs and hence, they must be modeled by a combined segment. Thee flow through this combined segment is a result of the sum of flow rate from all the segment's ICDs. This implies that the ICDs must be identical (Youngs et al., 2010).

3.7.2 Local Grid Refinement

Local Grid Refinement (LGR) allows areas requiring a higher level of simulation accuracy to have an enhanced grid definition. It can be reasonable to use in areas near wells or of complex geology. In comparison to the global model, the local model can be defined to have a greater number of layers. The parent block properties are transferred to the refined blocks if nothing else is specified. This is usually sufficient for wellbore refinement. Otherwise, the property values must be explicitly specified. The transmissibilities are automatically computed by the ECLIPSE simulator between the local and the global model (Schlumberger, 2014). A local refined grid system provides a reduction in the computational time compared to a fine grid system. Additionally, the accuracy of the local grid is significantly improved over the coarse grid results (Gourley & Ertekin, 1997).

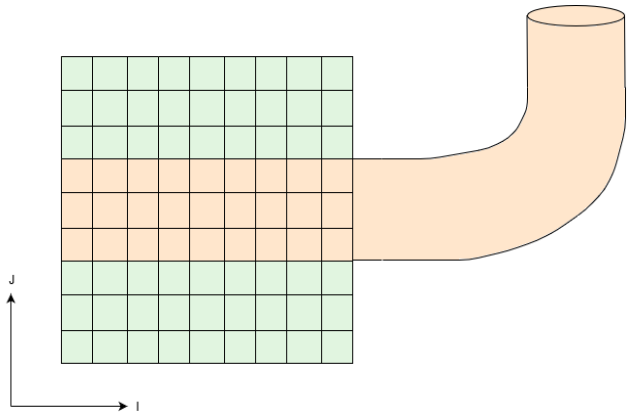

Figure 3.11: Example of a cartesian LGR in 2D, where the wellbore and well connection blocks are refined three times, in x- and y-direction.

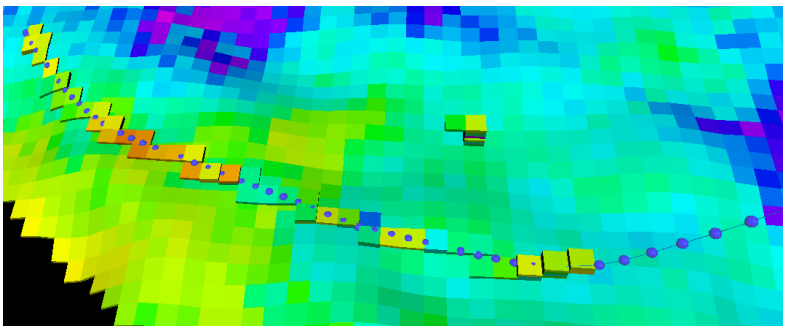

Figure 3.12: Illustrates a well trajectory crossing different grid blocks.

In reality, deviated and horizontal wells are crossing different grid blocks through the reservoir (**Figure 3.12**). As a solution to this, it is possible to amalgamate multiple local grid refinements into a single entity. Hence, a smaller number of refinements can be made along the wellbore in a zigzag pattern, to reduce the number of

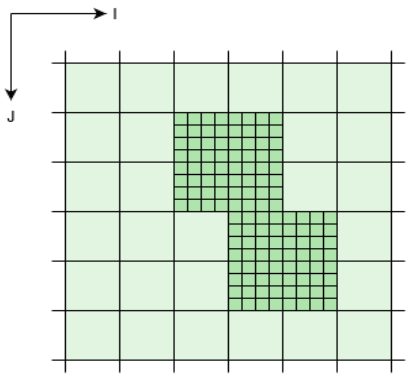

Figure 3.13: Two amalgamated refinements.

local cells and consequently, the simulation time (Schlumberger, 2014). An example of two amalgamated refinements can be seen in **Figure 3.13**.

3.7.3 Simulation Programs

3.7.3.1 ECLIPSE

ECLIPSE is the reservoir simulation software used in this project, originally developed by ECL and currently owned, marketed and further developed by Schlumberger (SERINTEL, 2017). Over 25 years, ECLIPSE has been the benchmark for commercial reservoir simulation, due to its robustness, speed and comprehensive capabilities. It can be used to model any type of reservoirs and covers all the reservoir models, while providing fast and accurate predictions of the reservoir's dynamic behavior (Schlumberger, 2018). There are several model formulations for the reservoir simulators, classified according to the system they are designed to simulate (Kleppe, 2007). The two main versions of ECLIPSE are:

- ECLIPSE 100
- ECLIPSE 300

ECLIPSE 100 is used to solve Black Oil equations and ECLIPSE 300 Compositional equations (Schlumberger, 2014). The Black Oil model is most commonly used in the petroleum industry and it is the model to be used in the simulation study in this thesis. Black Oil simulators solve multiphase, multidimensional fluid flow equations, where the properties are mainly dependent on pressure (Fanchi, 2006, p. 144).

3.7.3.2 Petrel

Another software program used in this project is Petrel – Petrel is a Schlumberger product, founded in 1996 and commercially released in 1998. The software can be used to create geological 3D reservoir models. It is a shared earth software, compatible with ECLIPSE and hence, provides the user with flexibility when adjusting and updating the reservoir simulation model. The software is used to visualize the simulation grid and to view the development of static and dynamic properties over the field's life time (Schlumberger, n.d.).

4 Inflow Tracer Technology in Maria Producers

The Inflow Tracer Technology can be used in complex subsea projects, along with long production tie-backs, which is the case for Maria, causing no extra risk to the operations (Siddiqui et al., 2017). For each Maria producer, the tracer carriers are installed adjacent to the ICD sandscreen completions, constructed on unperforated pipes (**Figure 4.1)**. This requires no changes to the design, as the sandscreen design includes spaces, where the tracers are placed. The inflowing fluids from the reservoir, contact the tracer system in the annular and tracer molecules are released. Together, it flows through the mesh grid in the sandscreens, through the ICD, then into the tubing (**Figure 4.1**) (Anopov et al., 2018).

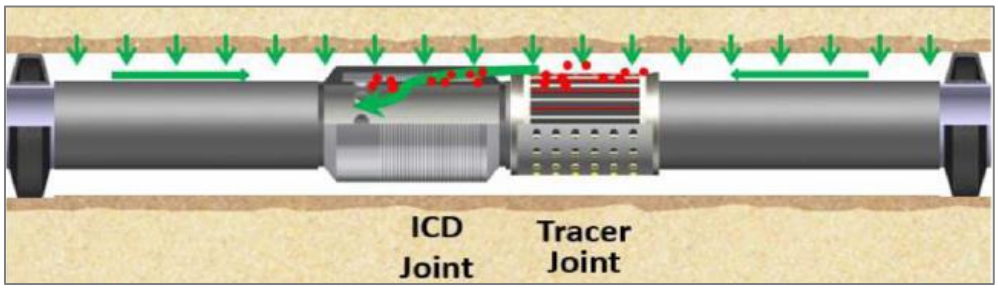

Figure 4.1: Tracer joint installed adjacent to an ICD joint in one compartment and the transportation path of the released tracer molecules (Anopov et al., 2018).

The tracer system is particularly designed for Maria, based on the field's reservoir parameters. The maximum flow rate of oil at sampling point at the host platform is 6500 Sm^3/day and water 1000 Sm^3/day. Low Solid Oil-Based Mud (LSOBM) is used as completion fluid. Of the total 160 unique chemical signatures, 40 oil tracers and 40 water tracers are qualified to be used for the Maria reservoir. The oil-soluble tracers have a 5 years' lifetime, while the water-soluble tracers 2,5 years, including well shut-in times. The tracer carriers are vented outwards (Mehdiyev, 2018).

Depending on the horizontal section length of the Maria wells, the section is segmented into seven to ten production zones. The tracer joints length varies from each producer, with an average length of 30 m from all the Maria joints. They are placed every 200 to 300 m in the reservoir, i.e. one tracer carrier represents the inflow from 200 to 300 m of the reservoir section. Each of the Maria tracer joints contains one OS and one WS tracer system

(Mehdiyev, 2018). As the Maria field is in an early phase of production, water breakthrough has not occurred in any of the wells. Hence, the water-soluble tracers remain dormant until contacted by water.

The initial clean-up of the Maria producers was performed at separate times. Hence, production fluid samples from each well were collected and analyzes for unique tracers, individually. However, after six months of production, all the field producers were shut-in simultaneously, such that when the production was restarted, commingled flow from all the wells were present at the sampling point. The best performing producers were restarted first, then the less performing producers came along. This was done to avoid disturbances in the fluid samples. Thus, all the unique tracer concentrations, representing one specific zone in one producer, are analyzed.

4.1 Interpreted Tracer Inflow Profile for Producer H-4

The Maria producer of major focus in this thesis is well H-4. It has seven tracer segments, where each joint has a length between 3 to 63 m and an average length of 20 m. Each tracer joint is representing the inflow from an average length of 239 m of the reservoir section. The tracer response was interpreted for quantification of the zonal inflow contribution, by RESMAN, at two well events; 1) The first well clean-up and 2) shut-in/restart of the well, after approximately six months of production. The inflow percentage profile along the horizontal section of H-4 for clean-up and restart, are presented in **Figure 4.2**. The measured data were of good quality.

During the first clean-up, all seven oil tracers were detected in the analysis, indicating that all zones were contributing to inflow. The expected heel-to-toe trend is observed, where the heel shows high contribution and decreasing towards the toe. The results after the well were shut-in for approximately two days and then restarted, after six months of production, shows a different profile; Extremely low tracer signals from the heel, OS-7 and OS-6. Both zone OS-7 and OS-1 were not qualified for inflow quantification. Therefore, as only low amounts of the tracers were detected, the zonal percentage contribution was estimated. No tracers were detected from OS-6. This gives rise to the question; Why is the heel not contributing to oil inflow anymore?

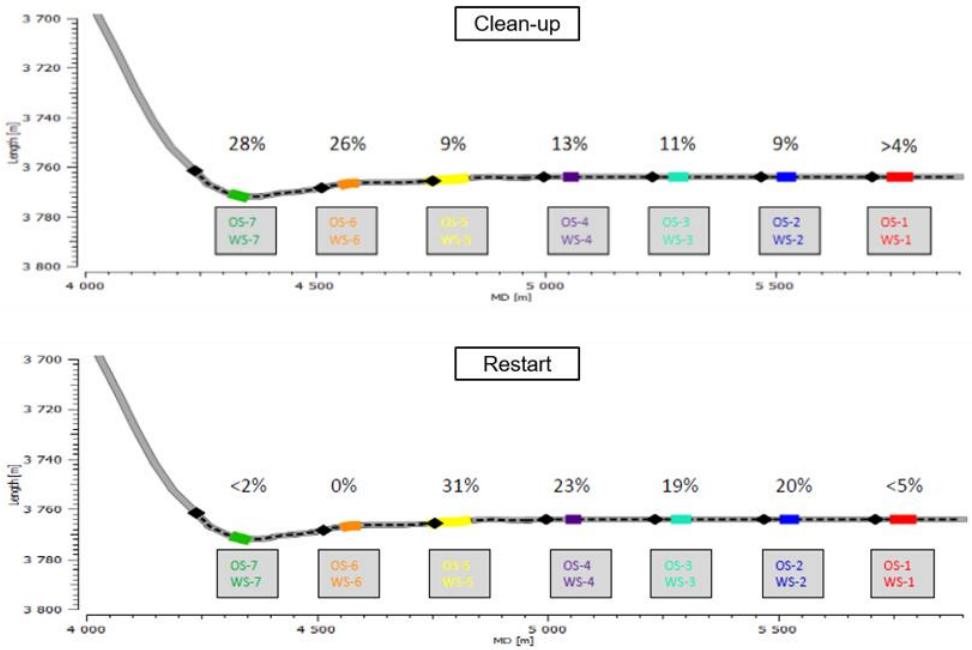

Figure 4.2: Quantitative inflow contribution along the horizontal section during clean-up and restart of well H-4.

The overall permeability of the formation is considered to be a static property, i.e. not expected to vary over time. The interpreted inflow profile (**Figure 4.2**) would indicate that something has changed in the reservoir after the tracer inflow from clean-up were interpreted. A potential reason for the heel of the well being unproductive after restart, could be due to severe skin damage of the near-wellbore formation, causing a reduction in the permeability of the given area. Another possible explanation could be due to mechanical related well issues, leaving zone OS-7 and 6 shut-in. This means that the well connections are closed off.

According to the RESMAN Interpretation Summary Report for the Maria field (Mehdiyev, 2018) from the clean-up and restart sampling, some general factors that can cause uncertainties in the tracer responses are for instance related to filter cake, ongoing clean-up, short shut-in times and choke openings. When the filter cake present in the given zone suddenly breaks, it will arrive at the surface fast, but it will start producing later than anticipated, compared to neighboring zones. Thus, the tracer decay and results in tracer signals will be affected, indicating a higher zonal inflow that it actually is. Moreover, choke openings can result in late arrival of the tracer peaks.

5 Description of Maria Base Case Model

This chapter describes the Base Case of the Maria-P50-Model, considered to be the reference case in this study, which is a full field reservoir model, provided by WINO. It is a Black Oil model, where the P50-approach is used as a good middle estimate. There are three phases present in the model; Oil, gas and water. In addition, the oil phase can contain some dissolved gas. This dynamic model has been updated according to a geological model and well test data. The model stretches over roughly 12 000 m from North-West to South-East direction. **Figure 5.1** shows the full field model map view of the upper layer. The simulated field is divided into a grid with 68 blocks in the x-direction, 239 in y-direction and 60 in z-direction. The mean dimensions of the cells in x-direction are 49 m, y-direction 50 m and z-direction 1,6 m. Furthermore, the Base Case gives an Original Oil In Place (OOIP) of 36.2 MSm^3 and a pore volume of 243.9 MRm^3.

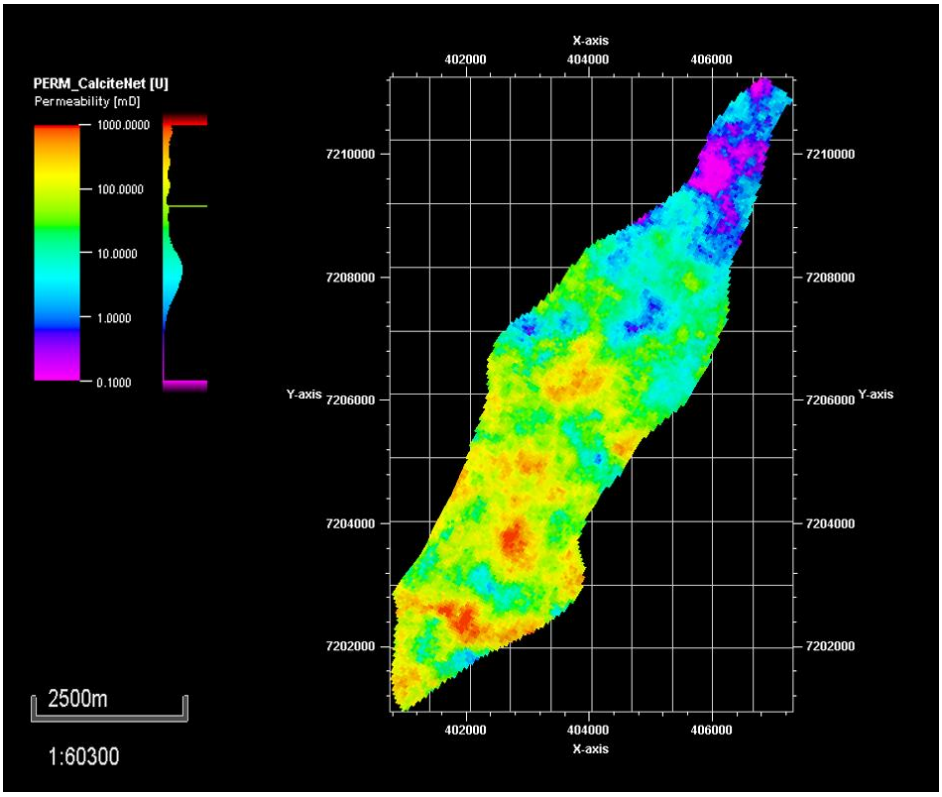

Figure 5.1: 2D illustration of the Maria full field model, coloured by permeability values, along k-layer 1.

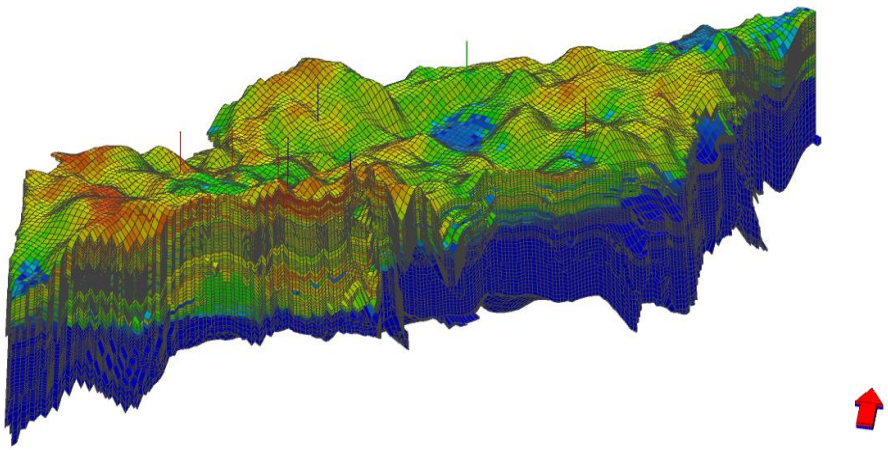

Figure 5.2: Visualization of the Maria simulation grid.

Grid Characteristics	
Grid dimensions	68 x 239 x 60
Total grid cells	975 120
Active grid cells	470 560
Grid cell dimensions (Mean)	49 x 50 x 1.6 m

Table 5.1: Maria simulation grid characteristics.

Lithostratigraphy		Zonation	Maria-P50-Model, k-layers
Fangst Group	Garn	Garn 2D	1 - 10
		Silt Barrier	11
		Garn 2C	12 - 19
		Silt Barrier	20
		Garn 2B	21 - 31
		Silt Barrier	32
		Garn 2A	33 - 38
		Silt Barrier	39
		Garn 1B	40 - 47
		Garn 1A	48 - 55
	Not	Not	56 - 60

Table 5.2: Reservoir zonation's from top, corresponding grid layers in the Maria-P50-Model.

The silt layers, specified in **Table 5.2**, are acting as vertical barriers. Therefore, they are modeled as separate layers having different reservoir properties than the surrounding formation. W.r.t. communication and pressure support from the water injection wells, the vertical permeability is the property of greatest interest.

5.1 Model Wells and Production Network

Five horizontal producers and two slanted injectors are modeled in the full field model. The producers' horizontal sections are mainly placed in the upper part of the reservoir, in Garn 2D, from k-layer 1-10. Both H-1 and G-4 are dipping into the top of the Garn 2C formation, k-layers 12-13 over short intervals. December 15th 2017, the producers H-4 and H-1 were put on stream in the model and two weeks later, the two water injectors, H-3 and G-3, started injecting. The remaining three producers came online later.

	Producers					**Injectors**	
Property	**H-1**	**H-2**	**H-4**	**G-1**	**G-4**	**H-3**	**G-3**
Gauge Depths [mTVD]	3600	3602	3591	3592	3604	3698	3703
Well Length [mMD]	6668	6851	5918	7451	7424	4400	4512
Max Inclination [deg]	94	92	92	92	96	61	61
Horizontal Section, k-layers	1 - 12	1 - 3	2 - 8	2 - 9	3 - 13	40 - 57	40 - 56

Table 5.3: Properties of the field producers and injectors.

The model is controlled by a production network. Due to the complex structure of the Maria field, the production pipelines are split up to make it easier to quality assure the pressure drop calculations.

Up to this time, the Base Case model has been history matched against BHP, while the observed oil production rates are entered in the model. The observed rates for producers and injectors s are defined by the WCONHIST- and WCONINJH-keywords, respectively. The producers are controlled by the observed liquid rate, LRAT, such that the historical rate will always be reproduced. The injectors are controlled by the injection rate, RATE. As the observed flow rates and pressures change with time, the keywords have to be repeated at

every timestep. At date November 27th 2018, the simulation time has exceeded the history time and the well is converted into a "regular" well for the purpose of forecasting. This is done by re-specifying the wells with the keywords WCONPROD and WCONINJE, respectively for producers and injectors.

The obtained matches between Base Case and the production data for four of the Maria producers can be seen in **Figure 5.3** and **Figure 5.4**. From **Figure 5.3**, it can be observed some deviation in BHP from the historical data for some of the well's time periods. Nevertheless, the simulation model is following the trend of historical data.

Additionally, 12 VFP curves are specified in the model for the producers and two for the injectors, using the VFPPROD and VFPINJ respectively. In the producers' VFP tables, flow rate, Tubing Head Pressure (THP), water cut, Gas Oil Ratio (GOR) and lift gas injection rate values are defined, while in the injectors' VFP tables, flow rate, THP and BHP values are defined.

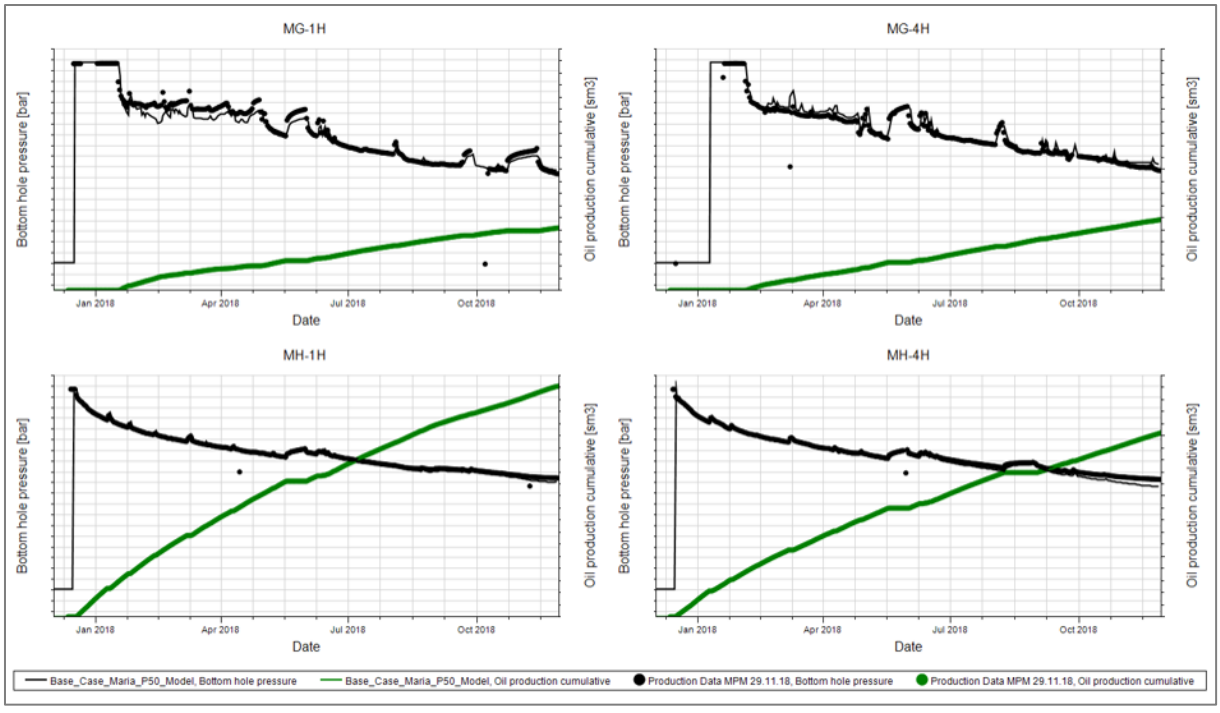

Figure 5.3: Maria-P50-Model BHP and cumulative oil production plotted together with the production data for four of the field's producers.

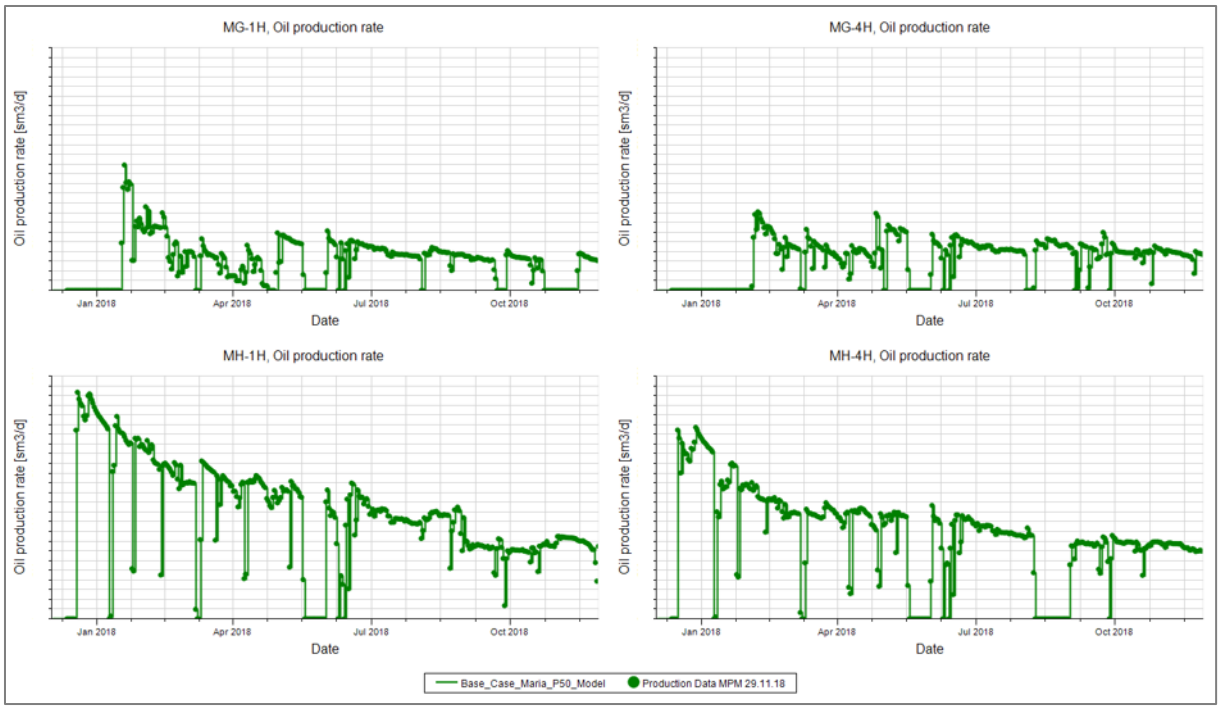

Figure 5.4: Maria-P50-Model oil production rate plotted together with production data for four of the field's producers.

5.2 Model Input Data

Some of the input reservoir and fluid parameters are presented in **Table 5.4**. To model the PVT data, the common Equation of State (EoS) model was made and the results were matched against the bottom hole samples from the Maria exploration and appraisal wells. The model was initialized to have two different PVT regions (PVTNUM), North and South, and five different equilibrium regions (EQLNUM) (**Figure 5.5**).

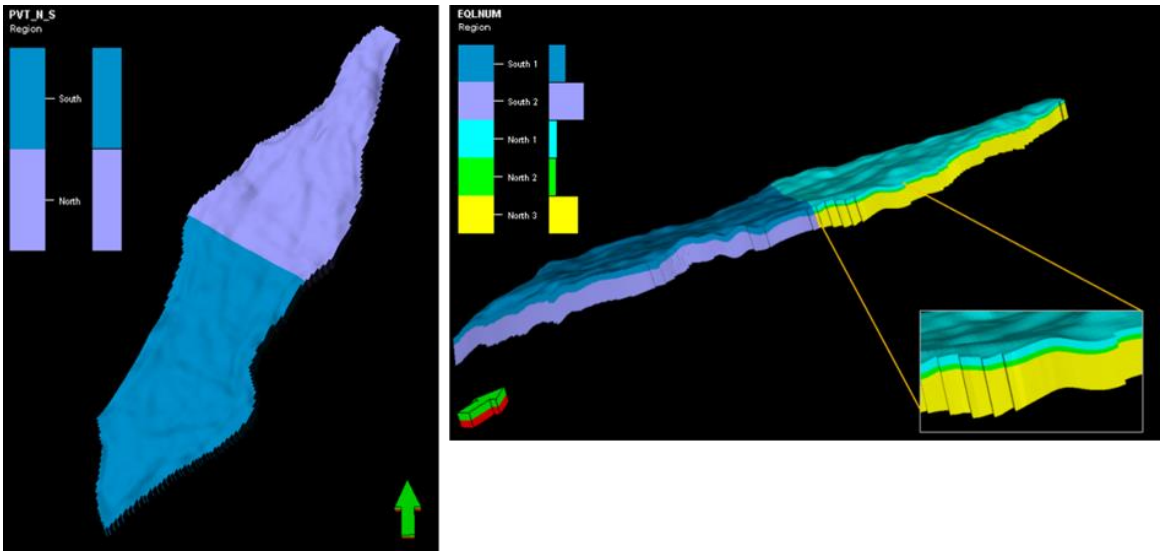

Figure 5.5: The two PVT regions and the five equilibrium regions of Base Case, respectively.

Base Case			
Property		**Value**	**Unit**
Oil Formation Volume Factor:	Southern Part:	1.50	Rm^3/Sm^3
	Northern Part:	1.46	
Water Formation Volume Factor at P_{ref}		1.05	Rm^3/Sm^3
Field Average Oil Viscosity		0.335	cP
Water Viscosity at T_{ref}		0.249	cP
Oil Density at Surface Conditions		831	kg/m^3
Water Density at Surface Conditions		1041	kg/m^3
Gas Density at Surface Conditions		1.04	kg/m^3
Dissolved Gas-Oil Ratio		30.6	Sm^3/Sm^3
Water Compressibility		$4.04 \cdot 10^{-5}$	1/bar
Rock Compressibility		$8.20 \cdot 10^{-5}$	1/bar

Table 5.4: Properties of the Maria Base Case.

5.3 Model Assumptions and Uncertainties

The greatest uncertainties in the Maria Base Case model are related to the Stock Tank Oil Originally In Place (STOOIP) and permeability. Additional assumptions and uncertainties of the model are presented in the following;

- No formation damage is modeled, through a skin value of zero for all the production wells.
- The model assumes anisotropic permeability, as the vertical and horizontal permeabilities, k_v and k_h, respectively, are different. The k_v/k_h-relation are very important in horizontal wells, where the reservoir heterogeneity cannot be neglected. The silt layers are modeled explicitly due to their effect on the vertical communication. Thus, the permeability in z-direction is modeled explicitly and not scaled by permeability in x- and y-direction. The horizontal permeability, i.e. permeability in x- and y-direction, are assumed to be equal in the model. This is a common and consistent assumption, as the Maria reservoir is considered to be relatively homogeneous in the x- and y-direction.

- Faults are predicted to be present from seismic interpretation, but none are detected this far. Therefore, no faults are included in the current reservoir model, which fits observed pressure communication between the production wells in Garn 2D.
- Due to no specification in the reservoir model, ECLIPSE treats all connection blocks along the entire well section to be perforations. The model does not contain a detailed modeling of the ICDs, due to little pressure drop across the ICDs. Thus, modeling the ICDs are expected to give no/very little impact on the results. Moreover, it will give a significant increase in the simulation time.
- The wellbore flowing pressure of the model is assumed to be constant over the horizontal well length. This implies that the pressure drop of the wellbore is neglected, as it is of small value compared to other pressure drops in the system. It could potentially cause errors in the well performance predictions and in the reservoir drainage pattern. For the Maria wells, this is considered to be a consistent assumption as the wellbore pressure losses along the horizontal length are small.
- Assume that no flow occurs at the boundaries of the model.
- The calculation of the J-functions is more uncertain than usual, as all Mercury Injection Capillary Pressure (MICP) measurements are made on endtrims. This is due to the permeability being calculated based on a correlation and not measured as if a plug sample is used. Consequently, this affects the saturation and hence the STOOIP.

5.4 Model Mechanisms and Uncertainties

In this subsection, mechanisms that are modeled in the Maria Base Case will be presented. As the model contains grid blocks of roughly 50 m in x- and y-direction, there could be uncertainties related to details of modeling the highly complex reservoir flow. One single value for each property and grid block is computed. The main uncertainties in the model are related to the geological and static properties of the reservoir. The Maria reservoir are considered to be relatively homogeneous, overall. As the Maria horizontal producers are of long lengths, they have a greater contact between the reservoir and wellbore, thereby increasing the probability of encountering heterogeneity. All the model producers are mainly located in the Garn 2D formation, which tend to be more or less heterogeneous compared to the underlaying formations. Hence, properties such as permeability, porosity and grain size vary locally. The distribution of permeability and porosity for the subdivision of Garn 2 can

be seen in **Figure 5.6** and **Figure 5.7**, respectively. Hence, a heterogeneity effect is present. It can have a dominating effect on how fluid flows through the reservoir.

The Maria drive mechanism is water injection for pressure support. There are no natural water drive taking place as the aquifer is too small. As of today, no water breakthrough is observed in the producers and strong pressure support is not part of the initial history matching of the tracer response. Therefore, the field producers are undergoing primary depletion. The model is set-up for water-flood pressure support, including multi-phase flow effects, but it is not a main consideration of this study. With the water drive not working fully, solution gas drive is supporting the production. As the reservoir oil is undersaturated, i.e. the reservoir pressure is above bubble point pressure, all gas is dissolved in the oil, and the oil expands due to compressibility, also referred to as an oil compressibility drive (Owusu et al., 2013).

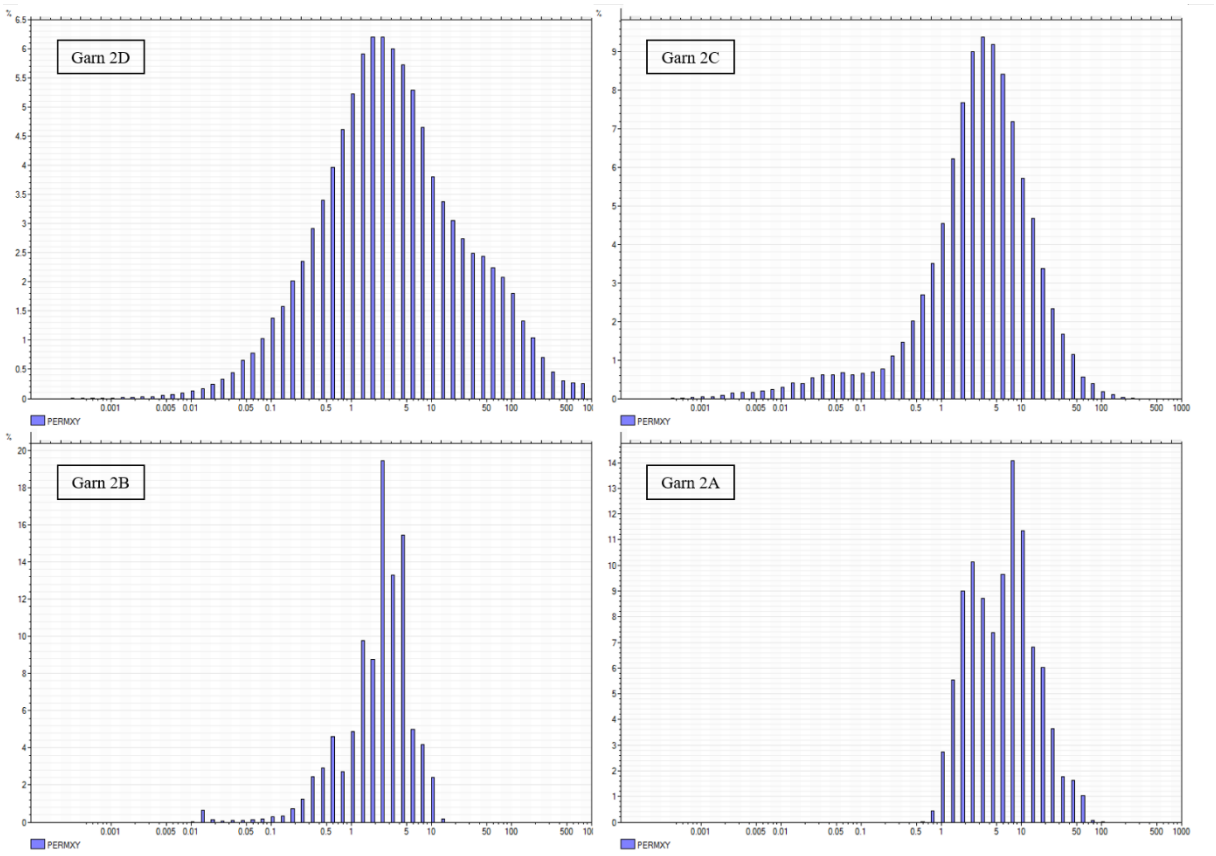

Figure 5.6: Permeability distribution in the sublayers of Garn 2, on a log-scale.

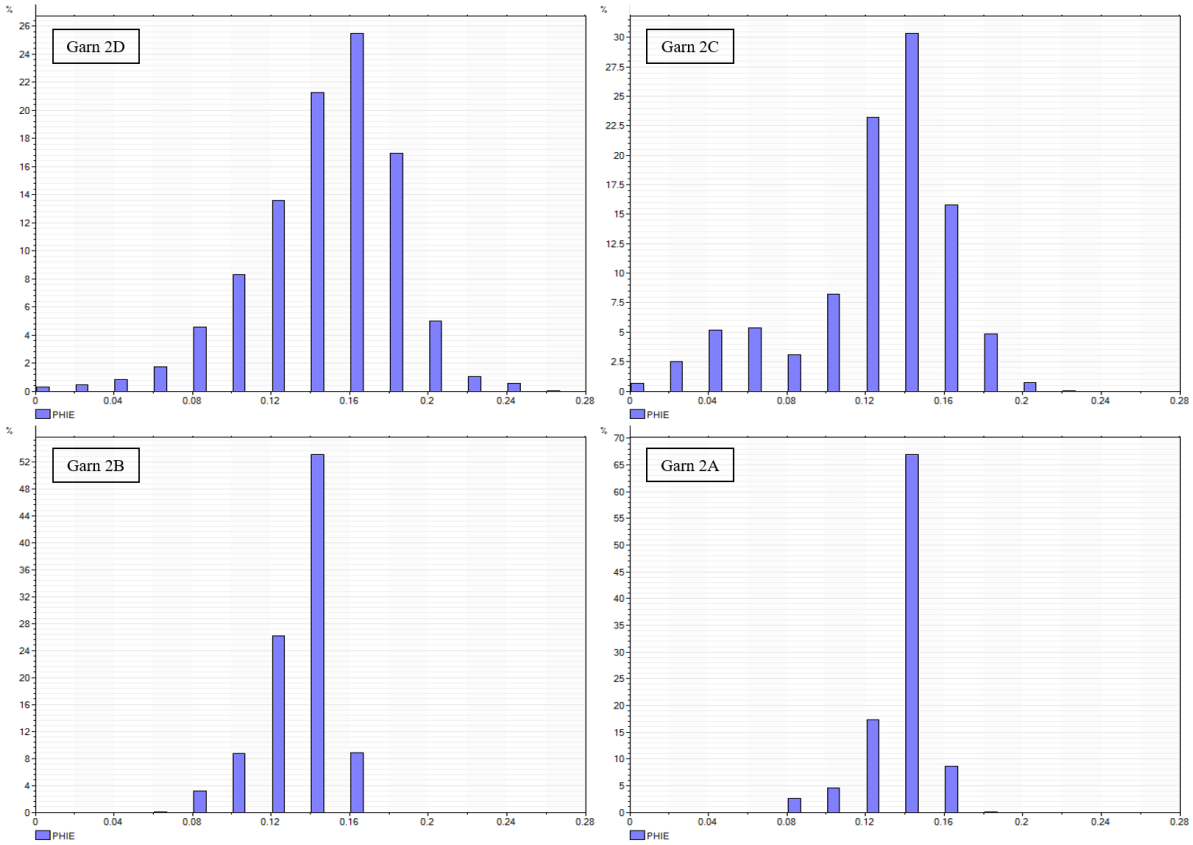

Figure 5.7: Porosity distribution in the sublayers of Garn 2.

6 Method

In the Result-section, I will review previous work on tracer analysis of the Maria field, performed by RESMAN (**Section 4.1**). Thereby, I will use the results to interpret the inflow from the reservoir along the horizontal section of Maria producer H-4.

Various parameters in the Maria-P50 reservoir model will be tuned for the purpose of matching the analyzed tracer inflow profile. As the interpreted inflow contributions from tracers are used as matching parameters, they are not directly implemented into the model. Hence, advection, dispersion and molecular diffusion mechanisms are not included in the reservoir model. The simulated inflow oil production rate results are extracted from Petrel into Excel, where the respective results are plotted and matched. Manual history matching is performed in this thesis.

6.1 Implementation of Interpreted Tracer Inflow Profiles

First and foremost, to be able to history match the zonal oil rate towards the interpreted inflow tracer profile, the reservoir model has to output the inflow rate profiles along the horizontal well section. To obtain this, the WRFTPLT-keyword is included in the SCHEDULE-section in the existing Maria simulation model; To request output of the PLT data for the current time step and all subsequent timesteps. The PLT provides output data for oil, gas and water rate, pressure, connection transmissibility factor, flow capacity and tubing flows, for each grid block having a connection to the well. The PLT oil rate is used to match against the interpreted inflow profile. The keyword is defined in the following way:

```
WRFTPLT
-- Well      RFT          PLT          Segment
-- Name      Data         Data         Data
H-4          NO           TIMESTEP     NO        /
/
```

In addition, the frequency of outputting the Restart-files is set to 10 000, i.e. every 10 000 report steps a file is created.

The inflow contribution of producer H-4 has been interpreted at two events; Well clean-up

and restart. The well clean-up was made to the drilling rig prior to production start. Therefore, the first date of production, 17th December 2017, is used as the corresponding date for the clean-up results. The well oil production rate for clean-up is around 2000 Sm^3/day. During shut-in and restart of the well, production curtailment 2nd June 2018, 17:00hrs, disturbed all the tracer's stability. Therefore, the date of restart when the well has stabilized is considered to be 3rd June 2018. The well oil production rate for restart has declined compared to clean-up rates, around 1200 Sm^3/day. These two events will be modeled in this thesis.

As the numerical interpreted tracer inflow from RESMAN is given as the zonal percentage of contribution, the inflow rate profile is calculated by multiplying it with the cumulative inflow rates for the corresponding date, acquired from production data. Moreover, the Maria numerical interpreted inflow profile for producer H-4, from clean-ups and restarts, was implemented into Petrel. This step is not of importance to perform this study, but a good way to clarify the chosen methodology. The MD placement of the tracer carriers, the zonal inflow percentage and rate profile, for producer H-4, were manually converted into a Petrel-readable format. It was further imported into the given software and plotted in a well section log.

The interpreted inflow rate profiles from tracers during clean-up and restart can be presented in well section logs, in Sm^3/day, together with the simulated PLT oil rate for each well connection (**Figure 6.1)**. A well connection is defined to be where the wellbore and the single grid block is communicating. In the well section log, the distance between the two dots are representing the tracer carrier length, where the carrier at shallowest MD correspond to the carrier of the heel; Black, with grey curve-filling, for clean-up data and white, with blue curve-filling, for restart. The first well track shows the formation layering, followed by the simulated PLT flow capacity, kh, colored red, and PLT oil rate for each connection, in green. Throughout this thesis, kh is defined as permeability times the horizontal well length, rather than the vertical formation height. The inflow percentage of the clean-up and restart are placed in the final track.

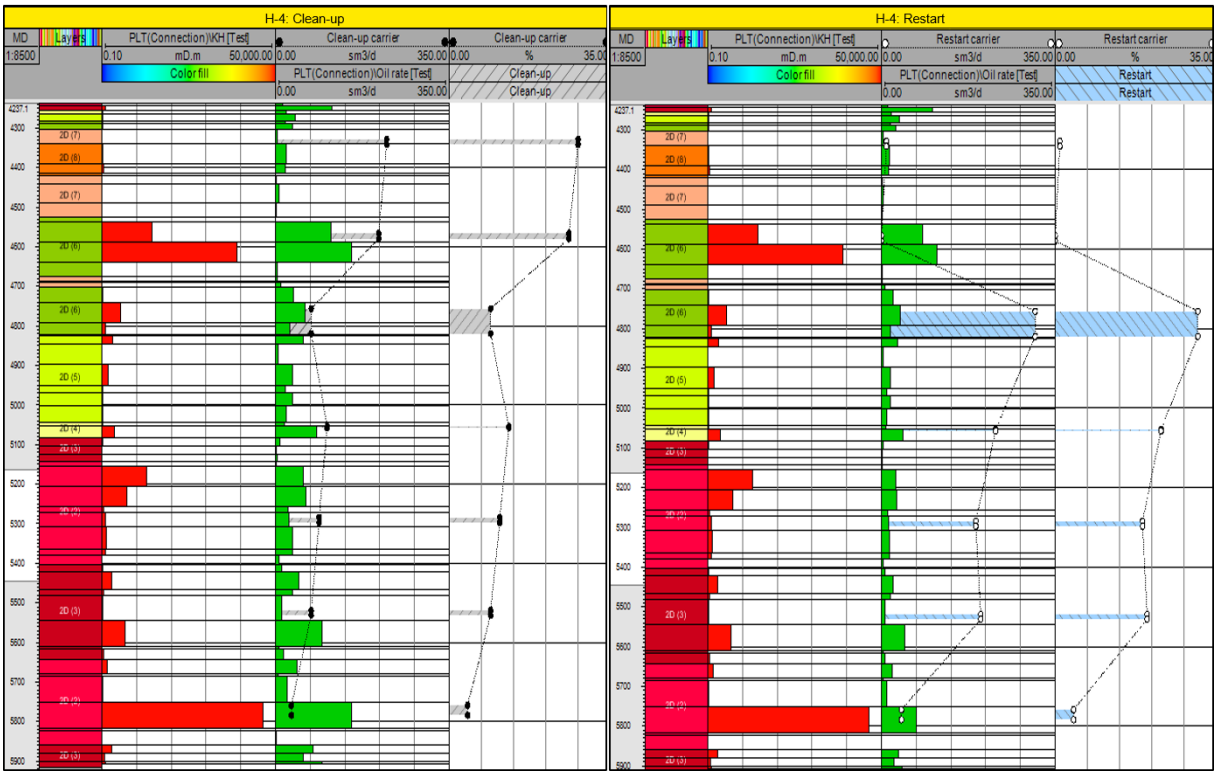

Figure 6.1: Well section log for the date of clean-up and restart, for Maria Base Case.

Furthermore, as mentioned in the introduction to this chapter, the interpreted inflow tracer data are not directly implemented into the model by following the specified procedure. Therefore, the history matching process is manually performed in Excel. The interpreted inflow profile obtained from tracers, for both clean-up and restart, are plotted; Cumulative oil rate plotted against the MD of the horizontal well section, for the respective events. The simulation cases are either adjusted in Petrel or ECLIPSE, and then run in Petrel. The PLT oil rate from the simulated case is extracted for the specific dates of clean-up and restart, into Excel. This extracted property presents the oil rate distribution along the MD of the horizontal section. As the tracers only generate one inflow oil rate value per tracer zone, i.e. one tracer carrier represents a specified amount of the surrounding formation, the simulated oil rate must be presented accordingly. Therefore, the simulated oil rates for each connection are added up to represent the surrounding formation, specified by the top and bottom formation depth of the numerical tracer data. Thus, the added zonal inflow data are plotted accordingly in the corresponding cumulative oil production rate plots in Excel, for the respective events, clean-up and restart.

The history matching process begins by altering properties in the Maria reservoir model and running the new simulation case, before extracting the simulated PLT oil rate distribution into Excel, repeating the same procedure as already explained. The process is continued in steps until a good match of the simulated inflow profile is obtained against the interpreted tracer inflow profile, for both events. In the Result section, the interpreted inflow contribution obtained from tracers will predominantly be considered as the correct representation of the well performance. Nevertheless, in the Discussion section, uncertainties related to the interpretation analysis of the chemical tracers, in addition to the reliability of the tracers in general, will be presented and put questions to.

6.2 History Matching Strategy

During history matching, modifications of parameters to improve the match can easily be made manually, directly into the ECLIPSE data file and then run in Petrel. Another method, offering more advanced options, is to update and run the model in Petrel. Petrel provides a visualization of the new field properties and thus, enables a better overview and consistency of the grid properties. Both methods are used in my project.

To select the tuning parameters is generally a difficult task in the history matching process. The parameters adjusted to match the inflow parameters from producer H-4 are listed below;

- Permeability in x- and y-direction (PERMX, PERMY)
- Porosity (PORO)
- Skin factor, i.e. reduced permeability in near-wellbore area

Another difficulty with the history matching process is that any modification on the parameters must be consistent and thus, lie within the range of values representing the Maria field. The main objective of the simulation process in this project is to match the simulated PLT oil production rate of the Maria-P50-Model against the interpreted inflow profile, to improve the history matching of producer H-4. Since the observed fluid production rates are already implemented into the Base Case model, using the WCONHIST-keyword in ECLIPSE, the well will roughly produce the correct amount of total fluid from the reservoir. Hence, the oil production rate match will not change when tuning matching parameters. This can be useful in the history matching process, where the BHP match is calculated,

accordingly. Thus, the BHP must also be matched for each tuning parameter.
The BHP values on the chart axes are anonymized due to restricted data. Thus, the BHP match quality are compared against the historical production data, either evaluated visually or as the relative percentage error, RELERR;

$$RELERR = \frac{P_{w,i} - P_w}{P_w} \cdot 100\% \qquad (6.1)$$

Where,

$P_{w,i}$ BHP of simulation case *i*

P_w Historical BHP

In the simulation process, two different areas, so-called bands, around the well will be considered; “Near-wellbore”-band and “Far from wellbore”-band (**Figure 6.2**). The area considered will be specified for each simulation case.

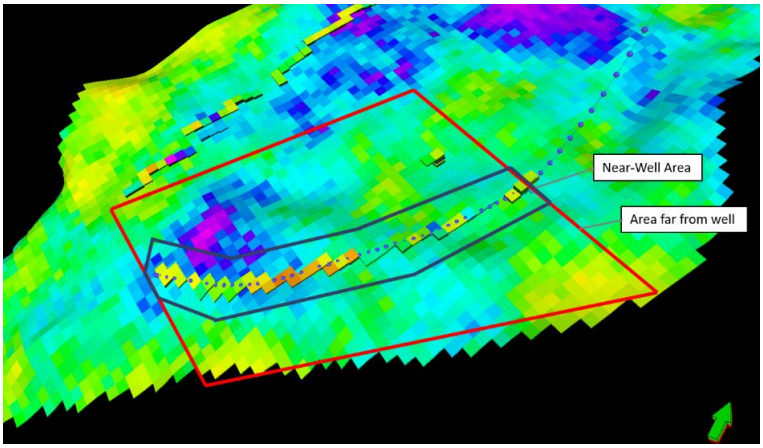

Figure 6.2: Illustration of the bands around the well, used in the simulation cases in the Result section.

A simplified model built in Excel and the reservoir model, Maria-P50-Model, are to be considered. Several case studies based on these models, for producer H-4, will be looked into and a short description of the different cases is presented in **Table 6.1** below. In the following sections, more detailed descriptions of the methodology for each simulation case are introduced.

The simulated PLT oil production rate will be presented in a plot of cumulative oil production

rate v.s. MD. Each simulation case will be compared to the interpreted inflow and inflow of Base Case, identified by blue and yellow lines, respectively, for all oil production rate plots.

Model	Case	Description
Simplified Model	**Case 1:** Simplified Model - Clean-up	Simulated oil rate match against interpreted inflow contribution from clean-up, using zonal permeability values calculated in the Simplified Model
	Case 2: Simplified Model - Restart	Simulated oil rate match against interpreted inflow contribution from restart, using zonal permeability values calculated in the Simplified Model
Reservoir Model	**Case 3:** Base Case	Initial simulated inflow profile match against interpreted inflow profile
	Case 4: Best History Match	
	→ **Case 4.1:** Match for Clean-up	Multipliers of PERMX, PERMY and PORO considered to obtain reservoir properties giving good match against interpreted inflow from clean-up and BHP, for area far from and near wellbore
	→ **Case 4.2:** Match for Restart	• Reservoir properties giving good match for oil production rate and BHP for clean-up, tested for restart • Severe positive skin and zones shut-in to obtain good match against interpreted inflow from restart and BHP
	Case 5: Multisegment Well	
	→ **Case 5.1:** Multisegment Well v.s. Non-Segmented Well	Comparison of simulated oil profile and BHP when well pressure drop is/not accounted for
Simplified Model & Reservoir Model	→ **Case 5.2:** Multisegment Well Model v.s. Simplified Model	Comparison of frictional pressure drop values in Multisegment Well Model and Simplified Model
	Case 6: Permeability Distribution	Comparison of the permeability distribution along the horizontal section in Simplified and Reservoir Model

Table 6.1: Short description of the case studies to look into in this thesis.

6.2.1 Simplified Model

6.2.1.1 Simplified Model Description

A simplified analytical model is created based on professor Rune Time's (2018) guideline for the well simulator problem. Simplification helps to extract essential trends to increase the understanding of the more complicated reservoir models. The model assumes single-phase flow in porous media, based on Darcy's law with radial geometry at steady state conditions. Furthermore, it is assumed to be uniform, with infinite reservoir boundaries, such that strong

boundary effects are not present. The case to be evaluated is when the well pressure, P_w, is greater than the bubble point pressure, P_b.

The main purpose of constructing this simplified model is to compute the zonal permeability distribution along the horizontal section of the wellbore, for the purpose of achieving a match to the interpreted inflow profile from tracers. The "Finite Difference Marching" method is used to calculate the pressure profile along a well consisting of a horizontal and vertical section. This implies that the well is divided into N imaginary segments, such that the flow is considered to go from one segment to the next. See **Figure 6.3** for illustration of the well segmentation. Since the segments are of short size, lengths between 200 to 280 m, the pressures are considered approximately constant from segment start to end. Additionally, by neglecting temperature effects, flow rates, pressure gradient and fluid data are considered constant along each segment. Hence, the fluid is considered to be incompressible. The reservoir is assumed to be layered, without any crossflow. In this Simplified Model, the reservoir pressure is assumed to be constant throughout the reservoir section. Two dates will be looked into in this model and hence, two reservoir pressure values are considered for the respective dates.

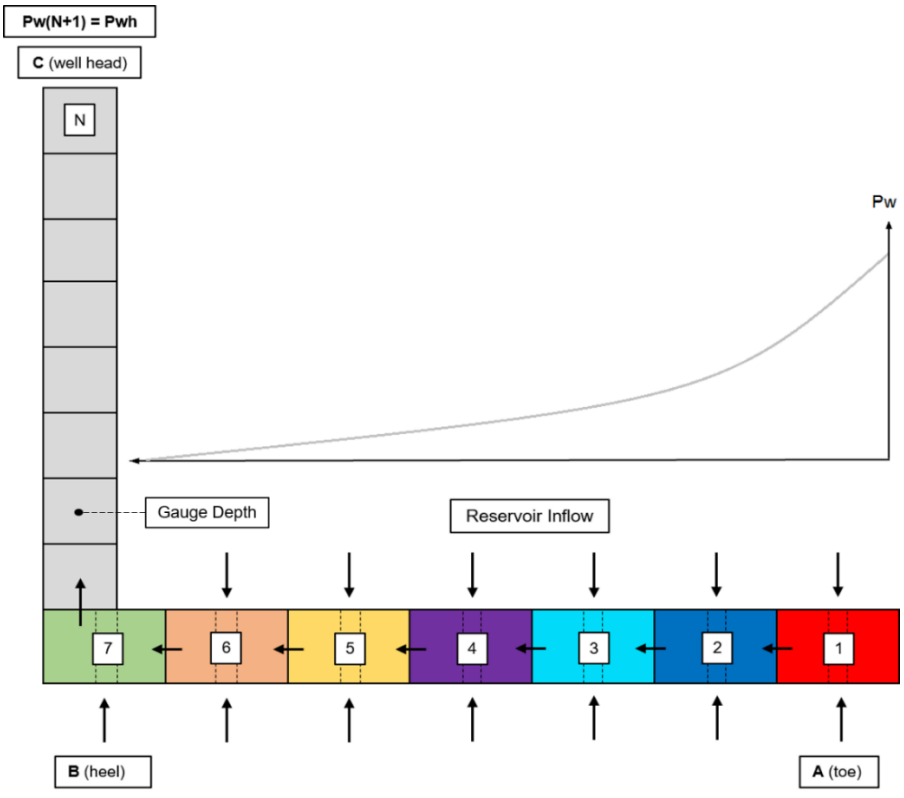

Figure 6.3: Well segmentation with the well pressure distribution plotted along the horizontal section, where the dotted lines are illustrating perforations.

The pressure at the toe, point A, $P_w(1) = P_A$, is given a "guessed" value, based on the well's production data, and eventually adjusted to match either the gauge pressure, P_{gauge}, or the well head pressure, P_{wh}. Based on these assumptions, the well pressure for the next segment, $P_w(i+1)$, can be calculated from the well pressure for segment i, $P_w(i)$, considering the total pressure loss, $\Delta l \cdot \frac{dP_w}{dl}$, by the equation:

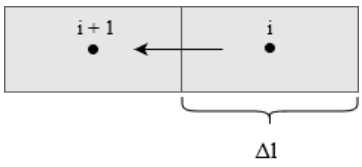

Figure 6.4: Flow from segment i to i + 1.

$$P_w(i+1) = P_w(i) + \Delta l \cdot \frac{dP_w}{dl}(l) \qquad (6.2)$$

Where,

Δl	Length of the segment, $\Delta l = l(i+1) - l(i)$ [m]
$\frac{dP_w}{dl}$	Total pressure gradient [bar/m]

The flow in the tubing is assumed to be turbulent, corresponding to a Reynold number greater than 4000. The friction factor, f, is a function of the Reynolds number, N_{Re}, tubing roughness, ε, and well diameter, D. The moody friction factor is considered in this simplified model. The Reynolds number relation is given by (Guo et al., 2007, p. 46);

$$N_{Re} = \frac{\rho \cdot v \cdot D}{\mu} \qquad (6.3)$$

Where,

ρ	Fluid density	[kg/m^3]
v	Fluid velocity	[m/s]
D	Well diameter	[m]
μ	Fluid viscosity	[cP]

The entire horizontal section is assumed to be at an average, constant depth of 3735 mTVDSS. Consequently, the hydrostatic pressure will remain constant throughout the horizontal section. For the horizontal section, there will only be frictional pressure drop varying from each segment. Pressure drop due to fluid acceleration is neglected as the tubing

diameter is assumed constant. Each segment in the horizontal section contains a perforation interval, such that the reservoir fluid flows into the well. In the vertical section, the hydrostatic pressure gradient becomes important. The MD is used to calculate frictional pressure loss in the vertical section, while the TVD for the hydrostatic pressure loss. Below, equations used to calculate the frictional, hydrostatic and total pressure gradient are given.

Frictional Pressure Gradient, $\left(\frac{dP_w}{dl}\right)_f$:

$$\left(\frac{dP_w}{dl}\right)_f = \frac{4}{D} \cdot f \cdot \frac{1}{2} \cdot \rho \cdot U^2 \qquad (6.4)$$

Where,

l	Running position along the well calculated from point A	[m]
f	Friction factor	[Dimensionless]
U	Flow velocity	[m/s]

Transforming the flow velocity into volumetric flow rate and by taking the unit conversion factor into account, the equation of the frictional pressure gradient becomes:

$$\left(\frac{dP_w}{dl}\right)_f = \frac{C_f \cdot f \cdot \rho \cdot Q^2}{D^5} \qquad (6.5)$$

Where,

Q	Cumulative volumetric flow rate along the well [Sm^3/day]
C_f	Unit conversion factor, values $4.34 \cdot 10^{-15}$

Hydrostatic Pressure Gradient, $\left(\frac{dP_w}{dl}\right)_h$:

$$\left(\frac{dP_w}{dl}\right)_h = \rho \cdot g \qquad (6.6)$$

Where,

g Gravity acceleration [m/s^2]

Total Pressure Gradient, $\frac{dP_w}{dl}$:

$$\frac{dP_w}{dl} = \left(\frac{dP_w}{dl}\right)_f + \left(\frac{dP_w}{dl}\right)_h \quad (6.7)$$

Ideally, the pressure at the outlet of the last well segment N at point C, $P_w(N+1)$, should be equal to the pressure at the well head, P_{wh};

$$P_w(N+1) = P_{wh} \quad (6.8)$$

There are several uncertainties related to this simplified procedure, as the well pressure is assumed to be greater than the bubble pressure throughout the entire well. In reality, the well pressure in the vertical section will decrease with decreasing depth and eventually, the well pressure will go below the bubble pressure. Hence, gas will boil out of the liquid, until phase equilibrium is obtained. Therefore, to avoid calculating the volumetric phase fractions and hence, the mixed fluid properties, an alternative approach is to use the measured pressure at the gauge depth to match against. Then there will be less uncertainty related to the assumption of the well pressure being higher than the bubble pressure. The match is obtained by modifying the guessed toe pressure, P_A, within given limits, such that the calculated pressure at the gauge depth corresponds to the measured gauge pressure.

When an acceptable low error in the well head pressure/gauge pressure is obtained, the pressure and velocity values are representative for the well flow. The error, ERR, in P_A, respectively, can be calculated by:

$$ERR = P_{wh} - P_w(N+1) = P_{wh} - P_{gauge} \quad (6.9)$$

By considering Darcy's law, describing the fluid's ability to flow through the porous media, an average permeability of each zone *i* can be calculated (**Equation (6.10)**). The equation is initially intended to be applicable for vertical wells, but it can be applied to horizontal wells by including the horizontal lengths, rather than the vertical height.

$$k_i = \frac{\mu_o \cdot B_o \cdot (ln\frac{r_e}{r_w}) \cdot Q_i}{c_f \cdot \Delta h_i \cdot (P_{res} - P_w^i)} \qquad (6.10)$$

Where,

k_i	Permeability for zone *i*	[mD]
B_o	Oil Formation Volume Factor	[Rm^3/Sm^3]
r_e	Drainage radius	[m]
r_w	Well radius	[m]
Q_i	Volumetric flow rate for zone *i*	[Sm^3/day]
Δh_i	Horizontal length of zone *i*	[m]
P_{res}	Reservoir pressure	[bar]
P_w^i	Well pressure for zone *i*	[bar]
c_f	Unit conversion factor, values $8.22 \cdot 10^{-3}$	

The parameters known in this analysis is the inflowing rate for each section, obtained from the tracer analysis, as well as the top pressure, i.e. the pressure at the well head or gauge pressure, the reservoir pressure, fluid data, well dimensions and the well trajectory depths (MD and TVD). In the horizontal section there are two main unknown parameters; The flowing well pressure along the well and the average permeability for each segment. There are also some uncertainties related to the friction factor and the drainage radius. The vertical section is treated as one segment and is not divided into smaller segment. This is considered to be a consistent assumption due to no perforations in the vertical section and hence, there is only flow along the well direction. Therefore, the well pressures are the only unknown values in the vertical section. Accordingly, the overall number of unknowns in this analysis with N_z segments is defined to be 2 N_z + 1 unknowns. For the horizontal section, N_z relations of Darcy's law are given, defined between the reservoir and the segments, and N_z pressure relations, defined between the segments. These relations include the frictional law as a function of rate. In the vertical section, there are no Darcy's law relations, but one pressure relation between the vertical and the top of the well. The vertical section can also be discretized as illustrated in **Figure 6.5**, where the segment pressure can be defined as the

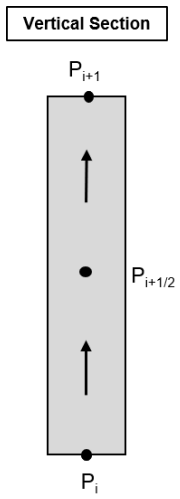

Figure 6.5: Discretization of vertical section.

average pressure, $P_{i+1/2}$, of the inlet and outlet pressure, P_i and P_{i+1}, respectively. The discretization method is not focused on in this thesis.

6.2.1.2 Case 1 and 2: Simplified Model – Clean-up and Restart

The length of the horizontal well segments is determined to be the exact same length as the zone that the tracers are representing of the formation (See **Table 11.1** in the Appendices for zone top and bottom depths). This is done for the model to be directly comparable with the interpreted inflow results, such that the inflow rate of each modeled section is given from the tracers. Using **Equation (6.10)**, the zonal permeability distribution of the reservoir from the Simplified Model is obtained. The calculated zonal permeability is used as the average for the corresponding zone and is specified into the ECLIPSE-file of the simulation Base Case, using the EQUALS-keyword in the GRID-section. The coordinates of each zones are specified, in addition to the permeability value. The permeability in both x- and y-direction, PERMX and PERMY, hereby referred to as PERMXY, are given the same values. The reservoir simulation model is further run in Petrel. Below, the keyword is specified for one of the zones;

```
EQUALS
-- Array      Array                    Coordinates
-- Name       Value        I1    I2    J1    J2    K1    K2
PERMX          100         1     30    55    61    1     10   /
PERMY          100         1     30    55    61    1     10   /
/
```

As the Maria production tubing roughness is not given, several tests have been made by adjusting the friction factor and the toe pressure in the Simplified Model in Excel, to obtain a calculated pressure equal to the measured gauge pressure, at gauge depth. The friction factor is assumed to be equal for the vertical and horizontal section, and for clean-up and restart. The properties of the incompressible fluid are taken to be the average value of the grid blocks around well H-4 and can be found in **Table 6.2,** in addition to the borehole radius;

Simplified Model – Input Data			
Property		**Value**	**Unit**
Oil Viscosity, μ_o		0.304	cP
Oil Density, ρ_o		639	kg/m^3
Oil Formation Volume Factor, B_o		1.50	Rm^3/Sm^3
Borehole Radius, r_w		0.0836	m
Drainage Radius, r_e		400	m
Gauge Depth		3591	mTVDSS
Gauge Pressure	Clean-up	373	bar
	Restart	253	bar
TVD of horizontal section		3735	mTVDSS

Table 6.2: Input data in Simplified Model.

For the pressure value of the toe to be within acceptable limits obtained from the clean-up and restart reports, the friction factor must be in the range of 0.0001 and 0.011. A friction factor exceeding the specified maximum value, results in the need of a higher pressure at the toe to approach the measured gauge pressure. Hence, a higher pressure of the toe than used for the maximum friction factor results in no pressure drawdown between the well toe and the reservoir. Likewise, for a friction factor lower than the minimum value specified, resulting in a too high pressure drawdown, according to the respective reports. Therefore, obtained permeability distribution from the two cases, minimum and maximum friction factor and their corresponding toe pressure, will be considered in the Result section, for both events, clean-up and restart, as the interpreted profiles are contrasting. Hence, Case 1 is defined to be the case study where the simulated oil production rate for the min and max friction factor are compared against the interpreted inflow from clean-up, while Case 2 is defined correspondingly but compared against the interpreted inflow from restart.

6.2.2 Reservoir Model

6.2.2.1 Case 3: Base Case

To begin with, the initial model, the Base Case of the Maria-P50-Model, is to be considered. The simulated PLT oil rate of the Base Case will be compared against the interpreted inflow

profile. Moreover, the initial BHP match will be presented.

The permeability distribution for the Base Case is to be obtained from the kh output data from the WRFTPLT output. The data will be extracted from Petrel into Excel and the connection's kh represented by the tracer zones will be added and further divided by the zone length. Hence, one average permeability value per tracer zone will be obtained.

6.2.2.2 Case 4: Best History Match

To pursue the best match between the simulated inflow and the interpreted inflow contribution for both clean-up and restart, they will be considered individually as the interpreted profiles are contrasting, Case 4.1 and 4.2, respectively.

Case 4.1: Match for Clean-up

The main strategy, to begin with, is to obtain a good match between the respective rates for clean-up to obtain an expected permeability distribution of the formation. This is done by adjusting the zonal multipliers of PERMXY, according to the ratios between the zonal rates. By using the multiplier application, the trends of the reservoir properties that are already captured in the Maria reservoir model when history matched against BHP and oil production rate is kept. This allows to adjust the values up and down and is an advantage, which might be lost when doing a fully manual history matching. The multiplier is specified in the following way using the ECLIPSE-keyword, MULTIPLY, in the GRID-section;

```
MULTIPLY
-- Array     Multiplication              Coordinates
-- Name      Constant      I1    I2     J1    J2    K1    K2
PERMX          2           1     34     23    69    1     10     /
PERMY          2           1     34     23    69    1     10     /
/
```

The first column specifies the property to be modified, followed by the multiplication constant. The i,j,k coordinates of the first and last blocks to be modified are specified, according to the chosen band (**Figure 6.2**).

When suitable zonal proportions between the PERMXY multipliers are found to match the interpreted clean-up profile within acceptable limits, the same zonal proportions are more or less multiplied up and down. Therefore, several values of the zonal multipliers will be considered in both the area far and near wellbore. The computed BHP for the simulation cases matching the inflow profile for clean-up are further matched against the historical BHP. If the matches for clean-up are showing poorer BHP matches than Base Case, multipliers of porosity, PORO, could be looked into.

Case 4.2: Match for Restart

Case 4.2.1: Clean-up Match for Restart

The reservoir properties, multipliers of PERMXY and PORO, corresponding to the Best Match for clean-up against the interpreted inflow profile from tracers and historical BHP, will be tested for the date of restart to see if it gives a correspondingly good match against the interpreted results for restart. If the resulting simulated oil rate match for restart are deviating from the interpreted contribution, other properties than permeability and porosity must have changed after clean-up was performed and thus, Case 4.2.2 to 4 will be looked into.

Case 4.2.2: Skin

By considering the reservoir properties of the Base Case, in addition to cases giving good match against interpreted inflow and BHP for clean-up, different cases of positive skin factors, up to a value of 150, are looked into.

To be able to add skin in the reservoir model, a new temporary simulation case must be run by specifying the value of skin for the given well, under the Completion Perforation Settings in Petrel. Hence, a corresponding simulation case must be run for all the different skin values to test. This has to be done to calculate the connection transmissibility factor for the given skin value. The resulting COMPDAT-keyword created in the SCHEDULE-section of the ECLIPSE-file, can be copied to the wanted simulation case.

Case 4.2.3: Shut-in of Zones OS-7 and 6

The connection of the specified zones can be shut-in column 6 of the COMPDAT-keyword for the respective date. No skin for the remaining producing zones is considered.

Case 4.2.4: Skin in OS-7 and Shut-in of OS-6

A study where increasing values of skin, from 30 to 150, are added to OS-7, while zone OS-6 is shut-in, is considered. For the remaining zones, a negative skin factor of 2 is added for all cases, for the permeability of the near-wellbore area to be improved and hence, expected to give a higher inflow.

Moreover, based on the different reservoir properties obtained for the various matches for clean-up are looked into to see which gives the best oil rate and BHP match for restart, for a given skin value of 70 in OS-7 and OS-6 shut-in.

6.2.2.3 Case 5: Multisegment Well

Case 5.1: Multisegment Well v.s. Non-Segmented Well

The well can be redefined to become a multisegment well, where the pressure losses in each segment of the horizontal section of the well are included. In the Base Case of the Maria-P50-Model, pressure losses in the well are neglected due to the assumption of constant wellbore flowing pressure. Therefore, the aim is to compare the simulated PLT oil rate and calculated BHP for the different cases and decide if the assumption made in the current Base Case model is consistent.

The well segmentation is performed using Petrel. The standard homogeneous flow model is considered, where the phases flow with the same velocity. Pressure drop due to fluid acceleration is not considered, only frictional and hydrostatic pressure drop. The BHP reference depth of the well is set equal to the depth of the well's top segment node. The wellbore is segmented up to this depth, which is at 3561 mTVDSS. Very large segments reduce the accuracy of pressure drop and fluid segregation calculations. Therefore, a simulation case with equal well segments of 50 m are tested, in addition to a case with 270 m segments. They are creating 35 and 8 segments, respectively, along the horizontal part of the wellbore. Another case, where the segments are of greatly varying size, using the Petrel

Segment Per Cell-option, are considered. This option ensures that each fluid entry to the wellbore is separately modeled and 64 segments are created.

When exporting the case from Petrel, the following ECLIPE-keywords are automatically generated from the defined data; In the Data-file the keyword WSEGDIMS appears and in the Schedule-file, WSEGITER, WELSEGS and COMPSEGS. The following keywords are manually specified in the Summary-section in ECLIPSE to output the data needed to compare with the Simplified Model and the tracer signals;

SPRD – Segment Pressure Drop
SPRDF – Segment Pressure Drop due to Friction
SPRDH – Segment Pressure Drop due to Hydrostatic

The reservoir model uses the Beggs & Brill flow correlation to calculate the pressure drop in a horizontal section, with a friction factor of 1. For the vertical section, the reservoir model uses a different correlation, Hagedom & Brown, and still maintaining a friction factor of 1.

Case 5.2: Multisegment Well Model v.s. Simplified Model

Another objective for redefining the well as a multisegment well is to compare the calculated friction and hydrostatic pressure loss of the segments against the calculated values obtained in the Simplified Model. Case 1 and 2B are to be considered. For the segments to be comparable with the Simplified Model, they are defined to have an equal length of 270 m. This divides the wellbore into eight segments, by which seven of them are placed in the horizontal section (**Figure 6.6**). This is done to segment the horizontal section in a similar way as the tracer carriers are representing the formation. The top and bottom measured depths of the segments are approximately equal

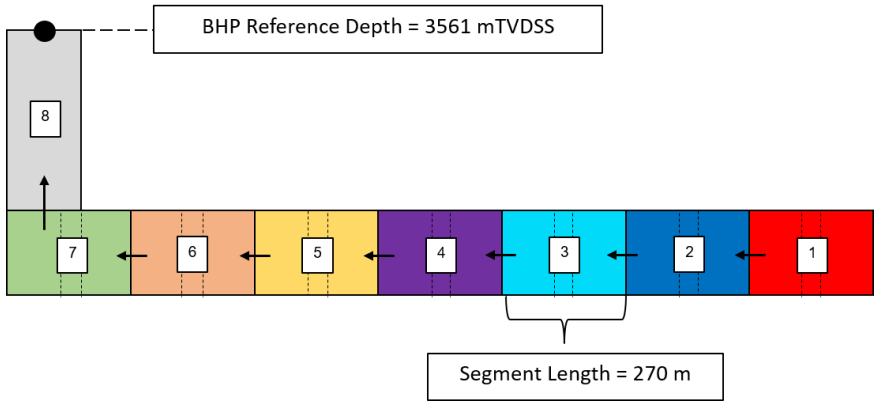

Figure 6.6: Illustration of the multisegment well.

to the top and bottom measured depth of the tracer zones.

6.2.3 Comparison of Simplified Model and Reservoir Model

6.2.3.1 Case 6: Permeability Distribution

The zonal permeability distribution of the Simplified Model, Case A and B, for both clean-up and restart, will be compared against the permeability distribution of the initial reservoir model, i.e. Base Case, and the simulation case showing the best oil rate match against the interpreted inflow profile from clean-up.

6.2.4 Local Grid Refinement

The well connection grid blocks of producer H-4 will be locally refined (**Figure 6.7**), by using the LGR feature in Petrel. This allows the grid resolution to be less than the physical displacement processes, causing numerical dispersion. The refinement of the wellbore grid is specified as N_x x N_y x N_z, defining the level of refinement in x-, y- and z-direction, respectively. To determine the optimal wellbore refinement of the model, a sensitivity analysis will be performed by varying the level of refinement. The levels will be increased from 3 to 9, resulting in the refined blocks having dimensions of around 16 to 5 m along x and y-direction. No refinement will be required in the z-direction, due to the initial grid blocks being sufficiently refined with a length of 1.6 m, i.e. $N_z = 1$. The runs to be used in this sensitivity analysis of refined wellbore is to be found in **Table 6.3** below. The refined grid blocks will be assigned the same value as the parent grid blocks in the global grid.

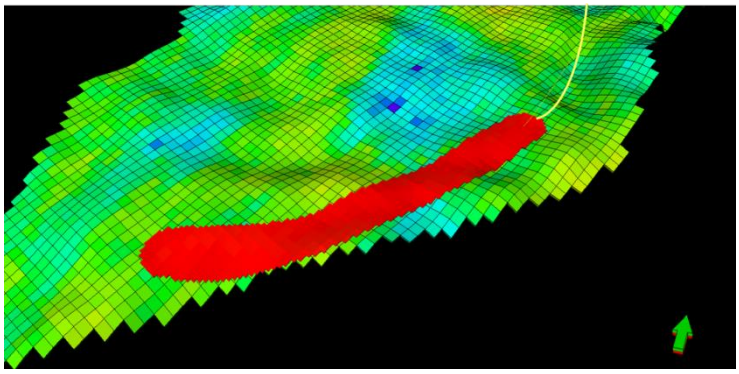

Figure 6.7: Local refined grid around producer H-4.

The case of the optimal refinement should show minor changes in the oil production rate and BHP, comparing to finer grid blocks, in addition to having a considerably lower Computer Processing Unit (CPU) time. These will be used as decision criteria for determining the optimal refinement case, through a compromise.

N_x	Refined length in x-direction [m]	N_y	Refined length in y-direction [m]	N_z
1	49.0	1	50.0	1
3	16.3	3	16.7	1
5	9.8	5	10.0	1
7	7.0	7	7.1	1
9	5.4	9	5.6	1

Table 6.3: Levels of refinements in the sensitivity analysis.

7 Results

7.1 Simplified Model

7.1.1 Case 1 and 2: Simplified Model - Clean-up and Restart

Presented in **Table 7.1**, Case 1A contains a friction factor of 0.0001 and well pressure at the toe, $P_{w,toe}$, of 382.06 bar. This results in a small error of -0.002 bar in the gauge pressure. The pressure drawdown between the reservoir and toe are calculated to be 3.9 bar, while at the heel 4.0 bar. Case 1B contains a friction factor of 0.011 and well pressure at the toe of 384.9 bar. A small error of -0.03 bar in the gauge pressure is obtained. The pressure drawdown at the toe is calculated to be 1.10 bar, while at the heel 3.6 bar.

Zones	Permeability Distribution [mD] of Simplified Model			
	Case 1: Clean-up		Case 2: Restart	
	Case 1A; f = 0.0001 , Pw,toe = 382.06 bar	**Case 1B**; f = 0.011 , Pw,toe = 384.9 bar	**Case 2A**; f = 0.0001 , Pw,toe = 262.05 bar	**Case 2B**; f = 0.011 , Pw,toe = 263.7 bar
OS-7	232.8	257.4	2.03	2.06
OS-6	249.3	467.6	0	0
OS-5	86.9	233.4	74.9	84.6
OS-4	126.5	398.7	56.7	66.8
OS-3	108.0	373.3	45.3	54.2
OS-2	85.9	309.7	46.9	56.3
OS-1	46.3	166.2	12.3	13.5

Table 7.1: Zonal permeability distribution of Simplified Model, Case A and B, from clean-up and restart.

A relatively equal permeability value for the heel, OS-7, for the two simplified cases after clean-up is observed. This can be explained by the pressure drawdown being of the approximately same size. For the other zones, Case 1B has a lower zonal drawdown. From Darcy's law for flow in porous media (**Equation (6.10)**), a lower drawdown leads to higher zonal permeabilities. Hence, higher permeabilities of the formation are required to deliver the same, specified inflow into the well. As Case 1B has the highest permeability values for all zones, the cumulative oil production is expected to be closer to the interpreted tracer profile

than Case 1A. From **Figure 7.1** below and **Table 11.2** in the Appendices, one can observe that this is not the case. It can likely be explained by the permeability of the heel segments, OS-7 and 6, in Case 1A, representing a higher fraction of the total permeability of all zones compared to the corresponding zones in Case 1B. Consequently, Case 1A obtains a higher inflow through the heel than Case 1B. From the model, it can also be observed that when the rate of inflow increases, the frictional pressure loss increases.

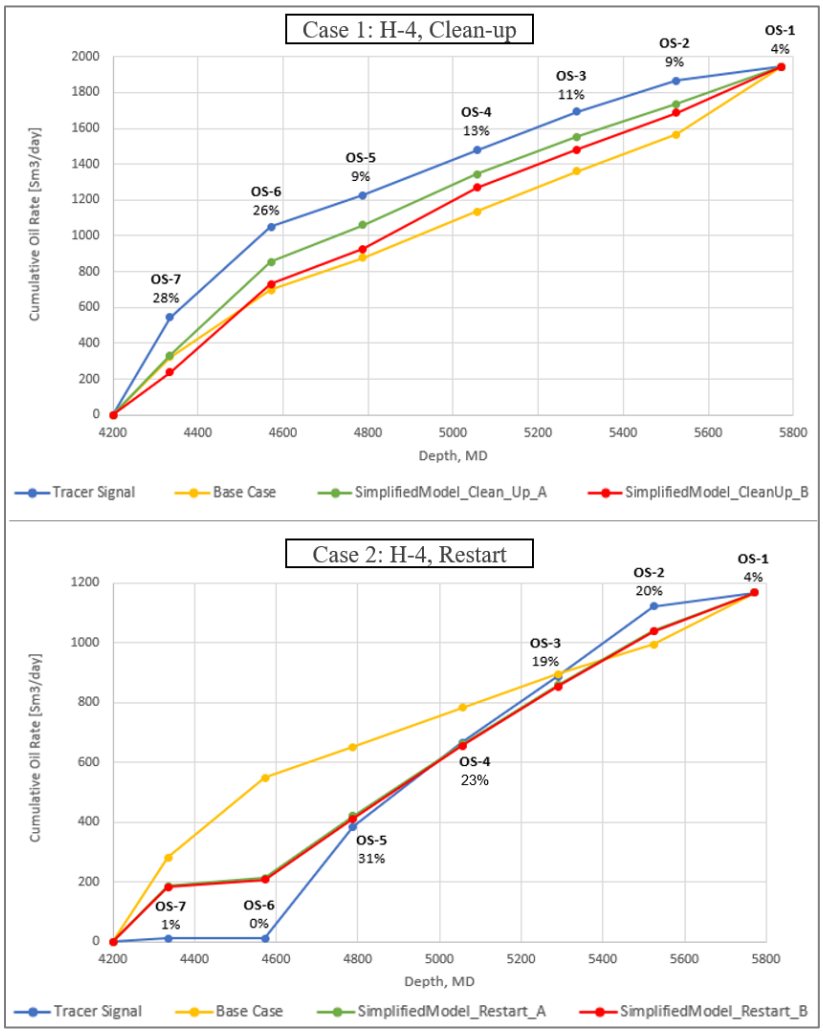

Figure 7.1: Simulated oil rate for both Case A and B of the Simplified Model against the reservoir model Base Case and interpreted inflow profile for clean-up, Case 1, and restart, Case 2.

Presented in **Table 7.1** for restart, Case 2A contains a friction factor of 0.0001 and well pressure at the toe of 262.1 bar. This results in a small error of -0.008 bar in the gauge pressure. The pressure drawdown between the reservoir and toe are calculated to be 9.7 bar, while at the heel 9.8 bar. Case 2B contains a friction factor of 0.011 and well pressure at the

toe of 263.7 bar. A small error of -0.03 bar in the gauge pressure is obtained. The pressure drawdown at the toe is calculated to be 8.1 bar, while at the heel 9.6 bar.

The zonal permeability after restart is less affected when adjusting the friction factor. The same trends as described for clean-up are observed but to a lesser extent. This can be explained by the rate after restart being less than the rate after clean-up and hence, the frictional pressure loss after restart is lower than after clean-up. Both Case 2A and 2B, are resulting in a higher pressure drawdown between the well and reservoir compared to clean-up and consequently, lower permeability values are obtained.

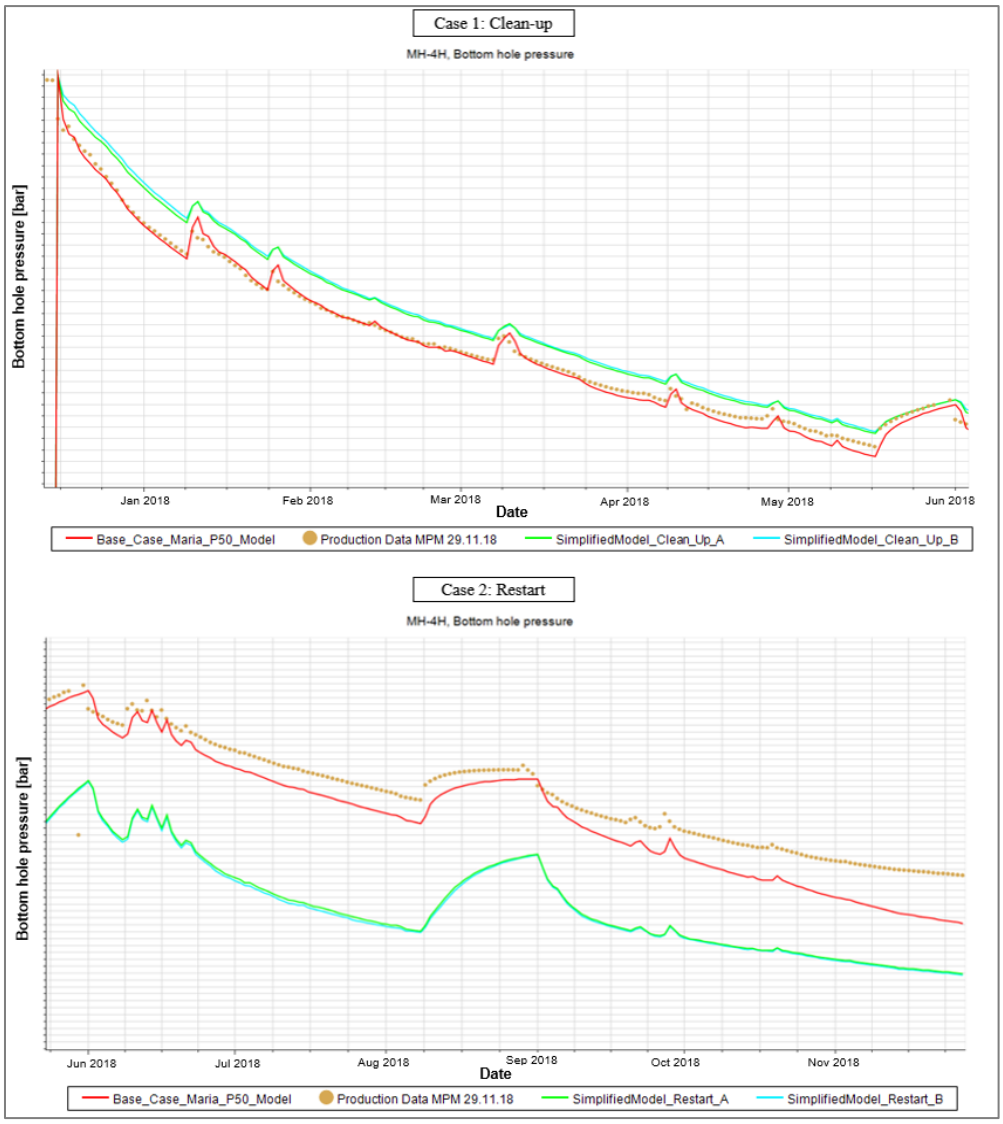

Figure 7.2: BHP match for Case A and B of the Simplified Model, for dates after clean-up, Case 1, and after restart, Case 2, in addition to the BHP match of the reservoir model Base Case, against historical BHP.

From the corresponding BHP match for Case 1 and 2, A and B, in **Figure 7.2**, it can be observed that the pressure is overestimated for Case 1, while underestimated for Case 2, compared to Base Case and the historical data. For both cases, Case A and B are resulting in closely similar matches.

7.2 Reservoir Model – Maria-P50-Model

7.2.1 Case 3: Base Case

The simulation PLT oil rate for Base Case for clean-up and restart can be observed in the well section **Figure 7.3**. The BHP match for Base Case compared to the historically measured BHP can be seen in **Figure 7.4**.

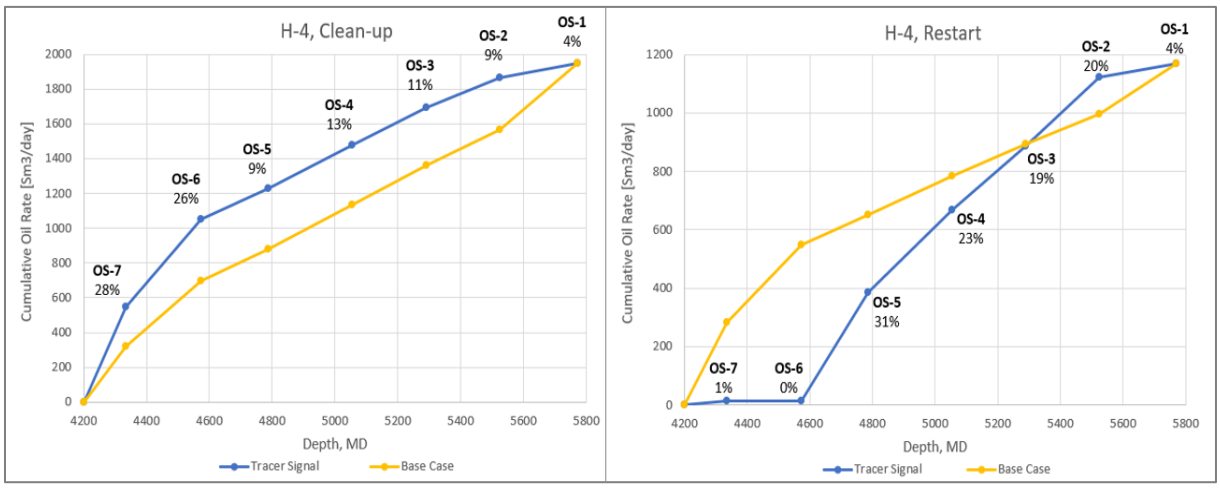

Figure 7.3: Simulated oil rate for Base Case against the interpreted tracer inflow, for clean-up and restart.

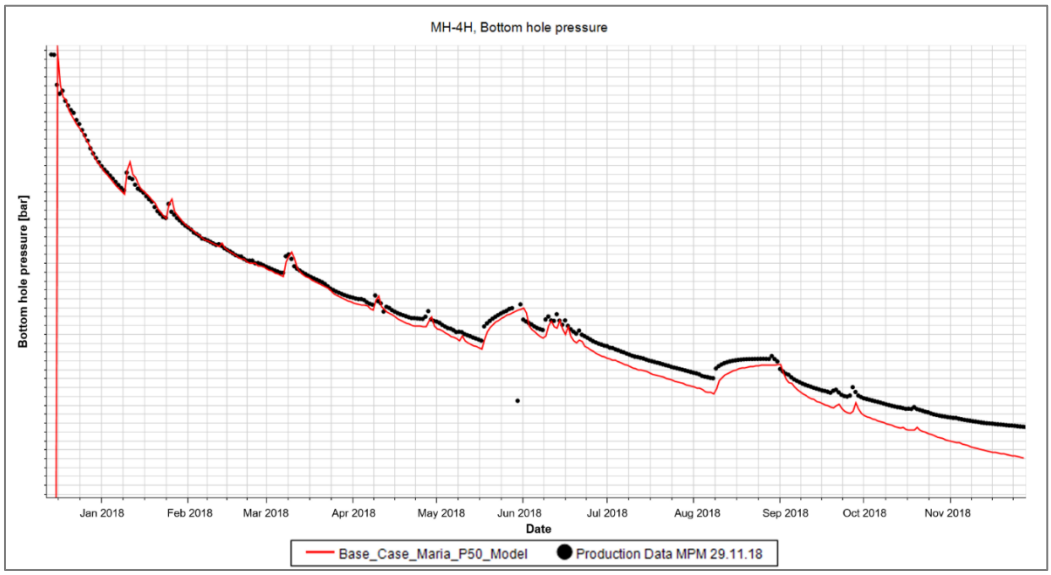

Figure 7.4: BHP match of Base Case against historical production data.

	Oil Production Rate [Sm^3/day]			
	Clean-up		Restart	
Zones	**Tracer Signal**	**Base Case**	**Tracer Signal**	**Base Case**
OS-7	544.6 (28%)	321.5	11.7 (1 %)	282.6
OS-6	505.7 (26 %)	376.9	0 (0 %)	266.6
OS-5	175.1 (9 %)	180.1	373.9 (31 %)	102.6
OS-4	252.9 (13 %)	257.4	280.4 (23 %)	131.4
OS-3	214.0 (11 %)	223.7	222.0 (19 %)	111.5
OS-2	175.1 (9 %)	205.8	233.7 (20 %)	100.9
OS-1	77.8 (4 %)	379.8	46.7 (4 %)	172.9
Total Rate	1945.2	1945.2	1168.5	1168.5

Table 7.2: Oil production rate for the tracer signals and the Base Case, for both clean-up and restart.

In **Figure 7.3**, it can be observed that simulated oil rate of the Base Case is not matching the interpreted inflow tracer profile, for either clean-up or restart. By comparing the respective numerical values (**Table 7.2**) after clean-up, it can be observed that the contribution of the heel, OS-7 and 6, are too low, while the toe, OS-1, is being too productive. The simulated inflow of the toe is contributing with 19.5 % contra the 4 % from measurements. The center zones, OS-5 to 2, of the Base Case are showing relatively similar inflowing rates as the inflow tracers and hence, these zones are more or less matching. After restart of the well, the Base Case is far off from matching the results of the tracers. Therefore, as expected, some parameters in the Maria Base Case must be adjusted to be able to match the interpreted tracer profile. The BHP match for Base Case shows relatively good results after clean-up of the well but starts deviating to a greater extent after restart of the well. At date 1st August, a relative error of -3.5 % between the Base Case BHP and production data is observed **Figure 7.4**.

The calculated zonal permeability distribution of Base Case is presented in **Figure 7.5** above. From the well section log for Base Case, for both clean-up and restart, **Figure 6.1**, it can clearly be observed that the connection oil rate is increasing with higher kh. Consequently, for a simulation zone to provide a higher inflow rate, the corresponding kh in the given zone must

be increased. This can be adjusted for by increasing the permeability of the zone, through multiplication of permeability in x- and y-direction. By increasing the porosity, on the other hand, a higher inflow through this zone can be obtained. Therefore, the horizontal permeability and porosity of the reservoir section considered to be the main parameters affecting the fluid inflow. From a sensitivity study performed by Wintershall to identify the properties having the largest impact on STOOIP, the permeability and porosity log were determined to be the key drivers. The directional permeability values can be hard to measure, thereby being among one of the most uncertain parameters in the model. Hence, the deviations between the clean-up tracer inflow data and simulated inflow are expected to be due to the uncertainties in porosity and permeability.

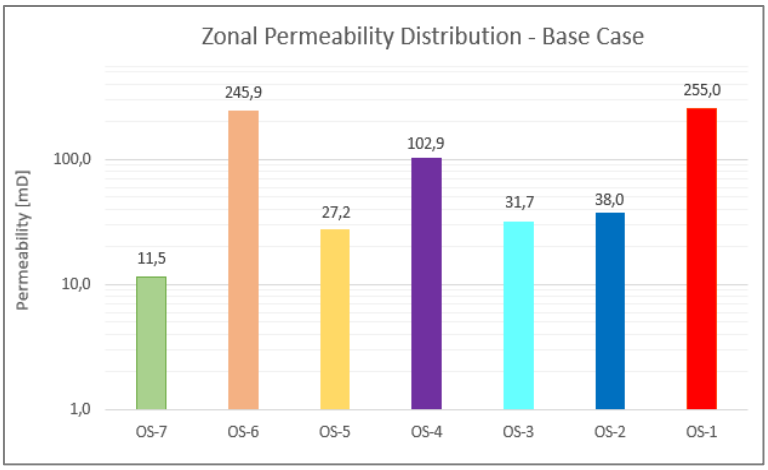

Figure 7.5: Zonal permeability distribution of Base Case, on a logarithmic scale.

Moreover, there are uncertainties related to skin damage in the model. An increase in the skin factor causes a decrease in the transmissibility factor for the connection between the grid cell and the wellbore. The deviations between the interpreted tracer inflow data from restart and inflow contribution from the simulation results are initially expected to be caused by skin effect. Hence, the main parameters tuned to obtain better matches of the inflow results are the horizontal permeability distribution and the porosity distribution for matching of clean-up data, while skin, which is also related to the permeability distribution in the near-wellbore area, for matching of restart data.

7.2.2 Case 4: Best History Match

7.2.2.1 Case 4.1: Match for Clean-up

"Far from Wellbore"-Band

Four different matches of the PLT oil rate to the interpreted inflow profile after clean-up, using various zonal multipliers of horizontal permeability, can be observed in **Figure 7.6**, by

considering the grid blocks of the band far from the well. The values of the various PERMXY multipliers utilized for the corresponding matches are presented in **Table 7.3** and the resulting zonal permeability values in **Table 11.3** in the Appendices.

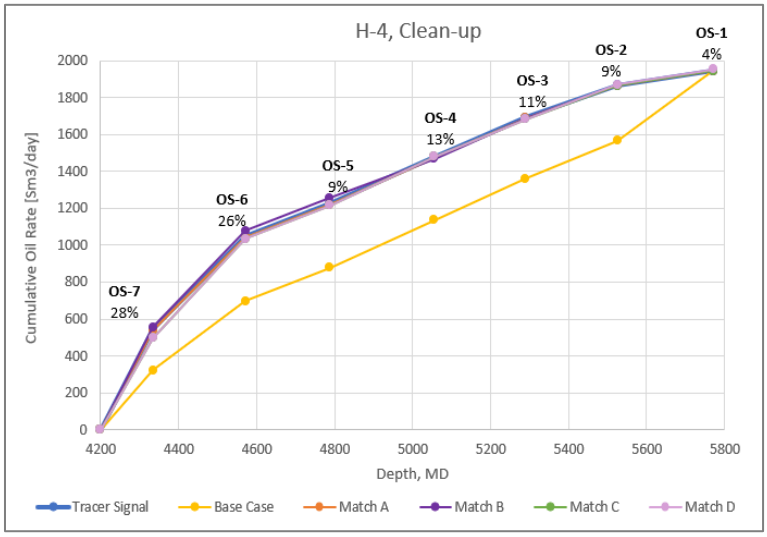

Figure 7.6: Simulated oil rate for different zonal permeability multipliers, against the interpreted inflow profile, for clean-up.

	Zonal Multipliers of PERMXY						
Cases	**OS-7**	**OS-6**	**OS-5**	**OS-4**	**OS-3**	**OS-2**	**OS-1**
Base Case	1.0	1.0	1.0	1.0	1.0	1.0	1.0
Match A	3.4	1.7	0.7	0.8	0.7	0.6	0.02
Match B	7.1	2.4	1.1	0.8	1.3	1.0	0.03
Match C	6.9	3.3	1.4	1.7	1.4	1.3	0.04
Match D	10.3	5.0	2.1	2.5	2.1	1.9	0.07

Table 7.3: Zonal PERMXY multipliers for the given simulation cases matching the interpreted inflow contribution for clean-up, considering the area far from well.

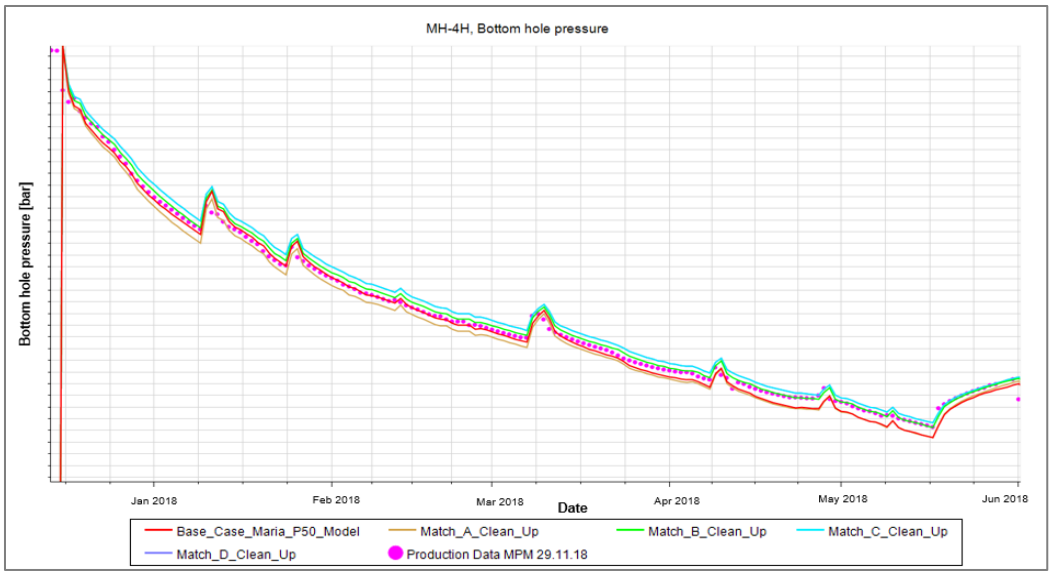

Figure 7.7: BHP match for different zonal permeability multipliers, for clean-up.

By comparing the numerical results of the PLT oil rate for the corresponding matches, **Table 11.4** in the Appendices, it can be observed that Match A is resulting in the closest match to the tracer results for each zone. At the BHP matches in **Figure 7.7**, it can be observed that Match B is closest to the measured BHPs. Match A results in a slightly underestimated BHP until the middle of June where it is approaching the Base Case. Both Match C and D are possessing the exact same BHPs, which are somewhat overestimated compared to the production data. From the ECLIPSE Print-file of the different matches, it can be observed that the pore volume and OOIP remain constant, i.e. alterations in permeability in x- and y-direction do not affect the pore volume and OOIP calculations.

To obtain better matches of BHP for the above cases, multipliers of porosity can be considered, in addition to the permeability multipliers. All the zones are considered to have the same porosity multiplier. For match A, an analysis is performed where three different multipliers are tested (**Table 7.4**), resulting in the following matches of oil production rate and BHP, **Figure 7.8** and **Figure 7.9**, respectively.

Cases	PORO Multipliers
Match A1	2
Match A2	0.5
Match A3	1.1

Table 7.4: Porosity multipliers for Match A.

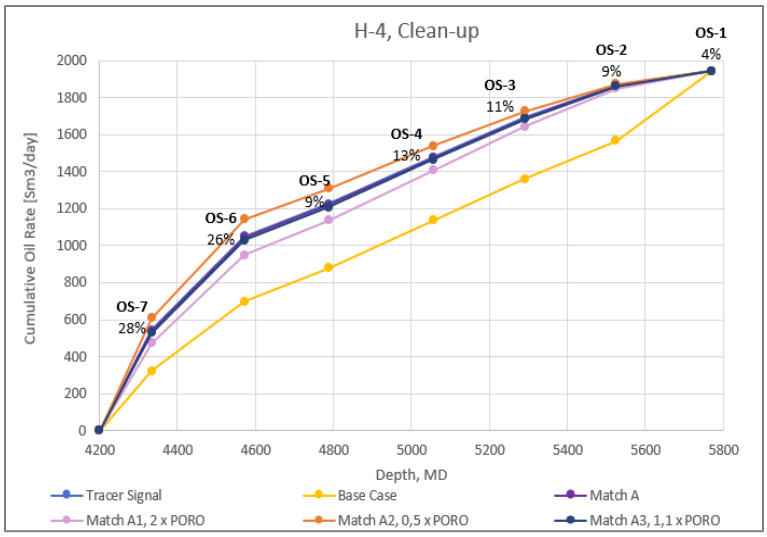

Figure 7.8: Simulated oil rate for different porosity multipliers of Match A, against the interpreted inflow profile, for clean-up.

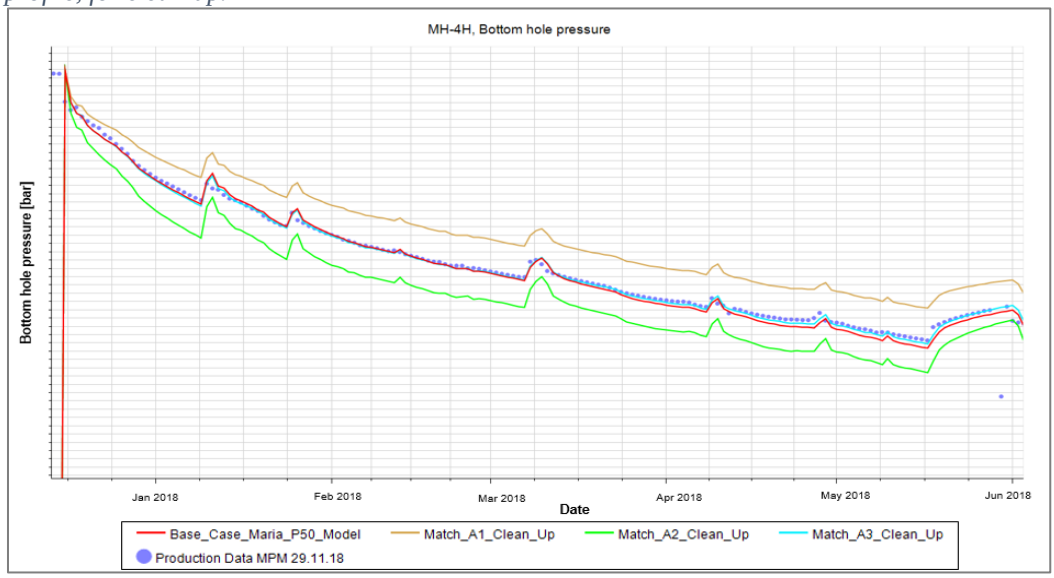

Figure 7.9: BHP match for different porosity multipliers of Match A, for clean-up.

From these figures, it can be observed that by doubling the porosity, Match A1, the oil production rate of the heel, OS-7 and 6, becomes less than for the interpreted inflow profile. The BHPs are highly overestimated. Moreover, the adjustments in the porosity value affect the material balance calculations; A doubling in porosity leads to an increased pore volume of 1.68 % and OOIP by 5.37 %, compared to the Base Case results. On the other hand, by halving the porosity of the formation, Match A2, the opposite results are obtained; The oil production of the heel is higher than of the interpreted tracer profile and the BHP match is distinctly underestimated. Hence, it results in a 0.80 % decrease in the pore volume and 2.57 % in the OOIP. By considering a more realistic multiplier, such as 1.1 x PORO, corresponding to Match A3, a good match of both oil production rate and BHP are obtained.

Hence, only a minor increase of 0.16 % in the calculated pore volume are obtained and 0.52 % increase in OOIP.

As the BHP match for Match B is relatively good by adjusting permeability alone, PORO multipliers are not looked into for this case. For Match C and D, PORO multipliers of 0.8 and 0.7, respectively, give good matches for BHP. Their new respective names are Match C1 and D1, and their oil rate match against interpreted inflow profile and resulting BHP are given in **Figure 7.10** and **Figure 7.11**. The matches result in a minor decrease in pore volume and OOIP compared to Base Case, 0.48 % and 1.03 % for Match C1 and 0.10 % and 1.55 % for Match D1, respectively.

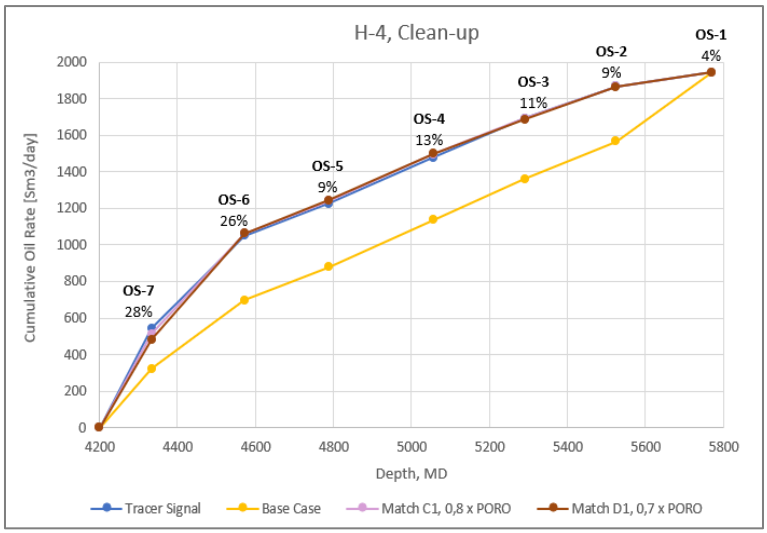

Figure 7.10: Simulated oil rate for porosity multipliers of Match C and D, against the interpreted inflow profile, for clean-up.

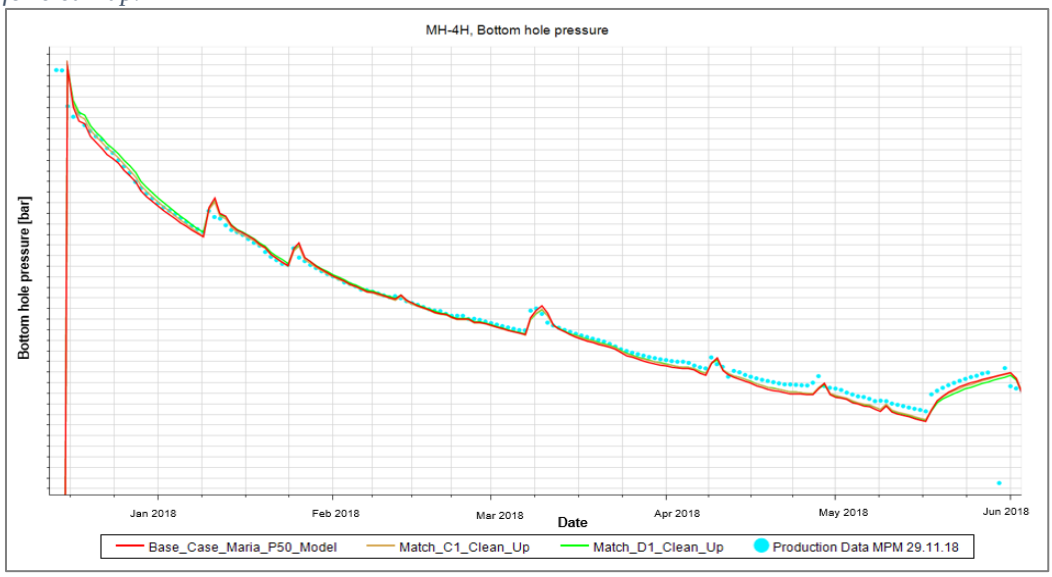

Figure 7.11: BHP match for porosity multipliers of Match C and D, for clean-up.

"Near-Wellbore"-Band

Applying the same PERMXY multipliers as for "Far from field"-band for the near-wellbore area, the simulated inflow rates of the heel are not great enough to match the interpreted inflow profile (**Figure 7.12**). Therefore, new matches must be investigated. Obtaining a good match after clean-up by considering the near-wellbore area, is found to be much more challenging. By adjusting the PERMXY multipliers accordingly, as done for the far from wellbore area, only minor adjustments in the PLT oil rate are achieved. Therefore, several matching cases were run to obtain Match E and F (**Figure 7.13** and **Table 7.5)**.

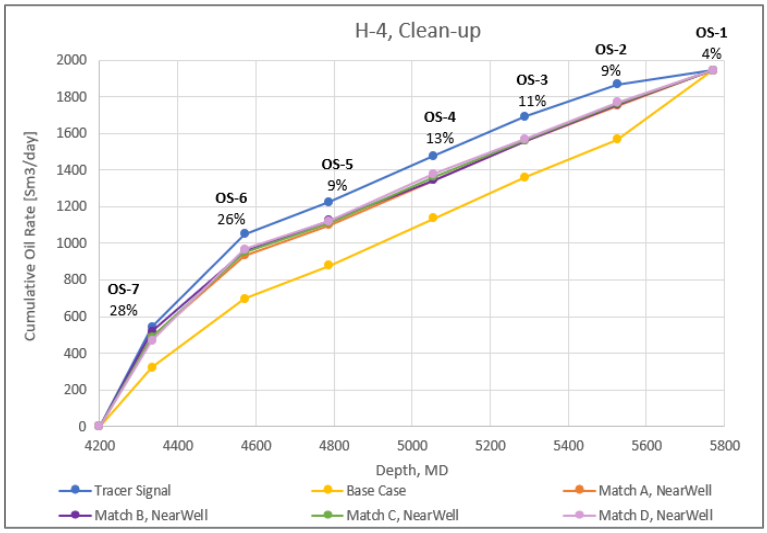

Figure 7.12: Simulated oil rate matches for the "Far from field"-band applied on the "Near-wellbore"-band, for clean-up.

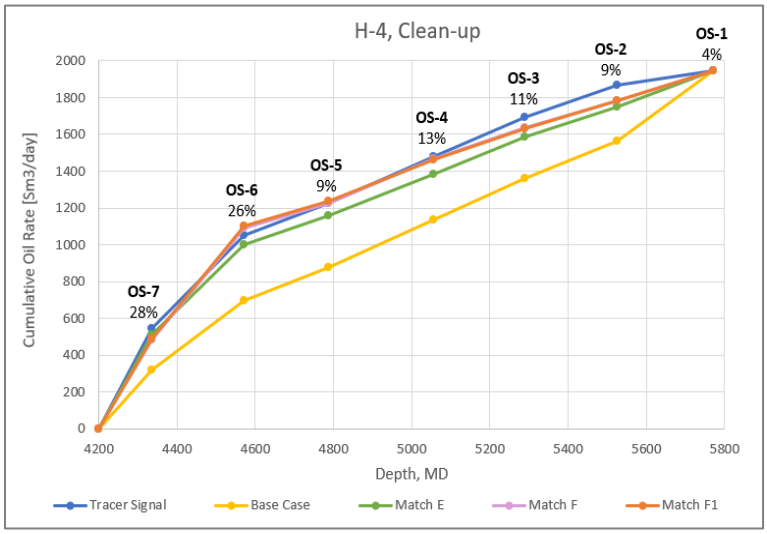

Figure 7.13: Simulated oil rate matches for the near-wellbore area, for clean-up.

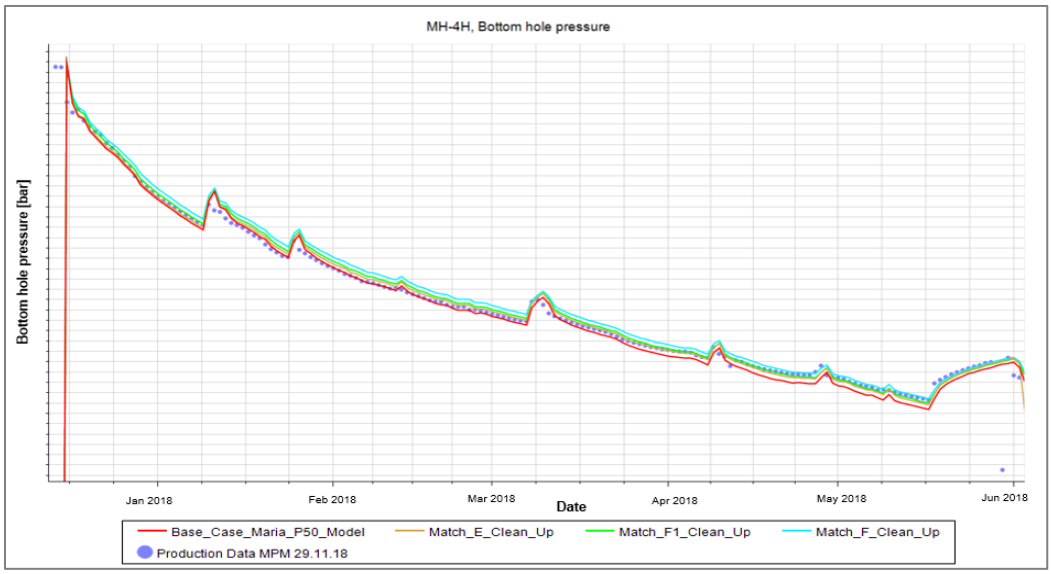

Figure 7.14: BHP matches for cases considering the near-wellbore area, for clean-up.

	Zonal Multipliers of PERMXY						
Cases	**OS-7**	**OS-6**	**OS-5**	**OS-4**	**OS-3**	**OS-2**	**OS-1**
Match E	4.5	2.7	0.3	0.6	0.1	0.1	0.000009
Match F	13.4	8.0	0.9	1.7	0.4	0.3	0.00003

Table 7.5: Zonal PERMXY multipliers for the given simulation cases matching the interpreted inflow contribution for clean-up, considering the near-wellbore area.

Match E is resulting in a relatively good BHP match (**Figure 7.14**) and hence, multipliers of PORO are not necessary to consider. On the other hand, Match F gives slightly overestimated BHP and PORO multipliers should, therefore, be looked into. Match F1, with 0.4 x PORO, gave a vaguely better BHP match (**Figure 7.14**). It deviates from the pore volume of the Base Case by a decrease of 0.10 % and a decrease of 0.35 % in OOIP.

By comparing the values of the zonal multipliers of PERMXY for the "Far from well"-band and Near-wellbore band, **Table 7.3** and **Table 7.5**, respectively, it can be observed that the multiplier value of the toe, OS-1, for the near-wellbore area, are much lower than when considering the area far from wellbore. Anyhow, in **Table 11.4** and **Table 11.5** in the Appendices, it can be observed that the toe for the near-wellbore area is contributing to a higher oil rate than in the far from wellbore area, even though the multiplier value is much lower. The multiplier values of PERMXY and PORO are confirmed by Maria reservoir engineers to be within a realistic range characterizing the field.

7.2.2.2 Case 4.2: Match for Restart

Case 4.2.1: Clean-up Match for Restart

In **Figure 7.15**, one of the obtained matches for clean-up, Match D1, is tested against values from restart to see if the same reservoir property values are matching. It is not expected to do so since **Figure 4.2** shows that the interpreted inflow from clean-up and restart are differing. The oil rate results from **Figure 7.15** indicate clearly that the reservoir properties matching the obtained clean-up profile do not match against the interpreted inflow profile from restart. Therefore, the next simulation cases will look into likely explanations of the non-flowing heel, based on the already obtained matches for the reservoir properties for clean-up. This means that new multipliers of PERMXY and PORO will not be looked into for restart, but those properties will be based on the good matches obtained for clean-up. Hence, parameters such as skin factor and shut-in of zones will be considered to match the interpreted inflow contribution during restart.

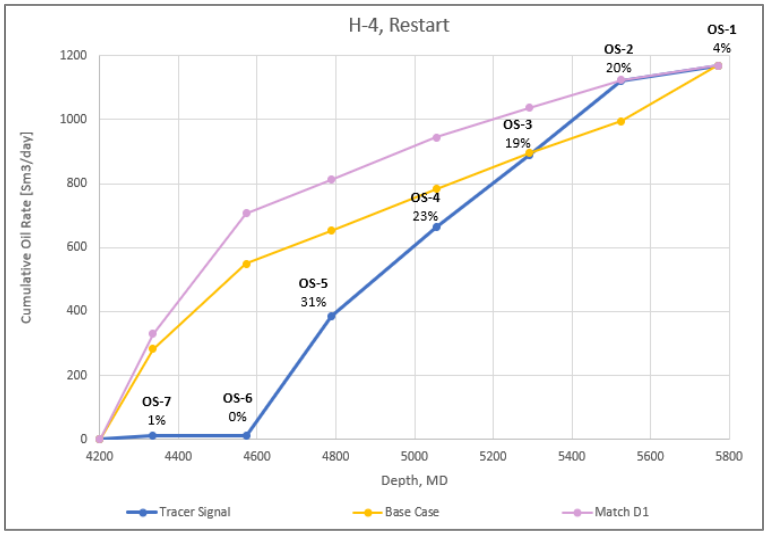

Figure 7.15: Simulated oil rate for restart, considering a simulation case, Match D1, matching the interpreted inflow rate profile for clean-up.

Case 4.2.2: Skin

To investigate if the non-contributing heel, OS-7 and 6, could be explained by containing severe skin damage in the given zones, a study of the Base Case is considered by adding different skin values to the well heel. The cumulative PLT oil rate distribution can be seen in **Figure 7.16** and the BHP in **Figure 7.17** for the corresponding cases. The notation S = 10 , 0 in **Figure 7.16**, corresponds to a skin of 10 for zone OS-7 and 6, and no skin for the

remaining zones. From the same figure, one can observe that the inflow rate of the heel becomes less with increasing skin, i.e. a better match against interpreted tracer inflow profile is obtained. The BHP match, on the other hand, becomes poorer, more underestimated, for increasing amount of skin in the heel.

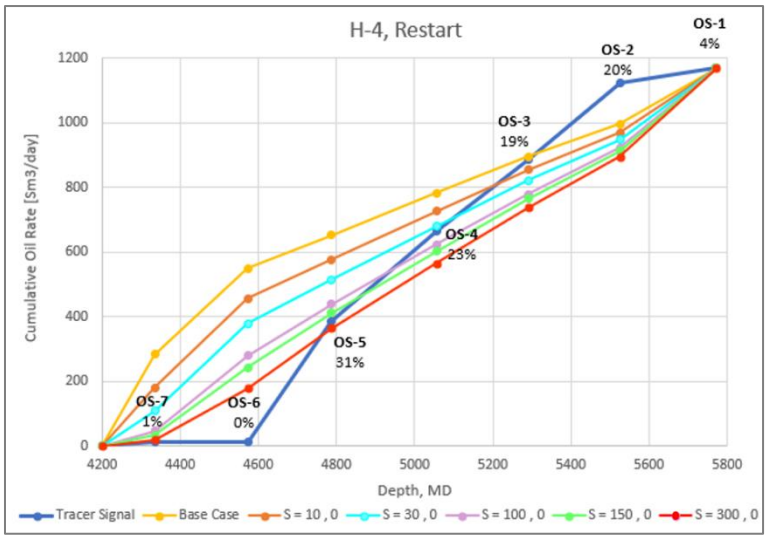

Figure 7.16: Simulated oil rate for Base Case with different skin values, against the interpreted inflow profile, for restart.

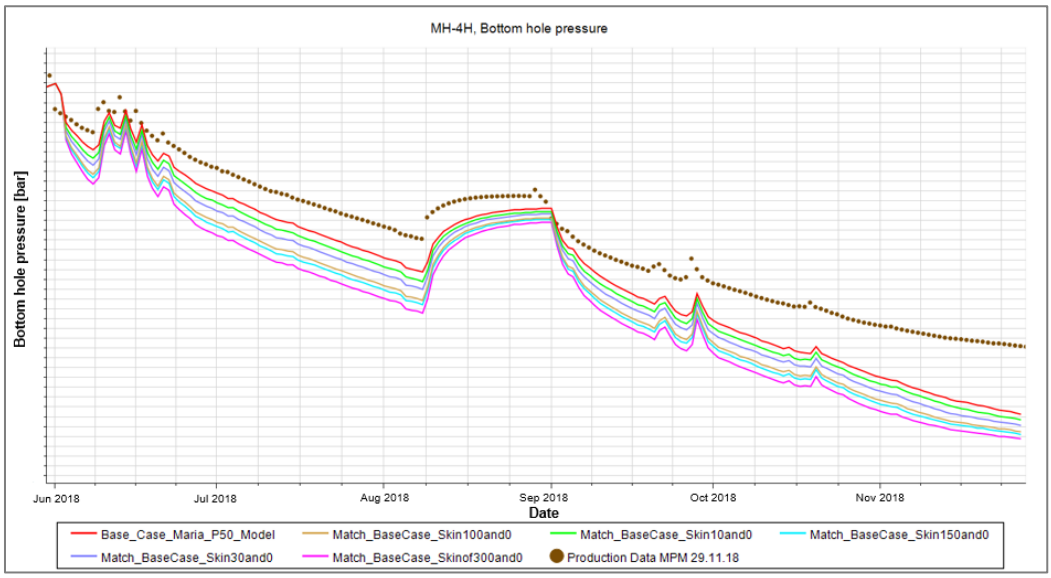

Figure 7.17: BHP matches for Base Case with different skin factors, for restart.

Another option is to add skin in the simulation cases already matching the tracer signals for clean-up. A study is performed for Match A3, using severe positive skin values for OS-7 and 6, while a negative skin value of 2 for zones OS-5 to 1. The corresponding simulated oil rate

distributions and BHP matches can be seen in **Figure 7.18** and **Figure 7.19**, respectively. The notation S = 300 , 500 , -2 in **Figure 7.18**, corresponds to a skin of 300 for zone OS-7, 500 for OS-6, and -2 for the remaining zones.

From the oil production rate in **Table 11.7** in the Appendices, it can be observed that a skin value of 300 in OS-7 and 500 in OS-6 give the closest match against the tracer signals. Equivalently as for the first study performed by altering the skin factor, the oil production rate of the heel reduces with increasing skin. Thus, the oil rate match approaches the interpreted inflow profile from tracer response with drastically increase in skin, while the BHP match becomes poorer.

The deviation between the PLT oil rate for different skin values and the tracer results are mainly caused by zone OS-6. The oil production rate of OS-6 shows the same decreasing trend with increasing skin, but the reduction rate is not high enough to match the interpreted tracer data entirely. This can be explained by a non-flowing zone corresponding to a skin factor approaching infinity.

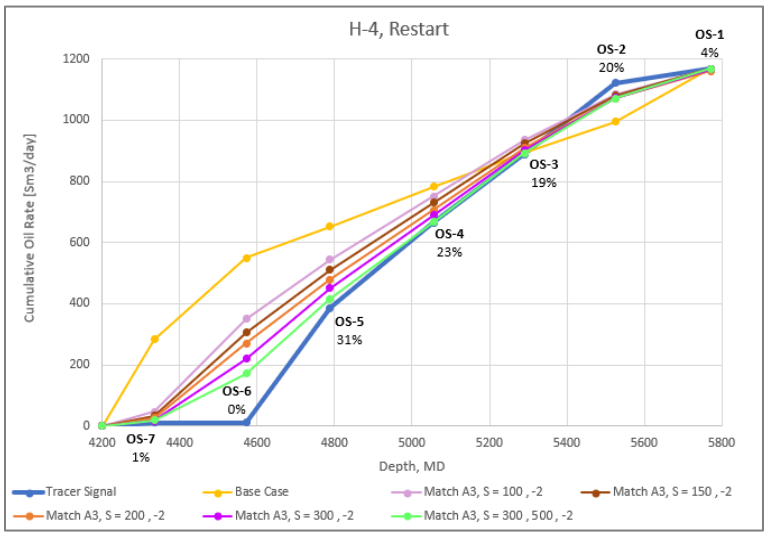

Figure 7.18: Simulated oil rate for cases of Match A3 with different skin values, against the interpreted inflow profile, for restart.

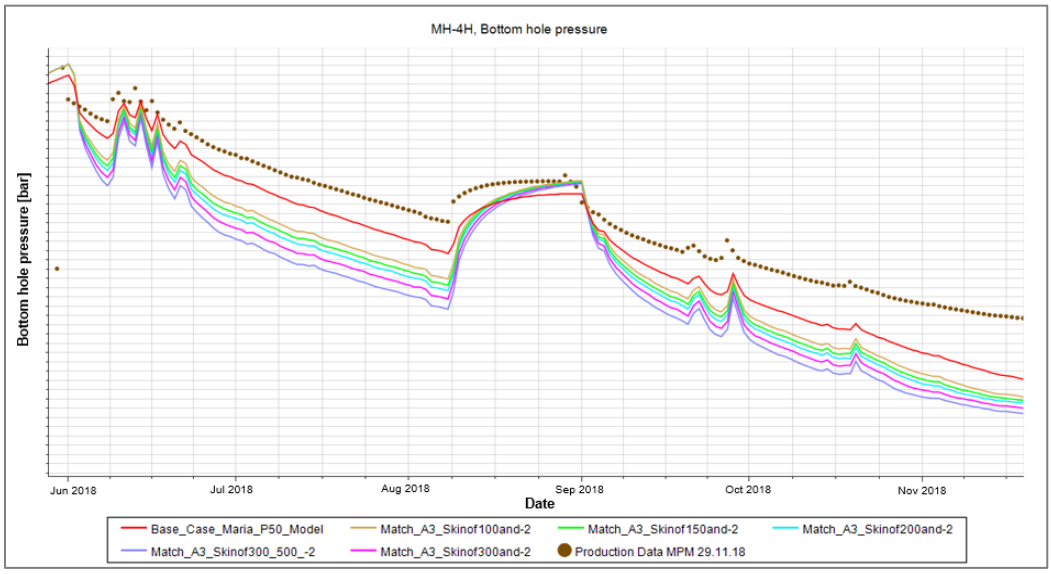

Figure 7.19: BHP match for cases of Match A3 with different skin values, for restart.

Case 4.2.3: Shut-in of Zones OS-7 and 6

Another option to simulate is to completely shut-in the zones of the heel, OS-7 and 6, to simulate how the inflowing oil rate distribution and the corresponding BHP match of the remaining zones turn out. The corresponding results for Base Case and Match A3, B, C1, D1 and E1 for clean-up, considering the heel shut-in, can be seen in **Figure 7.20** and **Figure 7.21**, respectively. No skin is modeled in any of the simulation cases for the remaining zones that are not shut-in. The oil production match after restart is giving relatively good results against the interpreted tracer inflow profile for the cases considering the "Far from well"-band, while Match E1 which are in the near-wellbore area shows a higher deviation (**Table 11.8** in the Appendices). On the other hand, the BHP match is far off from matching when two zones are shut, showing a significant deviation, where the BHP is highly underestimated. Match A3 shows the highest deviation from the production data with a relative error of -13.0 %, decreasing towards Match D1 with -7.0 %, on 1st August.

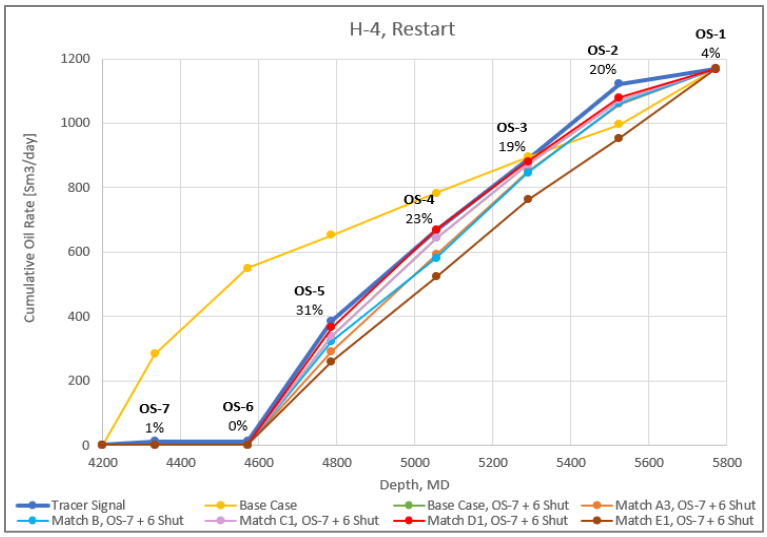

Figure 7.20: Simulated oil rate for different matches of the inflow from clean-up with the heel zones shut-in, against interpreted inflow profile, for restart.

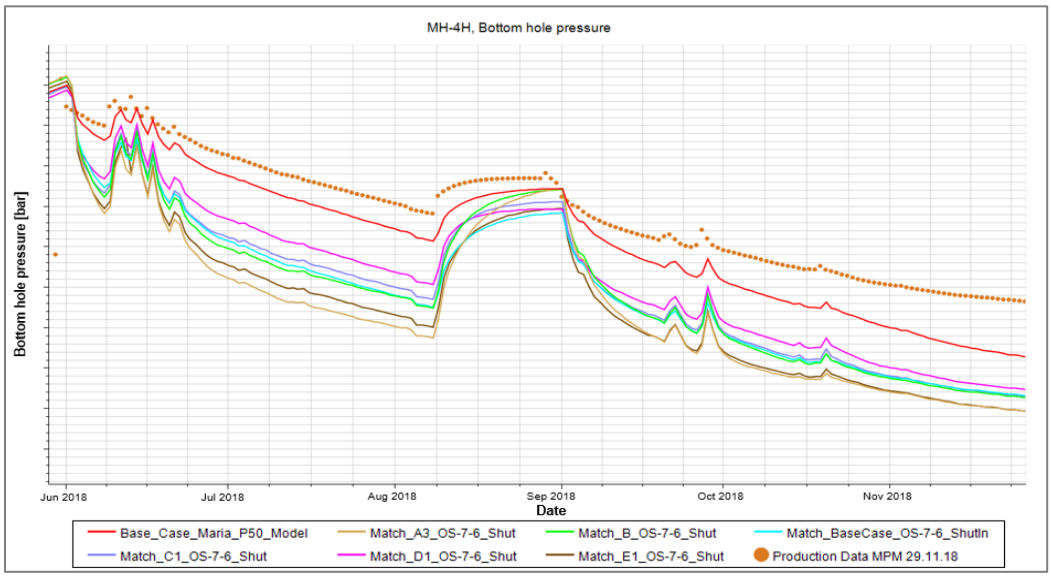

Figure 7.21: BHP matches for different matches of the inflow from clean-up with the heel zones shut-in, for restart.

Considering the heel zones shut-in, Match D1 for clean-up showed the best match against the zonal oil production, in addition to be the closest match for the BHP. However, the given results are not sufficiently close enough, for this to be a likely explanation of the unproductive heel.

Case 4.2.4: Skin in OS-7 and Shut-in of OS-6

An alternative to complete shut-in of both heel zones is to consider severe amounts of skin in zone OS-7 and shut-in zone OS-6, as OS-7 shows some tracer response. An analysis will be performed for Match D1 for clean-up by increasing the amount of skin in zone OS-7 and no modeling of skin in zones OS-5 to 1. It is based on Match D1 as it shows the best results on PLT oil rate and BHP matches for the cases tested this far, for clean-up. The following oil rate match and BHP match are obtained, **Figure 7.22** and **Figure 7.23**, respectively;

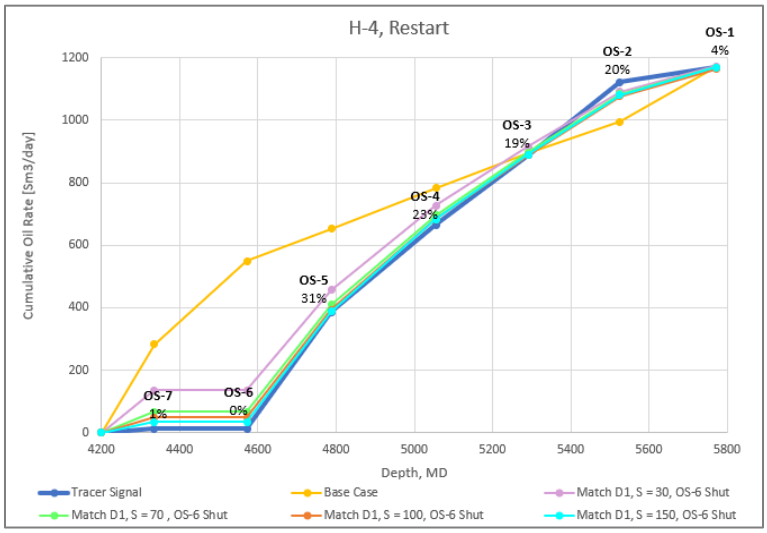

Figure 7.22: Simulated oil rate for Match D1 with the severe skin in OS-7 and OS-6 shut-in, against the interpreted inflow profile, for restart.

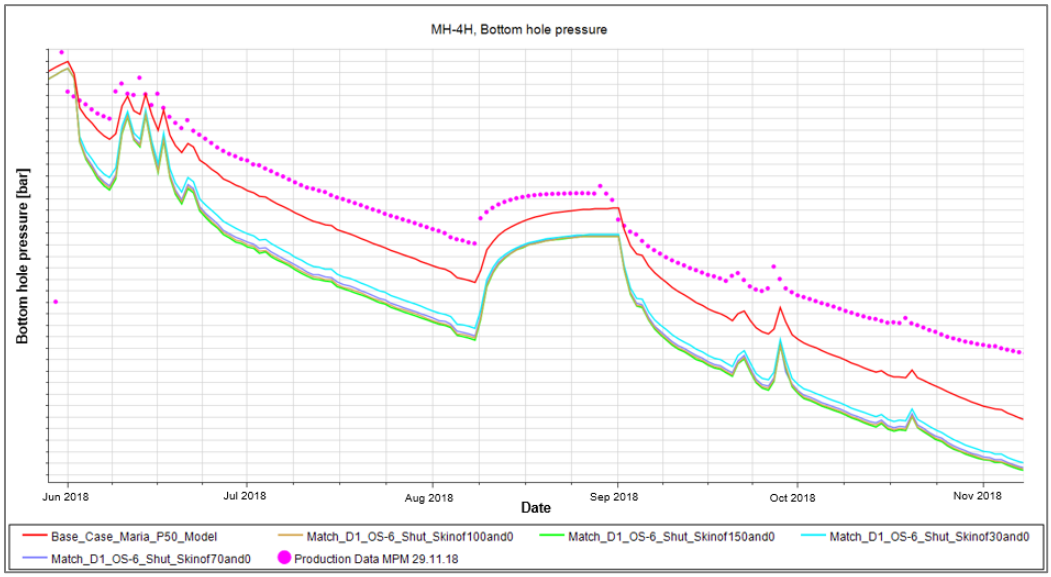

Figure 7.23: BHP matches for Match D1 with severe skin in OS-7 and OS-6 shut-in, for restart.

It can be observed that the simulated oil rate approaches the interpreted inflow profile at the heel with increasing skin factor. Hence, resulting in a slightly poorer BHP match.

Moreover, it is looked into which of the matches for clean-up, Match A3, B, C1, D1 and E1, or Base Case that are giving the best oil rate match to the interpreted inflow profile, in addition to best BHP match, when a skin value of 70 is applied in OS-7 and zone OS-6 shut-in. The resulting simulated oil rate match and BHP match can be seen in **Figure 7.24** and **Figure 7.24**, respectively.

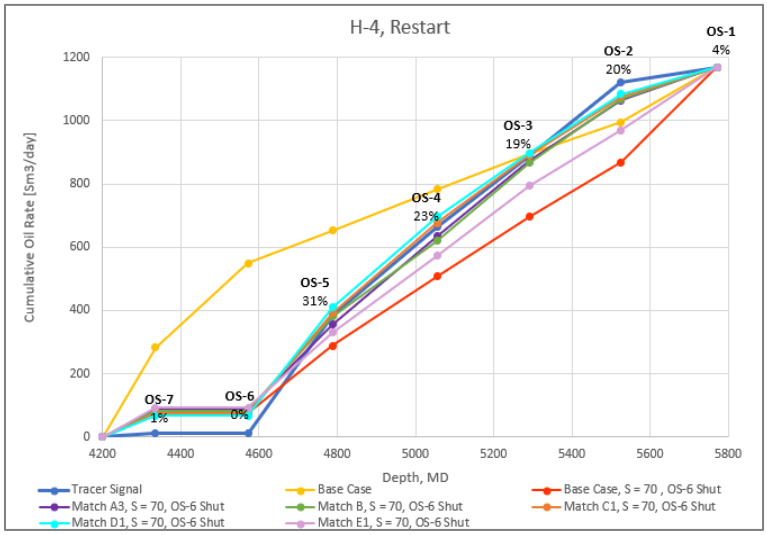

Figure 7.24: Simulated oil rate for different matches of the inflow from clean-up, with skin of 70 in OS-7 and OS-6 shut-in, against interpreted inflow profile, for restart.

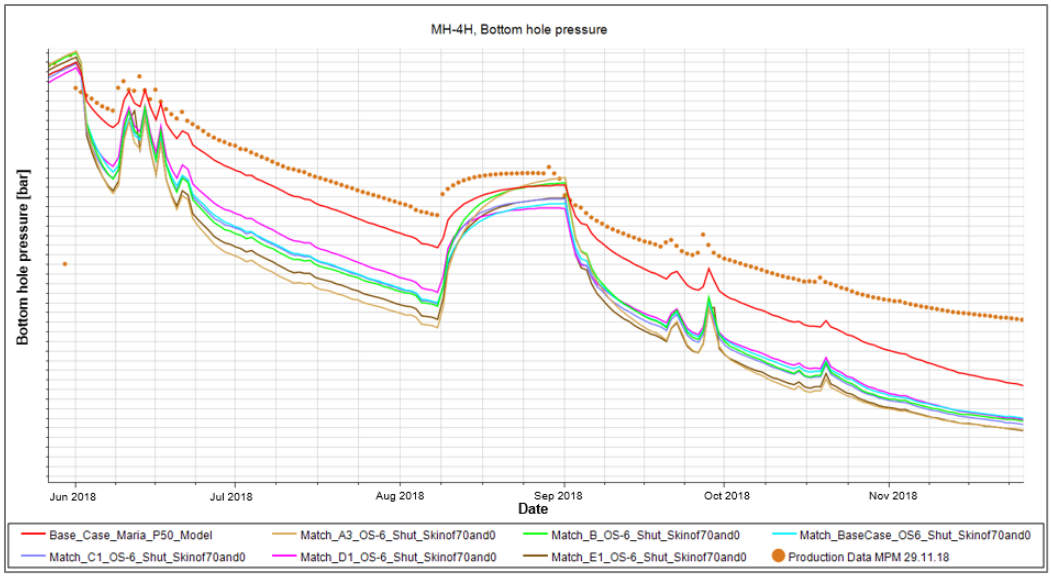

Figure 7.25: BHP match for different matches of the inflow from clean-up, with skin of 70 in OS-7 and OS-6 shut, for restart.

It can once again be observed, that Match D1 gives the best result of BHP, compared to Match A3, B, C1 and E, for clean-up. With a skin value of 70 in OS-7 and OS-6 shut, Match A3 shows the highest deviation from the production data with a relative error of -9.6 %, decreasing towards Match D1 with -6.5 %, at date 1st of August.

From all simulated cases for restart considered, it can be observed that by increasing the PERMXY multipliers for the match of clean-up, the BHP match becomes improved. From the matches considered above, Match D1 has the highest multipliers for all zones. Hence, it provides a result closer to the production data. Match C1, B, E and A are listed in decreasing multiplier order, which results in a poorer BHP match for each case.

Comparison of BHP for Match D1:

To get an idea of how the different BHP matches for Case 4.2 are relative to each other, they are plotted in the same figure, **Figure 7.26**. A lower Pressure Build Up (PBU) is needed to match the flowing pressure when skin alone is applied in the heel zone, than when the entire heel is shut-in and a combination between the two is applied. Moreover, a higher PBU is needed to match the flowing pressure when the heel is completely shut-in than for the combined case.

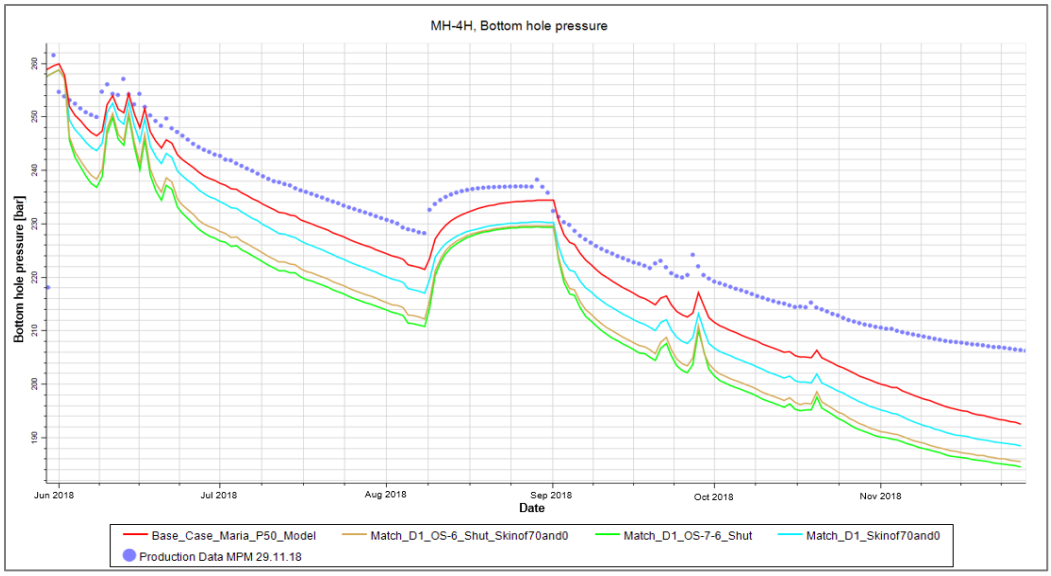

Figure 7.26: BHP match for different cases of Match D1; Skin, two zones shut-in and one zone shut-in, for restart.

For Match D1, one can observe that a skin factor of 70 in the heel give a relative error of -4.53 % from the BHP production data, while shut-in of OS-6 and skin of 70 in OS-7 -6.64 %, on 1st August. Shut-in of both zones of the heel gives the poorest BHP match, with a relative error of -7.29 %, on the same date.

7.2.3 Case 5: Multisegment Well

7.2.3.1 Case 5.1: Multisegment Well v.s. Non-Segmented Well

The simulated oil production rate for the different multisegment cases, for clean-up and restart, can be found in **Figure 7.27**. **Figure 7.28** shows the BHP matches, with two zoom-ins to display the deviations between the Base Case and multisegment wells.

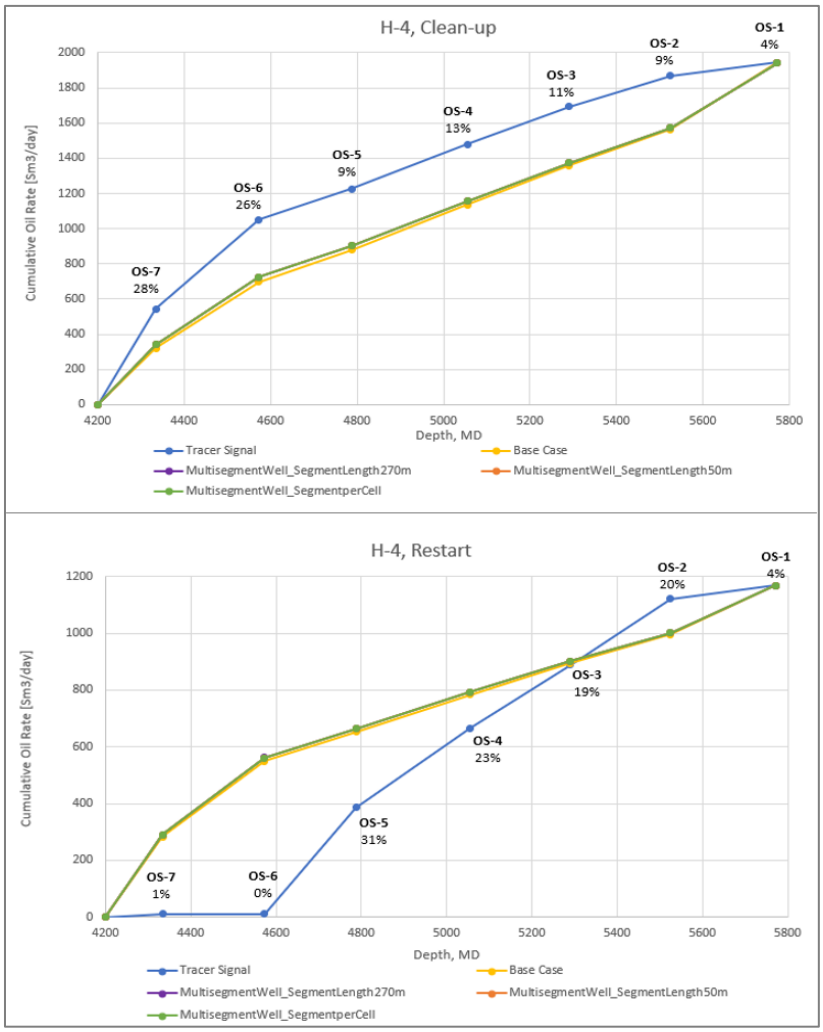

Figure 7.27: Simulated oil rate for multisegment wells, against interpreted inflow profile, for clean-up and restart.

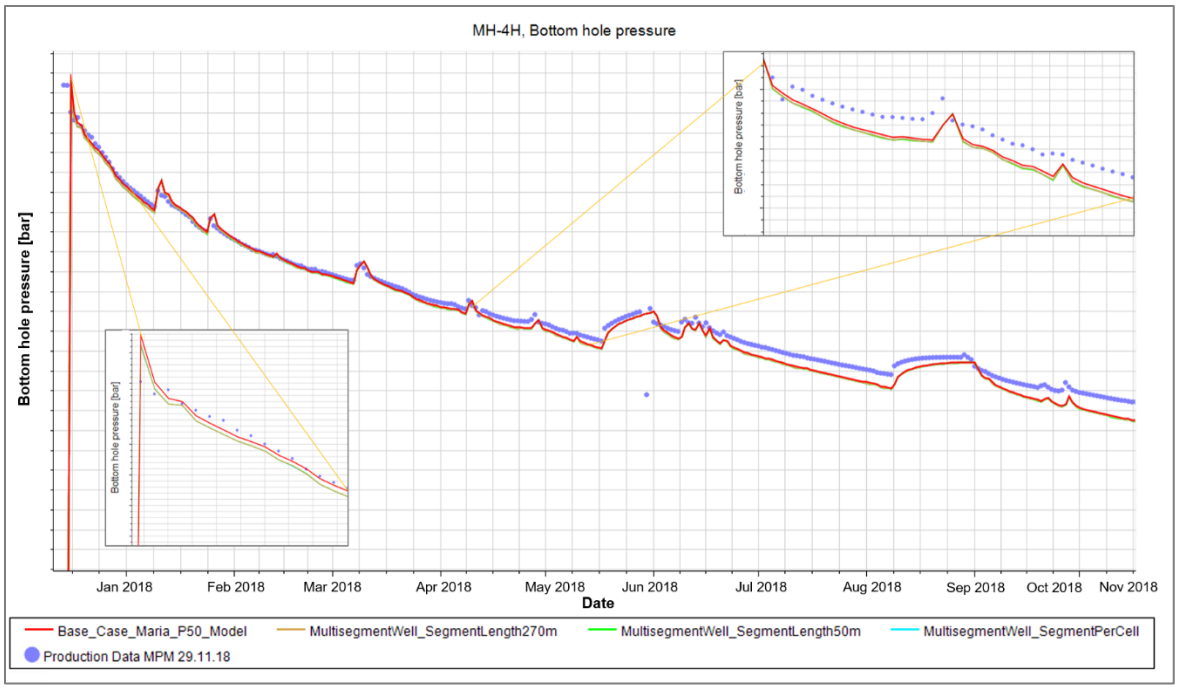

Figure 7.28: BHP match of multisegment well, with a closer look into two time periods.

The simulated oil production rates for the cases of multisegment well only show minor deviation from Base Case. The BHP is for the majority of times slightly below the BHP for the non-segmented well, Base Case, while sometimes they even coincide. They are deviating with a maximum relative error of -0.45 % and average deviation of approximately -0.20 %.

The cases of the different segment sizes tested show nearly the exact same result, deviating on the hundredth decimal place. Therefore, the segments are for all cases considered to be of small enough size for the pressure losses to be accurately calculated.

7.2.3.2 Case 5.2: Multisegment Well Model v.s. Simplified Model

In this subsection, the frictional and hydrostatic pressure losses of the 270 m equally-segmented reservoir model and the Simplified Model will be compared. The results are presented in **Table 7.6** and **Table 7.7**, for clean-up and restart, respectively.

	Clean-up					
	Simplified Model			Multisegment Well		
Zones	Frictional Pressure Loss [bar]	Hydrostatic Pressure Loss [bar]	Total Pressure Loss [bar]	Frictional Pressure Loss [bar]	Hydrostatic Pressure Loss [bar]	Total Pressure Loss [bar]
OS-1	0.000283	0	0.000283	0.0326	0.192	0.224
OS-2	0.00359	0	0.00359	0.0725	0.370	0.442
OS-3	0.0120	0	0.0120	0.152	0.00250	0.154
OS-4	0.0289	0	0.0289	0.245	-0.245	0.000651
OS-5	0.0450	0	0.0450	0.353	-0.148	0.205
OS-6	0.111	0	0.111	0.514	-0.0764	0.438
OS-7	0.245	0	0.245	1.31	11.1	12.4

Table 7.6: Presentation of the pressure losses in the wellbore after clean-up, in the Simplified Model compared to the multisegment well, with equal segment lengths of 270 m.

	Restart					
	Simplified Model			Multisegment Well		
Zones	Frictional Pressure Loss [bar]	Hydrostatic Pressure Loss [bar]	Total Pressure Loss [bar]	Frictional Pressure Loss [bar]	Hydrostatic Pressure Loss [bar]	Total Pressure Loss [bar]
OS-1	0.000102	0	0.000102	0.00769	0.187	0.195
OS-2	0.00442	0	0.00442	0.0178	0.360	0.378
OS-3	0.0140	0	0.0140	0.0387	0.00244	0.0411
OS-4	0.0342	0	0.0342	0.0642	-0.238	-0.174
OS-5	0.0752	0	0.0752	0.100	-0.145	-0.0446
OS-6	0.0755	0	0.0755	0.166	-0.074	0.0921
OS-7	0.0885	0	0.0885	0.501	10.8	11.3

Table 7.7: Presentation of the pressure losses in the wellbore after restart, in the Simplified Model compared to the multisegment well, with equal segment lengths of 270 m.

It can be observed that the frictional pressure losses of the Simplified Model, with a friction factor of 0.011, for both the clean-up and restart process, are of smaller size than present in the multisegment well, for all zones. In both models, the frictional pressure loss increases from toe to heel. After restart of the well, the deviation in pressure losses due to friction in the wellbore for the simplified and the multisegment well is slightly smaller than for clean-up. In summary, the calculated frictional pressure loss of the Simplified Model is underestimated. Therefore, to achieve a better match to the frictional pressure of the multisegment well, a higher friction factor is needed in the Simplified Model.

An observation is that the frictional pressure losses are of greater significance for clean-up than for restart of the well. As the Simplified Model assumes the entire horizontal section to be placed at a constant, average depth, the hydrostatic pressure loss becomes zero for all zones. Hence, the total pressure loss will be equal to the frictional pressure loss.

7.3 Comparison of Simplified Model and Reservoir Model

7.3.1 Case 6: Permeability Distribution

The zonal permeability distribution of the Base Case and Match D of the reservoir model (**Table 11.3** in the Appendices) will be compared against the permeability distribution of the two cases of the Simplified Model, Case 1 and 2, for both A and B (**Table 7.1**). The average permeability values for each zone are presented in a histogram in **Figure 7.29,** for clean-up and restart, on a logarithmic permeability scale. The zonal permeabilities are compared against the zonal rate from the interpreted tracer inflow, as there is a relation between inflow rate and zonal permeability. It can clearly be observed that an increased zonal oil rate gives a higher zonal permeability for the Simplified Model. Match D, which gives a good match to the clean-up interpreted inflow, follows the same trend; Where the zonal oil rate from Base Case is too low compared to its interpreted rate, the zonal permeability value is increased to give a higher inflow.

According to the obtained match to the interpreted profile for clean-up, Match D, the resulting reservoir properties of the heel is not poor. Hence, this does not reflect the low inflow through the heel, interpreted during restart. For restart, Base Case and Match D for clean-up show higher permeability than Simplified Model in the zones containing lower oil rate, i.e. heel zones and toe. Hence, the oil rate for Base Case and Match D in these zones are overestimated compared to the interpreted profile. As the Simplified Model uses the interpreted rates from tracer responses for calculating the zonal permeabilities, the values are lower for these zones.

Even though the reservoir model shows a similar effect as the Simplified Model on the relation between permeability and inflow rate for clean-up, the zonal average permeability values are deviating; In some zones, the zonal permeability of the reservoir model is much lower and in other cases higher than the Simplified Model. No reasonable trends are observed. Considering the clean-up data in **Figure 7.29**, the Simplified Model Case 1B has a zonal

permeability greater than Case 1A for all zones. This is commented on in **Section 7.1.1** and is explained by higher pressure drawdown for Case 1A, resulting in lower permeabilities needed to have the same inflow. For restart, the variations in permeability for Case 2A and B are less due to similar drawdown. However, Case 2B has a slightly higher permeability than Case 2A for all zones.

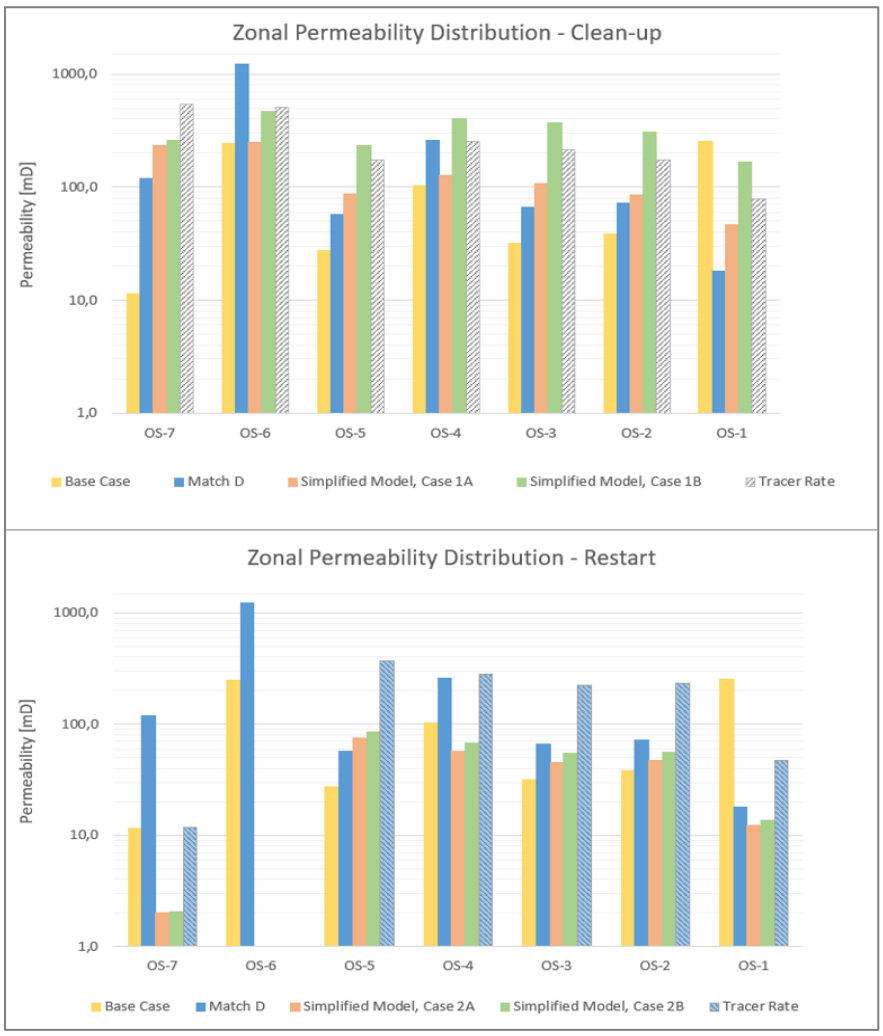

Figure 7.29: Zonal permeability distribution for clean-up and restart, for the reservoir and Simplified Model, on a logarithmic scale.

7.4 Local Grid Refinement

A sensitivity analysis of different refinements of the grid locally around the wellbore was performed, according to the different refined runs specified in **Table 6.3**. **Figure 7.30** shows the BHP through the first year of production and similar in **Figure 7.31**, but a zoomed-in version is provided. **Figure 7.32** illustrates the corresponding cumulative CPU time for the

given refinements, including Base Case.

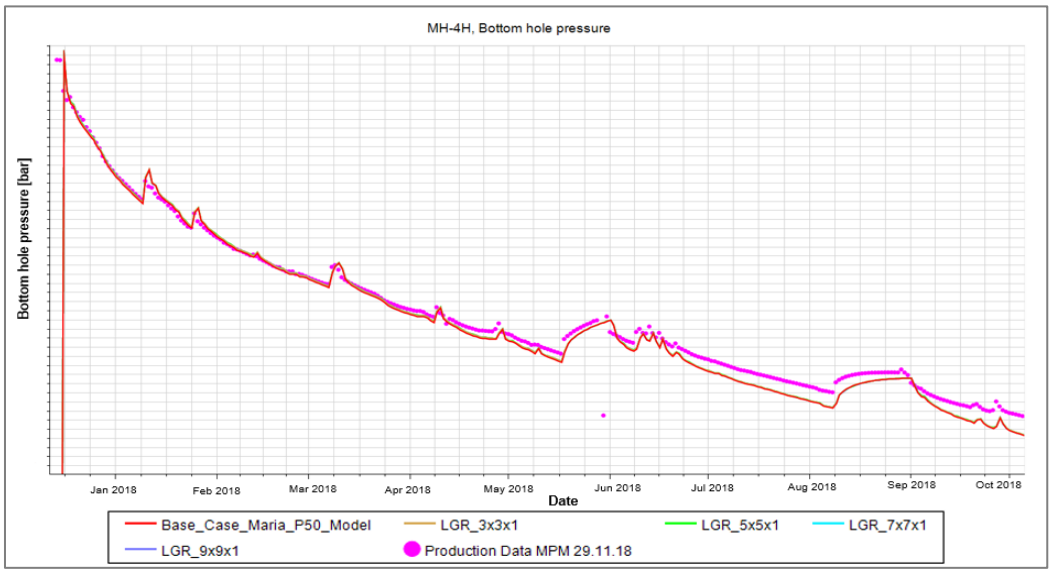

Figure 7.30: BHP match for the various local refinement levels.

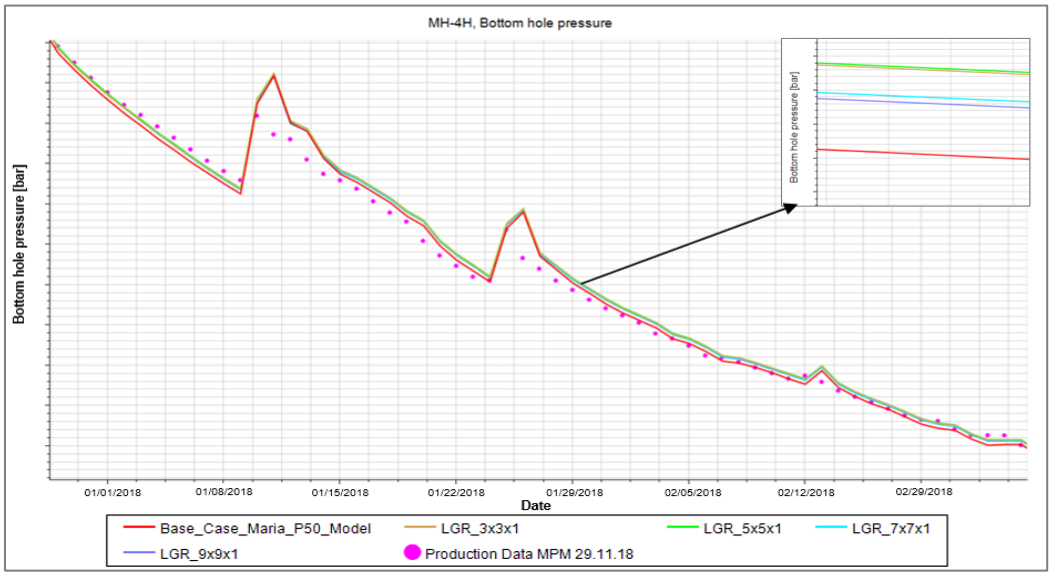

Figure 7.31: A closer look into the BHP match for the various local refinement levels.

Since the optimal refinement should be chosen through a compromise of minor changes in oil production rate and BHP compared to finer grid blocks, in addition to the having an acceptable CPU time, a combination of the parameters must be considered. The various refinements show little change in BHP and oil rate compared to the Base Case. The Base Case shows the least CPU time, increasing with finer grid blocks. At some specific times, the BHP Base Case (**Figure 7.31**) is matching the production data better than the LGRs, while at other

times it is oppositely.

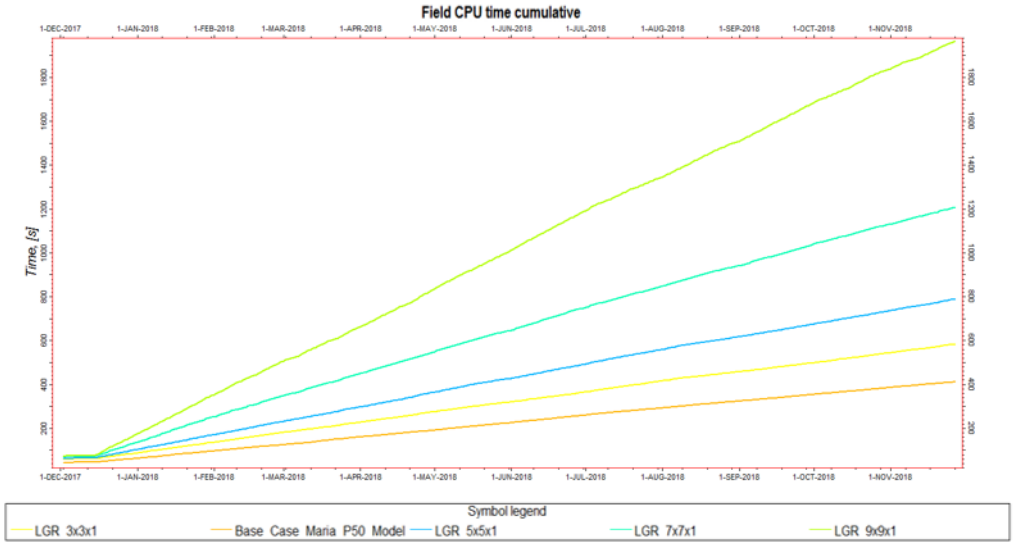

Figure 7.32: Cumulative field CPU time for the different Local Grid Refinements.

8 Discussion

First and foremost, it is important to mention that the P50-model considered in this thesis is one model out of a hundred similar cases for the Maria field that were used in an uncertainty study. Hence, only a presentation of the result from one of the model cases is provided. The uncertainty of the parameters having the greatest impact on the recoverable volumes is considered, to create P10, P50 and P90 statistical production profiles.

The reliability and uncertainty of the inflow tracer results are one of the main subjects to be brought up for discussion. Moreover, the Simplified Model representativity for the real system will be discussed, in addition to a comparison against the reservoir model. The result obtained from modeling will be evaluated, in addition to a discussion of other potential explanations of the non-productive heel. Additionally, it will be discussed if the pressure losses in the horizontal well section should be included or not in the Maria model, and which LGR is optimal for the given grid.

8.1 RESMAN Tracer Uncertainties

As one relatively short tracer carrier must represent the inflow from 200 to 300 meters of the horizontal reservoir section, i.e. the length of four to six grid blocks, it can be discussed how representative it is for the entire zone. Therefore, the accuracy of the tracer technology depends on the reservoir heterogeneity surrounding the specified well. Even though the Maria reservoir is considered to be relatively homogeneous, it can be observed in **Figure 7.5**, that the average permeability of the Base Case changes from zone to zone. Further, from the kh track in the well section log of the Base Case (**Figure 6.1**), one can observe that kh and hence, permeability, changes from each well connection in producer H-4, i.e. on an even smaller scale than the tracer zones. Consequently, one can argue that due to heterogeneities in the formation surrounding the H-4 producer, the inflow tracers cannot give an adequate description of the inflow contribution along the horizontal reservoir section.

Another aspect related to the reliability of the tracers is the accuracy of the analysis model utilized to quantify the tracer inflow percentage. RESMAN (M. Mehdiyev, personal communication, December 12, 2018) comments on the tracer quantification with respect to uncertainty range in an email in the following way; The Flush Out model has been validated

through a flow loop test. The uncertainty of the model was estimated to be 5 %. The flow conditions in the flow loop test are idealized and well-specific conditions, for instance, deviations, cross-flow, flow restrictions and multiple inflow points along the reservoir section, are not accounted for. Therefore, the uncertainty will depend on the well condition and the data quality, and hence, the fit to the model. Consequently, a specific number of uncertainties applicable to all well conditions does not exist. RESMAN points out that to reduce the uncertainty of the data, the estimated inflow rates should be compared to the permeability distribution of the reservoir, in addition to other available data.

The data quality for the Maria producers is in general good, which is observed by achieving expected curves for Flush-Out, in addition to good correlations in the clean-up and restart results, involving some discrepancy. There are some uncertainties in the tracer inflow results from producer H-4, related to the Flush Out model due to ongoing clean-up and short shut-in time. No tracer signals detected from OS-6 and unstable signals from OS-7. During shut-in and restart of the well, production curtailment 2nd June 2018, 17:00hrs disturbed all the tracer's stability. It is also significant to mention that similar tracer effects, as observed after restart for the H-4 producer, has been observed in other producers in the field. For producer H-2, the tracer signals for clean-up showed no inflow through the heel, while after restart the heel came in strong, being the zone of highest contribution to inflow. Likewise, for producer G-4, zone OS-8 and 7, located close to the heel, provide high inflow according to the interpreted clean-up tracer data. After restart of the well, the tracer concentration of the given zones fell below the detection limit early in sampling. This suggests that the zones suddenly stopped producing.

No actions have been taken to attempt to get the heel productive again, due to the presumably high uncertainty range in the tracer measurements. As it is expensive and challenging to access downhole in long horizontal, subsea wells, the engineers would need to know with high accuracy what is causing the obstacle, before any stimulations or acidizing treatments are performed. An idea could be to run a PLT to check if it confirms or disproves the inflow tracer results. If the results are coherent, treatment could be tested as an option. Restart sampling of producer H-4 is planned again in the future, which could re-confirm if heel tracers are present.

In **Section 3.2**, limitations and advantages of production logging tools to measure horizontal well inflow compared to inflow tracers, were presented. However, the focus was more related to the limitations of the PLTs and the many advantages of the tracer technology. As the inflow tracers are a relatively newly invented technology, the uncertainties and limitations are not that well identified as for the PLTs.

8.2 Simplified Model Assumptions

When considering the Simplified Model, assuming single-phase flow of oil under steady state conditions with radial geometry, several observations have been made related to the zonal pressure losses and permeabilities. From the given analytical model and its conditions, it was demonstrated that a higher tubing roughness, i.e. a higher friction factor, results in a lower pressure drawdown between the well segment and reservoir. Hence, resulting in a higher zonal permeability value needed to obtain the same inflow from the producers. These trends are observed when considering both the clean-up and restart interpreted inflow. The changes in permeability from restart are small, due to little variation in drawdown when considering the maximum and minimum friction factor. Moreover, it has been demonstrated that the frictional pressure increases with increasing rate of inflow. Therefore, due to the cumulative inflow increasing towards the heel, the frictional loss of the heel is greatest.

The commented trends are observed when keeping the fluid properties, reservoir pressure, zonal inflow rates, well dimensions and TVD of the horizontal section constant. Changes in the reservoir pressure along the horizontal section could be accounted for in the model to get a higher accuracy of the pressure drawdown and hence, permeability distribution. Moreover, hydrostatic pressure losses could be accounted for by not assuming a constant depth of the horizontal section. This would result in a more precise total pressure loss and hence, pressure drawdown and permeability distribution. The horizontal well model applies Darcy's relation for vertical wells, where the equation's vertical well length is replaced by the horizontal. Consequently, the assumption is made due to time restrictions. Hence, by considering relations for horizontal wells, for instance, Borisov relation for steady state flow, more precise output permeabilities are expected, as both the horizontal well length and the reservoir height are accounted for. By adding more accurate input into the model, the results are expected to show the same trends.

In advance, the calculated permeability distributions for clean-up and restart in the Simplified Model were expected to give a perfect match to the interpreted tracer inflow profile, as the inflow rates were used to calculate the zonal permeabilities. As it can be observed in **Figure 7.1**, this was not achieved. A potential explanation to this is due to the calculated model pressure at gauge depth being matched against the calculated gauge pressure and hence, restricting the frictional factor range that can be considered. Using this matching criterion, a friction factor higher than 0.011 will result in no drawdown between the well toe and the reservoir, thus, no inflow. When reducing the friction factor to a value of less than 0.0001, considered to be the minimum value in this study, the frictional pressure losses of the zones will be of approximately negligible size. Therefore, only minor differences in the permeability distribution will be obtained when reducing the friction factor further.

8.3 Comparison of Simplified Model and Reservoir Model

First and foremost, the Simplified Model is more transparent than the reservoir model, i.e. it is easier to detect which parameters are affecting the results. Accordingly, it is quicker to run. The reservoir model, on the other hand, is much more complex, consisting of dynamic properties and have several mechanisms and equations built into the model. Consequently, it is much more representative of the real system than the Simplified Model.

As the Simplified Model uses the zonal interpreted inflow, obtained by tracers, to calculate the permeability distribution along the horizontal reservoir section, the resulting zonal permeability is directly proportional to the inflow (**Equation (6.10))**. The same trend between permeability and inflow rate can be observed for the reservoir model, where the permeability of Match D for clean-up is increased to obtain a higher zonal inflow.

At this stage of production in the Maria well H-4, the assumption of single-phase flow of oil is appropriate. Hence, this assumption is not contributing to explain the deviations between the models. The main factors explaining the deviating results are that the permeability values for the two models are computed using different approaches and uncertainties in input data. The permeability values of the reservoir model are based on the observed relationship between core porosity and permeability measured at lab conditions, while the values of the Simplified Model are not determined based on porosity. Instead, they are computed based on simplified relations containing considerable uncertainties of the input data; Both viscosity and

oil formation volume factor are taken as average around the H-4 wellbore, while the drainage radius is estimated. Moreover, the zonal pressure drawdown is computed based on simplified pressure loss equations, which is further considering guessed friction factors and pressure at well toe. Another aspect of the deviating results is that the Simplified Model assumes one single pressure for an entire section zone, compared to the reservoir model considering pressure values for each grid block, thereby providing more accurate descriptions of the reservoir. Without doubt, there are uncertainties in the parameters of the reservoir model too (**Section 7.2.1**), but to a significantly lower extent. Therefore, there are more uncertainties related to the calculated permeability distribution of the Simplified Model and hence, the reservoir model is considered to be a more useful prediction tool.

From this, one can conclude that the most significant simplifications in the Simplified Model are related to pressure. Thus, pressure is regarded to be the main controlling factor to compute the zonal permeability distribution in the model. By considering changes in reservoir pressure along the horizontal well section, in addition to changes in depth of the horizontal section, i.e. account for hydrostatic pressure losses, higher accuracy of the pressure drawdown and hence, permeability distribution, is expected to be achieved in the model. Hence, a better match of the simulated oil rate to the interpreted inflow profile from tracer response is expected to be achieved. Moreover, by segmenting the horizontal section into smaller sections, more precise well pressure distribution is expected. However, this implies that the inflow must be known on a smaller scale than available from the inflow tracer technology.

8.4 History Matching of Inflow Contributions

As the parameters implemented in the Maria reservoir model are obtained from a combination of geological models, well logs, core samples, production data, etc., in addition to the dynamic model being history matched against oil production rate and BHP, the main trends of the reservoir properties are expected to already be captured. Therefore, the history matching methodology considered in this thesis is to use multipliers of the tuning parameters, such that the trends of the model's reservoir properties are maintained.

The obtained simulation matches for clean-up are not the only answer to this problem, as there is multiple combinations of input parameters that can result in a history match being equally-good. Hence, history matching can be considered as a non-unique problem. There

exist plenty of different simulation cases matching the interpreted tracer inflow results, by tuning multipliers of horizontal permeability and porosity. Therefore, matches with greatest deviation between them were considered, while still representing realistic values of the Maria reservoir. The horizontal permeability was considered to be the main tuning parameters affecting the fluid inflow along the reservoir section. Excellent matches were achieved against the interpreted contribution from clean-up tracer results, by adjusting PERMXY and PORO within acceptable margins, while honoring the BHP over six months of production. This means that the tracer data adds values to open-hole log information to characterize simulation model properties.

Matches of the inflow profile during clean-up were easier achieved considering the area far from wellbore than the near-wellbore area. This could potentially be explained by the well pressure pulses reaching further than the defined grid of the near-wellbore area. Moreover, the multiplier values of the toe in the near-wellbore area are much lower than when considering the area far from wellbore.

According to Denney (2010), in long horizontal wellbores of homogeneous reservoirs, the heel is expected to give the highest inflow contribution. The interpreted tracer inflow contribution of producer H-4 from restart deviates from this expected trend with approximately no inflow from the heel zones. It is hard to determine which of the simulated cases that fits the interpreted inflow data from restart best. Discrepancies between the simulated oil production rate and the BHP matches are present for all the simulated cases; A good oil rate match gives a poor BHP match, and vice versa. Nevertheless, from the obtained simulation results to match the restart inflow profile, it is observed that the BHP match approaches the production data by increasing the multiplier of PERMXY for clean-up, for all cases of skin, zones shut-in and a combination between the latter two. Hence, even higher PERMXY multipliers were considered for matching the clean-up, but these were only resulting in minor improvements of the BHP match and as the zonal multipliers are increased even further, they will not be within representable values of the Maria field. Therefore, greater PERMXY multipliers will not be considered in this thesis and Match D1 for clean-up is considered to contain the most representable static property values of the formation.

According to the interpreted inflow results from clean-up, the Base Case permeability value

of the heel zones in the reservoir model should be greater. Contrarily, the low average permeability value of OS-7 better reflects the low inflow from the interpreted result from restart. Then the non-flowing zone OS-7 could partially be explained by poor zonal reservoir properties. This explanation could not be transferred to zone OS-6 as Base Case contains a relatively high average permeability value in the respective zone.

Skin is regarded to be a relative quantity and it can, therefore, be discussed what the maximum skin value of a zone is. For that reason, increasing skin values, up to 500, were considered to match the inflow measurements of the heel. Increasing skin resulted in a better match of the inflow profile, but an opposing effect for the match of BHP. An infinitely high skin factor must be applied to zone OS-6 to match the no-inflow, resulting in an even worse BHP match. Moreover, from a reservoir engineering point of view, it seems unusual in real reservoirs that the heel contains extreme amounts of skin, while the rest of the horizontal section is unaffected or has improved performance. Hence, these extremely high skin values tested for the heel are not very likely in real reservoirs.

Achieving a good BHP match with skin proved to be hard, resulting in poorer well productivity than observed. Additionally, there is no clear decline in productivity observed in producer H-4, which would indicate an increase of skin damage, which is expected for sudden changes. The increasing skin factor of the heel could be a single event or it might decline over time. The latter case is more likely, but it can be challenging to model skin over time in a model. Additionally, it is hard to find a skin damage mechanism to explain losses of the entire heel section, in a 500 m long zone. One mechanism could be explained by scale formation around the heel, but it is disproved due to no water present. Well collapse could be another explanation, but it usually restricts the entire well from flowing, which is not the case for H-4. Another potential mechanism is fines migration, in which production fluid particles bridge the near-wellbore pore throats and thus, cause production impairment of the well (You & Bedrikovetsky, 2018).

As huge skin values could not result in low enough simulated inflow through the heel, complete blocking of the heel connections was tested, in addition to a combination between skin and zone shut-in. Despite the relatively good matches against the interpreted inflow profile from restart, an acceptable BHP match was far from being achieved. Thereby,

excluding that mechanically related restrictions are present in the wellbore.

According to Ohaegbulam et al. (2017), some parts of long horizontal wellbores can be choked due to pressure losses, leaving that wellbore part unproductive. This could be a likely event if the pressure losses were of large size, which is not the case for Maria producer H-4.

8.5 Evaluation of Inflow Profile in H-4

It is not to be excluded that no/minor response of the heel tracers for producer H-4 could be explained by incorrect tracer measurements. Three potential explanations will be presented in the following;

One explanation could be due to sand blocking the tracer carriers such that the inflowing fluid will not get in contact with the chemical tracers, before entering the well. If this is the case, then the heel is flowing in reality, but the tracer joints are not successfully managing to release their molecules. Anyhow, it might not be realistic that sand is only blocking the tracer joints surrounding the heel. No similar reducing effect is seen in the interpreted contribution for the remaining zones.

Moreover, another thought is that wax or asphaltenes could block the tracer screens of the heel to prevent fluid inflow to the well. However, wax is proved not possible for the reservoir temperature of this field, while asphaltenes are considered to be very unlikely as fluid tests never predicted asphaltene issues in the reservoir. A drop in productivity would be expected if asphaltenes were blocking the screens. As asphaltene precipitation is pressure dependent, it could potentially have a bigger effect in other field producers having lower flowing pressures than H-4.

Even though the OS tracers should last up to five years, a logistical thought could be that there are no tracer molecules left in the zones due to too high inflow in the heel. This means that there is inflow through the heel after restart, with no tracer response. This hypothesis could be confirmed by the result from the clean-up, showing high inflow rates through both OS-7 and 6, compared to the other zones. Therefore, it is realistic that it is the heel zones that are empty, as all zones have the same amounts of tracer molecules incorporated in the polymer to be comparable in the sample analyses. Furthermore, as only a natural reduction is

observed in the well productivity until date of restart and good oil rate and BHP matches are achieved to the clean-up inflow profile, it indicates that the heel is really flowing, but not their corresponding tracers.

RESMAN (M. Mehdiyev, personal communication, June 06, 2019) is not supporting the above theory as they consider it unlikely that the tracers of the heel section are empty at this early stage. The tracer systems are specifically created for the inflow, reservoir pressure and temperature for the Maria producers. As OS-7 in H-4 show some signals during restart, they claim that this would not be possible with empty tracer carriers. Their interpretation of producer H-4 after restart is that there is flow from the heel section, but it is very low. Moreover, they support their explanation by describing that when low inflow through a zone, the transported heel tracer signals will be diluted into the total field volume, as all producers are restarted simultaneously, such that the tracer signals will be masked.

Despite this, it could be that OS-6 was empty and OS-7 almost empty at the time of restart, as only minor inflow is interpreted from this zone. This theory is disproved if only minor tracer molecules are detected from OS-7 and 6 in future restart interpretation. The tracer signals being lost somehow, e.g. all tracer molecules spent, is concluded to be one of the most likely explanations of the disappearing heel inflow mystery.

8.6 Multisegment Well

Case 5.1: Multisegment Well v.s. Non-Segmented Well

The Maria-P50-Model Base Case does not model the pressure losses in the wellbore. Therefore, by segmenting the horizontal well section, the effect of the frictional and hydrostatic pressure losses along the wellbore are included. The pressure differences obtained between the multisegment well model and Base Case are considered to be negligible compared to other uncertainties. Accordingly, they are not having a big effect in this Maria well and so are not relevant for the tracer behavior.

Furthermore, modeling the pressure drops across the ICDs is a comprehensive study. Due to the limiting time given, this is not considered in this thesis. Wintershall has already performed a detailed simulation case to model the ICDs, drawing the conclusion that there is a very little

pressure drop across them. Consequently, they have very little impact on the final results. The combination of a significant increase in the overall simulation time and little impact on the final results indicates that the assumption of neglecting the pressure drop across the ICDs is consistent.

By including a higher level of details in the reservoir model, the elapsing time of the simulation will increase accordingly. Although, by including the pressure losses, additional factors are taken into account in the model, resulting in a more accurate model. However, by neglecting the pressure losses, only minor deviations are caused between the detailed and less-detailed case. Therefore, no modeling of the pressure losses is considered to be adequate for the purposes of this simulation model, thereby assuming a constant wellbore flowing pressure for the horizontal section.

According to Novy (1995), the frictional pressure losses are negligible in horizontal wells of short size, considering single-phase oil and gas. The Maria producers are considered to have long horizontal well lengths. Novy did not give any definition of lengths regarded as short and long sections. Therefore, as the friction is demonstrated to be of negligible size in Maria producer H-4, it may be that the well is short enough to experience this. He concluded that friction would be of greater importance in long horizontal wells, due to the drawdown being depleted by the frictional pressure loss.

Case 5.2: Multisegment Well Model v.s. Simplified Model

A likely reason for the frictional pressure loss being slightly higher for clean-up than restart for both the multisegment well model and the Simplified Model, is due to the inflowing oil rate being higher at this time. According to Dikken (1990), another explanation of the frictional pressure losses being lower at the date of restart could be due to skin damage in the near-wellbore. He demonstrated that the frictional losses are reduced with skin present in horizontal wells.

Moreover, as demonstrated for the Simplified Model, the multisegment well model also experiences increasing frictional pressure losses from toe to heel, which is expected as the cumulative inflow rate increases towards the heel. The frictional pressure losses of the Simplified Model are underestimated compared to the multisegment well. Hence, an

increasing frictional factor is needed to obtain higher losses.

Due to the Simplified Model assuming a constant depth of the H-4 horizontal section, hydrostatic pressure losses are not accounted for. Therefore, the total pressure losses of the Simplified Model are not comparable to the multisegment well model. Regardless if the hydrostatic pressure losses would be accounted for in the Simplified Model, there could be deviations in the pressure losses from the reservoir model due to different relations used for calculating pressure losses. The Simplified Model uses the simple Darcy flow relation, while the reservoir model Beggs & Brill. On top of that, another uncertainty related to how comparable the zones of the Simplified Model are to the zones of the multisegment well, is present. The zones of the Simplified Model are equal to the top and bottom depth of the tracers, while the multisegment top and bottom depths are slightly deviating from these zones. Hence, the segments in the simplified and the multisegment models are not representing the exact same reservoir zone length.

8.7 Local Grid Refinement

LGR was tested around the H-4 wellbore to see if there were considerable uncertainties related to the size of the grid blocks. As the Base Case shows little change in oil rate and BHP compared to the finer grids and provides the most effective simulation time, no refinements are needed for this model. This means that the current grid blocks around the wellbore are of small enough size to be able to capture the dynamic trends of the reservoir.

8.8 Future Study

- Perform similar history matching studies for the other field producer's inflow against their corresponding interpreted tracer inflow contributions.
- Incorporate new inflow tracer data when available, to keep the reservoir simulation model updated and re-confirm previous tracer results.
- Look into the expected results for the water tracers, when water breakthrough occurs in the wells.

9 Conclusion

The main aim of this study, to match the simulated inflow to the interpreted tracer inflow profiles for producer H-4, for the Maria reservoir model and an analytical, simplified model, is met. Based on the simulation results, the following conclusions can be drawn;

- An excellent match of the simulated oil rate, against the interpreted inflow profile from clean-up tracer results, was achieved, by adjusting PERMXY and PORO within acceptable margins, while honoring the BHP over the production period. Consequently, one can conclude that the clean-up tracer data adds value to open-hole log information, in long horizontal wellbores to characterize simulation model properties.
- Severe skin damage and complete blocking of the well connections of the 500 m long heel, cannot solely explain the interpreted well restart performance, as good BHP matches are not achievable. Additionally, a clear decrease in the well productivity of H-4 is not observed, thereby strengthening the stated conclusion.
- No major reduction in the well productivity and the good oil rate matches achieved to the clean-up inflow profile could indicate that the zones of the heel during restart are really flowing, but not their corresponding tracers. Therefore, one can conclude that the non-productive heel could either be explained by incorrect tracer measurements or tracer signals being lost somehow, e.g. tracer molecules spent.
- The Maria Reservoir Model is more complex, taking more parameters, mechanisms and equations into account, than the Simplified Model, which is better for understanding the main controlling parameters. Both models experience an increasing permeability trend with zonal inflow. The simplifying assumption of constant reservoir pressure and depth of the horizontal section is considered to have the greatest impact on the oil rate results. Thus, by taking these into account, higher accuracy of drawdown and hence, permeability distribution, is expected. The reservoir model is significantly more representative of the reservoir. Thus, a more useful prediction tool.
- The pressure losses along Maria producer H-4 show a minor impact on the results, and so are not relevant for the tracer behavior. It is therefore concluded that the multisegment well option is not needed for the given producer.
- Moreover, it is concluded that the current size of the grid blocks around the wellbore is able to capture the dynamic trends of the reservoir. Hence, no LGR needed.

10 References

Abbasy, I., Ritchie, B., Pitts, M. J., White, B. J., & Jaafar, M. R. (2010). Challenges in Completing Long Horizontal Wells Selectively. *SPE Drilling & Completion*, *25*(02), 199–209. https://doi.org/10.2118/116541-PA

Al-Ali, H. A., Salamy, S. P., & Haq, S. A. (2000). *The Challenges of Detecting Gas Entries in Horizontal Well by Using Integrated Production Logging Tool, Case Study*. Presented at the SPE/CIM International Conference on Horizontal Well Technology, Calgary, Alberta, Canada. https://doi.org/10.2118/65528-MS

Andresen, C. A., Williams, B., Morgan, M., Williams, M. T., Crumrine, T. W., Bond, A. J., & Franks, J. D. (2012). *Interventionless Surveillance in a Multilateral Horizontal Well*. Presented at the IADC/SPE Drilling Conference and Exhibition, San Diego, California, USA. https://doi.org/10.2118/151241-MS

Anopov, A., Alshuraim, F., Shammeri, F., Jacob, S., & Leung, E. (2018). *Permanent Downhole Chemical Tracer System for Wireless Surveillance and Optimizing Well Production*. Presented at the SPE/IADC Middle East Drilling Technology Conference and Exhibition, Abu Dhabi, UAE. https://doi.org/10.2118/189364-MS

Archer, R. A., & Agbongiator, E. O. (2005). Correcting for Frictional Pressure Drop in Horizontal-Well Inflow-Performance Relationships. *Society of Petroleum Engineers*, *20*(01), 1–5. https://doi.org/10.2118/80528-PA

Bao, K. (2016, January). *Multi-segment Wells and Well Modeling*. Presentation presented at the OPM meeting, Oslo.

Bennetzen, M. V., & Hviding, G. (2019, February). Value of Information (VOI) from Continuous Monitoring and Digitization of the Wellbore using Chemical Tracers. *First Break*.

Bjørlykke, K., & Avseth, P. (2010). *Petroleum Geoscience: From Sedimentary Environments to Rock Physics*. Heidelberg; New York: Springer Berlin Heidelberg.

Brice, B. W., & Miranda, J. R. (1992). *Production Impacts on Delta P Friction in Horizontal Production Wells*. Presented at the SPE Latin America Petroleum Engineering Conference, Caracas, Venezuela. https://doi.org/10.2118/23666-MS

Bybee, K. (2010). Reservoir-Management Practices in the Offshore Oil Fields of Saudi Arabia. *Journal of Petroleum Technology*, *62*(01), 49–51. https://doi.org/10.2118/0110-0049-JPT

Carpenter, C. (2018). Lessons From 10 Years of Monitoring with Chemical Inflow Tracers. *Journal of Petroleum Technology*, *70*(09), 81–83. https://doi.org/10.2118/0918-0081-JPT

Carvalho, V., LaVoie, S., & Williams, B. (2015, February). The Evolution of Production Logging. *Oilfield Technology Magazine*.

Chandran, T. P., Talabani, S. A., Jehad, A. S., Al-Anzi, E. H. D., Clark, R. A., & Wells, J. C. (2005). *Solutions to Challenges in Production Logging of Horizontal Wells Using New Tool*. Presented at the International Petroleum Technology Conference, Doha, Qatar. https://doi.org/10.2523/IPTC-10248-MS

Cho, H., & Shah, S. N. (2001). *Prediction of Specific Productivity Index for Long Horizontal Wells*. Presented at the SPE Production and Operations Symposium, Oklahoma City, Oklahoma. https://doi.org/10.2118/67237-MS

Civan, F. (2016). *Reservoir Formation Damage: Fundamentals, Modeling, Assessment, and Mitigation* (3rd ed.). Amsterdam, Netherlands: Gulf Professional Publishing.

Denney, D. (2010). Analysis of Inflow-Control Devices. *Journal of Petroleum Technology*, *62*(05), 52–54. https://doi.org/10.2118/0510-0052-JPT

Dikken, B. J. (1990). Pressure Drop in Horizontal Wells and Its Effect on Production Performance. *Society of Petroleum Engineers*, *42*(11). https://doi.org/10.2118/19824-PA

Dowley, J. (2016, September). *Maria Field Development*. Presentation presented at the NPF Stavanger. NPF Stavanger.

Dyrli, A. D., & Leung, E. (2017). *Ten Years of Reservoir Monitoring with Chemical Inflow Tracers - What Have We Learnt and Applied Over the Past Decade?* Presented at the SPE Kuwait Oil & Gas Show and Conference, Kuwait City, Kuwait. https://doi.org/10.2118/187677-MS

Fanchi, J. R. (2006). *Principles of Applied Reservoir Simulation* (3rd ed). Amsterdam; Boston: Gulf Professional Pub.

Fleming, A. J. A., & Appleby, R. (2006). *Wellbore Clean up Best Practices: A North Sea Operator's Experience*. Presented at the SPE/IADC Indian Drilling Technology Conference and Exhibition, Mumbai, India. https://doi.org/10.2118/101967-MS

Fossen, H. (2008). *Geologi - Stein, mineraler, fossiler og olje*. Bergen: Fagbokforlaget.

Gourley, E. N., & Ertekin, T. (1997). *Application of a Local Grid Refinement Technique to Model Impermeable Barriers in Reservoir Simulation*. Presented at the SPE Eastern Regional Meeting, Lexington, Kentucky. https://doi.org/10.2118/39216-MS

Guan, L., Du, Y., Johnson, S. G., & Choudhary, M. K. (2005). Advances of Interwell Tracer Analysis in the Petroleum Industry. *Journal of Canadian Petroleum Technology*, *44*(05). https://doi.org/10.2118/05-05-TN2

Guo, B., Lyons, W., & Ghalambor, A. (2007). *Petroleum Production Engineering: A computer-assisted approach*. Amsterdam: Gulf Professional Publishing.

Joshi, S. D. (1991). *Horizontal Well Technology*. Tulsa, Okla: PennWell Pub. Co.

Kleppe, H. (2007). *Reservoir Simulation - Course compendium in PET660, Reservoir Simulation*. University of Stavanger.

Kumar, M., Joshi, V., & Sharma, P. (2015). Application of Inflow Control Devices in Horizontal Well in Bottom Water Drive Reservoir using Reservoir Simulation. *International Journal of Engineering Research & Technology (IJERT)*, *4*(4). https://doi.org/10.17577/IJERTV4IS041092

Langaas, K., Jeurissen, E., & Hailu, K. A. (2017). *Combining Passive and Autonomous Inflow Control Devices in a Tri-Lateral Horizontal Well in the Alvheim Field*. Presented at the SPE Annual Technical Conference and Exhibition, San Antonio, Texas, USA. https://doi.org/10.2118/187288-MS

LR Senergy. (2016). *ICD Study for Producers, Wintershall Norge AS* [Internal Report].

Lu, J., Zhu, T., Dinh, A., Tiab, D., & Escobar, F. H. (2013). Pressure Drawdown Equations for Multiple-Well Systems in Circular-Cylindrical Reservoirs. *Asian Research Publishing Network (ARPN)*, *8*, 459–464.

Mehdiyev, M. (2018). *Interpretation Presentation: Summary of Maria Restart #1, 01.-04. June 2018, Wintershall*. RESMAN.

Mehdiyev, M., & Rivero, L. (2018). *On Site Clean-up Interpretation Report, Maria H-2H, Wintershall*. RESMAN.

Morales, R. H., Brown, E., Norman, W. D., DeBonis, V., Mathews, M., Park, E. I., & Brown, D. (1996). Mechanical Skin Damage on Wells. *Society of Petroleum Engineers*, *1*(03). https://doi.org/10.2118/30459-PA

Morozov, O. N., Andriyanov, M. A., Koloda, A. V., Shpakov, A. A., Simakov, A. E., Mukhametshin, I. R., … Prusakov, A. V. (2017). *Well Performance Wireless Monitoring with Stationary Intelligent Tracer Systems on the Prirazlomnoye Oilfield*. Presented at the SPE Russian Petroleum Technology Conference, Moscow, Russia. https://doi.org/10.2118/187767-MS

Novy, R. A. (1995). Pressure Drops in Horizontal Wells: When Can They Be Ignored? *SPE Reservoir Engineering*, *10*(01), 29–35. https://doi.org/10.2118/24941-PA

Ohaegbulam, M., Izuwa, N., & Onwukwe, S. (2017). Analysis of Wellbore Pressure Drop on Horizontal Well Performance. *Oil & Gas Research*, *03*(02). https://doi.org/10.4172/2472-0518.1000138

Owusu, P. A., DeHua, L., Nyantakyi, E. K., Nagre, R. D., Borkloe, J. K., & Frimpong, I. K. (2013). Prognosticating the Production Performance of Saturated Gas Drive Reservoir: A Theoretical Perspective. *International Journal of Mining Engineering and Mineral Processing*, *2*(2), 24–33. https://doi.org/10.5923/j.mining.20130202.02

Ovchinnikov, K., Buzin, P., Katashov, A., Dubnov, O., & Agishev, R. (2017). *Production Logging in Horizontal Wells without Well Intervention*. Presented at the SPE Russian Petroleum Technology Conference, 16-18 October, Moscow, Russia. https://doi.org/10.2118/187751-MS

Ozkan, E., Sarica, C., & Haci, M. (2002). Interpretation of Horizontal-Well Production Logs: Influence of Logging Tool. *SPE Production & Facilities*, *17*(02), 84–90. https://doi.org/10.2118/77295-PA

RESMAN. (n.d.). Products & Services - Inflow Distribution. Retrieved June 2, 2019, from www.resman.no/site/products-services/inflow-distribution/

Rollins, J. T., & Taylor, L. C. (1959). Using Heat in Combination with Solvents To Clean Up Formation Flow Channels. *Journal of Petroleum Technology*, *11*(10), 33–36. https://doi.org/10.2118/1110-G

Salman, A., Kurtoglu, B., & Kazemi, H. (2014). *Analysis of Chemical Tracer Flowback in Unconventional Reservoirs*. Presented at the SPE/CSUR Unconventional Resources Conference – Canada, Calgary, Alberta, Canada. https://doi.org/10.2118/171656-MS

Schlumberger. (2014). *ECLIPSE Technical Description, Version 2014.1*.

Schlumberger. (2018). ECLIPSE Industry-Reference Reservoir Simulator. Retrieved February 20, 2019, from Schlumberger Software website: https://www.software.slb.com/products/eclipse

Schlumberger. (n.d.). Petrel E&P Software Platform. Retrieved April 29, 2019, from https://www.software.slb.com/products/petrel

Semikin, D., Senkov, A., Surmaev, A., Prusakov, A., & Leung, E. (2015). *Autonomous ICD Well Performance Completed with Intelligent Inflow Tracer Technology in the Yuri Korchagin Field in Russia*. Presented at the SPE Russian Petroleum Technology Conference, Moscow, Russia. https://doi.org/10.2118/176563-MS

SERINTEL. (2017). Reservoir Simulation Software. Retrieved February 20, 2019, from Oil & Gas Portal website: http://www.oil-gasportal.com/reservoir-simulation/software/

Sheely, C. Q. (1978). Description of Field Tests to Determine Residual Oil Saturation by Single-Well Tracer Method. *Journal of Petroleum Technology*, *30*(02), 194–202. https://doi.org/10.2118/5840-PA

Siddiqui, M. A., Al-Mutairi, M., Mankala, R., Qayyum, S., Prusakov, A., Leung, E., … Al-Ali, A. (2017). *On/Off ICD Well Performance Assessment below an ESP Using Intelligent Chemical Inflow Tracer Technology in a Brown Field in Kuwait*. Presented at the SPE Annual Technical Conference and Exhibition, San Antonio, Texas, USA. https://doi.org/10.2118/187185-MS

Skaugen, E. (2010). *Petroleumsproduksjon - Course compendium in PET200, Production of oil and gas*. University of Stavanger.

Time, R. (2018). *Guideline for the Well Simulator Problem - Course compendium in PET650*. University of Stavanger.

Tomich, J. F., Dalton, R. L., Deans, H. A., & Shallenberger, L. K. (1973). Single-Well Tracer Method to Measure Residual Oil Saturation. *Journal of Petroleum Technology*, *25*(02), 211–218. https://doi.org/10.2118/3792-PA

Williams, B. (2017). *On-Demand Reservoir Inflow Monitoring for Improving Reservoir Management Decisions*. Presented at the SPE Annual Technical Conference and Exhibition, San Antonio, Texas, USA. https://doi.org/10.2118/187421-MS

Williams, B., & Carvalho, V. (2013). Intelligent Inflow Tracers Obtain Information with Less Risk, Cost. *Journal of Petroleum Technology*, *65*(09), 50–55. https://doi.org/10.2118/0913-0050-JPT

Wintershall. (2015a). *Maria - Plan for Development and Operation* [Internal Report].

Wintershall. (2015b). *Maria - Plan for Development and Operation: Subsurface Support Document* [Internal Report].

Wintershall. (2017a). *Clean-Up Guidelines* [Internal Document].

Wintershall. (2017b). *Maria Field - Reservoir Management Plan* [Internal Report].

Wintershall. (2018, August). *Factsheet - Maria Subsea Field*. Retrieved from https://www.wintershall.no/fileadmin/assets/05_Documents/05.1_Factsheets/Factsheet_Maria_en.pdf

Yan, J., Jiang, G., Wang, F., Fan, W., & Su, C. (1998). Characterization and Prevention of Formation Damage During Horizontal Drilling. *Society of Petroleum Engineers*, *13*(04). https://doi.org/10.2118/52892-PA

You, Z., & Bedrikovetsky, P. (2018). *Well Productivity Impairment Due to Fines Migration*. Presented at the SPE International Conference and Exhibition on Formation Damage Control, 7-9 February, Lafayette, Louisiana, USA. https://doi.org/10.2118/189532-MS

Youngs, B., Neylon, K., & Holmes, J. (2010, May). Multisegment Well Modeling Optimizes Inflow Control Devices. *World Oil*.

11 Appendix

Appendix A: Numerical Inflow Tracer Data

	Tracer Depths [mMD]				Zonal Interpreted Inflow	
Zones	**Carrier Top**	**Carrier Bottom**	**Zone Top**	**Zone Bottom**	**Clean-up**	**Restart**
OS-7	4328	4341	4238	4515	28 %	1 %
OS-6	4566	4579	4515	4756	26 %	0 %
OS-5	4756	4819	4756	4996	9 %	31 %
OS-4	5054	5057	4996	5234	13 %	23 %
OS-3	5284	5297	5234	5470	11 %	19 %
OS-2	5519	5531	5470	5710	9 %	20 %
OS-1	5759	5784	5710	5910	4 %	4 %

Table 11.1: Top and bottom depth of the tracer carriers and the formation that the unique tracers represent, for producer H-4, in addition to the zonal interpreted inflow percentage.

Appendix B: Numerical Simulation Results

Simplified Model

Case 1 and 2: Simplified Model - Clean-up and Restart

	Oil Production Rate [Sm^3/day]			
	Case 1: Clean-up		**Case 2: Restart**	
Zones	**Case 1A**; f = 0.0001 , Pw,toe = 382.06 bar	**Case 1B**; f = 0.011 , Pw,toe = 384.9 bar	**Case 2A**; f = 0.0001 , Pw,toe = 262.05 bar	**Case 2B**; f = 0.011 , Pw,toe = 263.7 bar
OS-7	331.8	238.5	186.7	183.5
OS-6	523.0	490.7	25.9	24.8
OS-5	206.2	196.5	208.0	203.0
OS-4	283.1	342.1	240.4	244.0
OS-3	208.4	212.6	197.7	197.8
OS-2	184.0	207.4	182.5	185.2
OS-1	208.7	257.4	127.5	130.1
Total Rate	1945.2	1945.2	1168.7	1168.4

Table 11.2: Simulated oil production rate for Case 1 and 2 of the Simplified Model.

Case 4.1: Match for Clean-up

	Zonal Permeability [mD]				
Zones	**Base Case**	**Match A**	**Match B**	**Match C**	**Match D**
OS-7	11.5	39.1	81.7	79.4	118.5
OS-6	245.9	418.0	590.2	811.5	1229.5
OS-5	27.2	19.0	29.9	38.1	57.1
OS-4	102.9	82.3	82.3	174.9	257.3
OS-3	31.7	22.2	41.2	44.4	66.6
OS-2	38.0	22.8	38.0	49.4	72.2
OS-1	255.0	5.1	7.7	10.2	17.9

Table 11.3: Zonal permeability values of the simulated matches for clean-up, using PERMXY-multipliers.

	Oil Production Rate [Sm^3/day]				
Zones	**Tracer Signal**	**Match A**	**Match B**	**Match C**	**Match D**
OS-7	544.6 (28 %)	537.1	556.7	496.3	496.3
OS-6	505.7 (26 %)	506.3	519.8	539.7	539.7
OS-5	175.1 (9 %)	176.5	178.5	180.2	180.2
OS-4	252.9 (13 %)	253.2	212.3	263.0	263.0
OS-3	214.0 (11 %)	216.2	219.5	203.6	203.6
OS-2	175.1 (9 %)	175.0	178.7	180.9	180.9
OS-1	77.8 (4 %)	81.0	79.6	81.4	81.4
Total Rate	1945.2	1945.3	1945.1	1945.1	1945.1

Table 11.4: Simulated oil rate for the different matches, considering PERMXY multipliers, of interpreted clean-up data, in the "Far from well"-band.

	Oil Production Rate [Sm³/day]		
Zones	**Tracer Signal**	**Match E**	**Match F**
OS-7	544.6 (28 %)	511.5	479.9
OS-6	505.7 (26 %)	491.6	608.3
OS-5	175.1 (9 %)	154.8	136.7
OS-4	252.9 (13 %)	227.1	240.9
OS-3	214.0 (11 %)	203.1	169.6
OS-2	175.1 (9 %)	163.5	149.0
OS-1	77.8 (4 %)	193.7	160.7
Total Rate	1945.2	1945.3	1945.1

Table 11.5: Simulated oil rate for the different matches, considering PERMXY multipliers, of interpreted clean-up data, in the near-wellbore area.

Case 4.2: Match for Restart

Case 4.2.2: Skin

	Oil Production Rate [Sm³/day]					
Zones	**Tracer Signal**	**Skin = 10 , 0**	**Skin = 30 , 0**	**Skin = 100 , 0**	**Skin = 150 , 0**	**Skin = 300 , 0**
OS-7	11.7 (1 %)	180.2	107.7	46.4	33.4	18.5
OS-6	0 (0 %)	275.5	270.8	232.4	209.2	160.7
OS-5	373.9 (31 %)	120.3	136.7	160.7	169.6	185.1
OS-4	280.4 (23 %)	149.8	164.5	182.8	189.4	201.0
OS-3	222.0 (19 %)	127.8	140.8	156.8	162.5	172.7
OS-2	233.7 (20 %)	115.7	127.6	142.3	147.6	156.8
OS-1	46.7 (4 %)	199.3	220.4	247.2	256.8	273.7
Total Rate	1168.4	1168.6	1168.5	1168.6	1168.5	1168.5

Table 11.6: Simulated oil rate considering different skin factor in the heel, in the Base Case, for restart.

	Oil Production Rate [Sm^3/day]					
Zones	**Tracer Signal**	**Skin = 100 , -2**	**Skin = 150 , -2**	**Skin = 200 , -2**	**Skin = 300 , -2**	**Skin = 300 , 500 , -2**
OS-7	11.7 (1 %)	46.4	33.4	26.4	16.4	19.7
OS-6	0 (0 %)	304.9	271.5	244.4	203.5	152.0
OS-5	373.9 (31 %)	192.4	206.6	216.9	231.5	244.6
OS-4	280.4 (23 %)	207.9	219.0	227.1	238.8	251.7
OS-3	222.0 (19 %)	184.7	194.6	202.0	212.4	224.0
OS-2	233.7 (20 %)	148.5	156.5	162.4	170.8	180.1
OS-1	46.7 (4 %)	83.8	87.0	89.4	92.8	96.4
Total Rate	1168.4	1168.6	1168.6	1168.6	1166.2	1168.5

Table 11.7: Simulated oil rate for different skin values considering Match A3 for clean-up, for restart.

Case 4.2.3: Shut-in of Zones OS-7 and 6

	Oil Production Rate [Sm^3/day]						
Zones	**Tracer Signal**	**Base Case**	**Match A3**	**Match B**	**Match C1**	**Match D1**	**Match E1**
OS-7	11.7 (1 %)	0	0	0	0	0	0
OS-6	0 (0 %)	0	0	0	0	0	0
OS-5	373.9 (31 %)	227.6	291.3	322.8	339.0	365.5	258.9
OS-4	280.4 (23 %)	234.2	300.8	257.8	304.0	303.8	263.4
OS-3	222.0 (19 %)	201.9	258.3	266.1	228.3	212.2	239.8
OS-2	233.7 (20 %)	183.5	208.7	215.7	200.8	197.6	191.8
OS-1	46.7 (4 %)	321.4	109.4	106.1	96.4	89.5	214.7
Total Rate	1168.4	1168.6	1168.5	1168.5	1168.5	1168.5	1168.6

Table 11.8: Simulated oil rate for heel zones shut-in, considering different matches of clean-up.

Case 4.2.4: Skin in OS-7 and Shut-in of OS-6

	Oil Production Rate [Sm^3/day]				
Zones	**Tracer Signal**	**Skin = 30 , 0**	**Skin = 70 , 0**	**Skin = 100 , 0**	**Skin = 150 , 0**
OS-7	11.7 (1 %)	132.2	67.2	49.1	33.9
OS-6	0 (0 %)	0	0	0	0
OS-5	373.9 (31 %)	321.1	342.9	349.0	354.1
OS-4	280.4 (23 %)	270.0	286.6	291.2	295.1
OS-3	222.0 (19 %)	188.5	200.1	203.4	206.1
OS-2	233.7 (20 %)	175.7	186.5	189.5	192.0
OS-1	46.7 (4 %)	81.0	85.3	86.4	87.4
Total Rate	1168.4	1168.5	1168.6	1168.6	1168.6

Table 11.9: Simulated oil rate OS-6 shut-in and OS-7 with different skin values, considering Match D1 for clean-up.

	Oil Production Rate [Sm^3/day]						
Zones	**Tracer Signal**	**Base Case**	**Match A3**	**Match B**	**Match C1**	**Match D1**	**Match E1**
OS-7	11.7 (1 %)	73.3	86.9	80.9	76.0	67.2	92.2
OS-6	0 (0 %)	0	0	0	0	0	0
OS-5	373.9 (31 %)	213.9	269.1	299.6	315.7	342.9	238.3
OS-4	280.4 (23 %)	219.8	278.0	239.7	284.3	286.6	242.8
OS-3	222.0 (19 %)	189.1	238.3	247.1	213.3	200.1	220.7
OS-2	233.7 (20 %)	171.8	192.6	200.5	187.8	186.5	176.6
OS-1	46.7 (4 %)	300.7	103.6	100.8	91.7	85.3	197.9
Total Rate	1168.4	1168.6	1168.5	1168.6	1168.8	1168.6	1168.5

Table 11.10: Simulated oil rate OS-6 shut-in and skin of 70 in OS-7, for different matches of clean-up.

Case 5: Multisegment Well

Case 5.1: Multisegment Well v.s. Non-Segmented Well

	Oil Production Rate [Sm^3/day] – Clean-up			
Zones	**Base Case**	**Segment Length 270 m**	**Segment Length 50 m**	**Segment per Cell**
OS-7	321.5	340.9	341.2	341.4
OS-6	376.9	383.5	383.2	382.7
OS-5	180.1	179.2	178.9	179.0
OS-4	257.4	252.4	252.4	252.4
OS-3	223.7	217.5	217.5	217.4
OS-2	205.8	199.7	199.8	199.7
OS-1	379.8	367.9	368.2	368.2
Total Rate	1945.2	1941.1	1941.2	1940.8

Table 11.11: Simulated oil rate for different segment lengths of the multisegment well, for clean-up.

	Oil Production Rate [Sm^3/day] – Restart			
Zones	**Base Case**	**Segment Length 270 m**	**Segment Length 50 m**	**Segment per Cell**
OS-7	282.6	289.5	289.6	289.7
OS-6	266.6	272.4	271.2	271.0
OS-5	102.6	102.4	102.2	102.3
OS-4	131.4	129.2	129.5	129.6
OS-3	111.5	109.4	109.5	109.5
OS-2	100.9	98.6	98.7	98.7
OS-1	172.9	167.0	167.7	167.7
Total Rate	1168.5	1168.5	1168.4	1168.5

Table 11.12: Simulated oil rate for different segment lengths of the multisegment well, for restart.